OPERATION HARDTACK—PROJECT 2.1

410997

Shipboard Radiation from Underwater Bursts

M. M. Bigger
H. R. Rinnert
H. A. Zagorites
U.S. Naval Radiological Defense Laboratory
San Francisco, CA

24 March 1961

NOTICE:

This is an extract of WT-1619, Operation HARDTACK, Project 2.1.

Extracted version prepared for
Director
DEFENSE NUCLEAR AGENCY
Washington, DC 20305-1000

BEST COPY AVAILABLE

1 September 1985

REPORT DOCUMENTATION PAGE

1a REPORT SECURITY CLASSIFICATION UNCLASSIFIED			1b RESTRICTIVE MARKINGS		
2a SECURITY CLASSIFICATION AUTHORITY N/A since Unclassified			3 DISTRIBUTION AVAILABILITY OF REPORT Approved for public release; distribution is unlimited.		
2b DECLASSIFICATION DOWNGRADING SCHEDULE N/A since Unclassified					
4 PERFORMING ORGANIZATION REPORT NUMBER(S)			5 MONITORING ORGANIZATION REPORT NUMBER(S) WT-1619(EX)		
6a NAME OF PERFORMING ORGANIZATION U.S. Naval Radiological Defense Laboratory	6b OFFICE SYMBOL (If applicable)		7a NAME OF MONITORING ORGANIZATION Defense Atomic Support Agency		
6c ADDRESS (City, State, and ZIP Code) San Francisco, CA			7b ADDRESS (City, State, and ZIP Code) Washington, DC		
8a NAME OF FUNDING SPONSORING ORGANIZATION	8b OFFICE SYMBOL (If applicable)		9 PROCUREMENT INSTRUMENT IDENTIFICATION NUMBER		
8c ADDRESS (City, State, and ZIP Code)			10 SOURCE OF FUNDING NUMBERS		

			PROGRAM ELEMENT NO	PROJECT NO	TASK NO	WORK UNIT ACCESSION NO

11 TITLE (Include Security Classification)
OPERATION HARDTACK—PROJECT 2.1
Shipboard Radiation from Underwater Bursts, Extracted Version

12 PERSONAL AUTHOR(S)
Bigger, M.M.; Rinnert, H.R.; and Zagorites, H.A.

13a TYPE OF REPORT	13b TIME COVERED FROM _____ TO _____	14 DATE OF REPORT (Year, Month, Day) 610324	15 PAGE COUNT 111

16 SUPPLEMENTARY NOTATION This report has had sensitive military information removed in order to provide an unclassified version for unlimited distribution. The work was performed by the Defense Nuclear Agency in support of the DoD Nuclear Test Personnel Review Program.

17	COSATI CODES		18 SUBJECT TERMS (Continue on reverse if necessary and identify by block number)
FIELD	GROUP	SUB GROUP	Hardtack Gamma Radiation
18	3		Underwater Bursts Radiation Measurements
6	18		Radiation Doses

19 ABSTRACT (Continue on reverse if necessary and identify by block number)
The principal objectives of this project were: (1) the determination of total gamma-radiation dose and dose rate histories aboard three moored ships exposed to radiological environments at locations of possible operational interest about the surface zeros of two underwater nuclear detonations, shots Wahoo and Umbrella; (2) estimation of remote-source gamma-radiation dose and dose-rate histories at exposed weather-deck locations aboard ships; (3) estimation of total gamma-radiation dose and dose-rate histories in the water adjacent to the ships; and (4) measurement of gamma-ionization decay of a fallout sample collected on one ship a few minutes after each shot.

Although radiation from the water may have influenced the compartment/deck dose-rate ratios to a considerable degree at later times, the contribution of contaminated water to the total dose observed aboard the ships was probably of little significance.

20 DISTRIBUTION AVAILABILITY OF ABSTRACT ☒ UNCLASSIFIED/UNLIMITED ☐ SAME AS RPT ☐ DTIC USERS	21 ABSTRACT SECURITY CLASSIFICATION UNCLASSIFIED	
22a NAME OF RESPONSIBLE INDIVIDUAL Mark D. Flohr	22b TELEPHONE (Include Area Code) (202) 325-7559	22c OFFICE SYMBOL DNA/ISCM

DD FORM 1473, 84 MAR   83 APR edition may be used until exhausted   SECURITY CLASSIFICATION OF THIS PAGE
All other editions are obsolete

FOREWORD

Classified material has been removed in order to make the information available on an unclassified, open publication basis, to any interested parties. The effort to declassify this report has been accomplished specifically to support the Department of Defense Nuclear Test Personnel Review (NTPR) Program. The objective is to facilitate studies of the low levels of radiation received by some individuals during the atmospheric nuclear test program by making as much information as possible available to all interested parties.

The material which has been deleted is either currently classified as Restricted Data or Formerly Restricted Data under the provisions of the Atomic Energy Act of 1954 (as amended), or is National Security Information, or has been determined to be critical military information which could reveal system or equipment vulnerabilities and is, therefore, not appropriate for open publication.

The Defense Nuclear Agency (DNA) believes that though all classified material has been deleted, the report accurately portrays the contents of the original. DNA also believes that the deleted material is of little or no significance to studies into the amounts, or types, of radiation received by any individuals during the atmospheric nuclear test program.

OPERATION HARDTACK— PROJECT 2.1

SHIPBOARD RADIATION FROM UNDERWATER BURSTS

M. M. Bigger, Project Officer
H. R. Rinnert
H. A. Zagorites

U. S. Naval Radiological
    Defense Laboratory
San Francisco, California

3 — 4

ABSTRACT

The principal objectives were: (1) the determination of total gamma-radiation dose and dose-rate histories aboard three moored ships (destroyers) exposed to radiological environments at locations of possible operational interest about the surface zeros of two underwater nuclear detonations, Shots Wahoo and Umbrella: (2) estimation of remote-source gamma-radiation dose and dose-rate histories at exposed weather-deck locations aboard ship: (3) estimation of total gamma-radiation dose and dose-rate histories in the water adjacent to the ships; and (4). measurement of gamma-ionization decay of a fallout sample collected on one ship a few minutes after each shot.

The ships, which were equipped with operating washdown systems, were instrumented with film badges and gamma-intensity-time recorders (GITR's). The film badges and unshielded GITR's supplied radiation data at locations representing major battle stations; GITR's submerged in the water supplied some data on underwater radiation: and a fallout collector connected to a fully shielded GITR supplied gamma-ionization decay data.

Radiation histories were obtained on only one ship for Shot Wahoo. Although histories were obtained on all three ships for Shot Umbrella, some data was lost because of shock damage.

At least 95 percent of the total dose observed on the washed weather decks was attributed to radiation from airborne radioactivity. After Shot Umbrella, weather-deck dose accumulation (to 75 percent of final values) ranged between 600 r received within H - 26 seconds at 1,900 feet from surface zero and 50 r received within H + 150 seconds at 7,900 feet from surface zero. After Shot Wahoo, the dose accumulation was slower, but the final deck doses were about 300 r higher, despite the fact that the ships were from 1,000 to 2,000 feet farther away from surface zero than was the case for Shot Umbrella. For nuclear-weapon-delivery situations simulated by the two closer-in ships, temporary immobilization could result in lethal or near-lethal doses.

After Shot Wahoo, the majority of compartments received doses in excess of 500 r aboard the closest ship and in excess of 200 r aboard the next-to-closest ship. After Shot Umbrella, the two ships received doses in excess of 200 r in many compartments.

Ratios of dose or dose rate in compartments to dose or dose rate on washed weather decks were dependent upon changes in radiation-source geometries and upon the presence of contaminants within the ships. The long-term dose ratios ranged between 0.1 and 0.7 for nonmachinery spaces, and between 0.02 and 0.2 for machinery spaces.

Although radiation from the water may have influenced the compartment deck dose-rate ratios to a considerable degree at later times, the contribution of contaminated water to the total dose observed aboard the ships was probably of little significance.

After Shot Umbrella, gamma-ionization decay was measured for the periods between H + 0.1 and 11.5 hours and between H + 23.0 and 34.9 hours. No decay measurements were obtained for Shot Wahoo.

FOREWORD

This report presents the final results of one of the projects participating in the military-effect programs of Operation Hardtack. Overall information about this and the other military-effect projects can be obtained from ITR-1660, the "Summary Report of the Commander, Task Unit 3." This technical summary includes: (1) tables listing each detonation with its yield, type, environment, meteorological conditions, etc.; (2) maps showing shot locations; (3) discussions of results by programs; (4) summaries of objectives, procedures, results, etc., for all projects; and (5) a listing of project reports for the military-effect programs.

PREFACE

Project 2.1 gratefully acknowledges its indebtedness to the following organizations and personnel for their contributions to the project:

W. B. Lane, U. S. Naval Radiological Defense Laboratory, for the general concept and details he developed for collection of early-time decay samples.

R. K. Fuller, Project 2.2, for implementing the collection and handling of the early decay sample in the field.

Task Unit 6 of Task Group 7.1, for furnishing and processing the 1,700 film badges used for technical measurements.

Personnel of Task Element 7.3.1.5, the Task Group 7.3 Decontamination Unit, who showed a high degree of initiative and cooperation in installing the film badges aboard ship, in sample recovery, and in sorting and handling the many film badges required.

The officers and crews of the Task Group 7.3 Special Projects Unit, who manned the three target ships, for their frequent and cheerful assistance in maintaining support equipment, accomplishing repair and alteration work, and furnishing work parties when requested.

F. K. Kawahara, Project 2.2, for much needed help in reducing the gamma-radiation data required for the final report.

CONTENTS

FIGURES

9

10

11

12

Chapter 1

INTRODUCTION

1.1 OBJECTIVES

The principal objectives were: (1) the determination of total gamma-radiation dose and dose-rate histories aboard three moored ships (destroyers) exposed to radiological environments at locations of possible operational interest about the surface zeros of two underwater nuclear detonations, Shots Wahoo and Umbrella; (2) estimation of remote-source gamma-radiation dose and and dose-rate histories at exposed weather-deck locations aboard ship; (3) estimation of total gamma-radiation dose and dose-rate histories in the water adjacent to the ships; and (4) measurement of gamma-ionization decay of a fallout sample collected on one ship a few minutes after each shot.

An additional objective was the provision of preproduction evaluation, production liaison, instrument-maintenance consultation, and a field maintenance facility for all projects using GITR's developed by the U. S. Naval Radiological Defense Laboratory (NRDL).

1.2 TERMINOLOGY

In this report, total gamma-radiation dose indicates the combined contributions of all radiation sources that affect the detectors. Doses and dose rates are specified to apply to air absorption only.

1.3 BACKGROUND AND THEORY

It is of interest to the Navy to find out whether the minimum safe standoff distance for anti-submarine nuclear-weapon-delivery ships is determined by radiological effects or by physical damage. (Standoff distance is defined as the distance of surface zero from the ship at the time of detonation.) Each tactical maneuver by the ship, during and after delivery of the weapon, will have associated with it physical shock and radiation effects. For a given weapon detonated under a specific set of environmental conditions, the shock effects will be chiefly dependent upon the ship's position and orientation with respect to surface zero at the time of shock arrival, whereas the radiation effects will be dependent upon integration (with respect to time) of the shipboard dose rates received at each position along the entire track of the ship.

Because it was not feasible to have the test ships actually perform representative tactical maneuvers in the radiological environments, doses for such maneuvers were not measured directly. The alternative was to obtain data for specific locations, which would be useful for the calculation of dose rates aboard ships performing maneuvers in hypothetical weapon deliveries.

Parameters of interest in determinations of shipboard dose rates include: (1) the magnitudes of radiation sources on the surfaces of the ship, in the surrounding and remote air, and in the surrounding and remote water; (2) the ingress of contaminants into the interior of the ship; and (3) the attenuation afforded by the ship's structures or machinery with respect to the several

13

radiation sources. Some of these parameters have been previously investigated, principally for other than underwater-detonation conditions.

In past calculations of shipboard radiation attenuation, the major emphasis has been given to residual contamination on ships' weather surfaces (Reference 1), with some work done for a ship enveloped in a radioactive volume of air (Reference 2), assuming monoenergetic gamma radiation and uniform contamination in an idealized geometry. (Shielding calculations are in progress at NRDL, which for both residual contaminant and remote-source radiation take the entire radiation-energy spectrum into account and which eliminate much of the need for idealized geometries in the case of remote-source radiation.)

Gamma radiation from sources outside a ship has been investigated during various phases of the fallout environment from land-surface and water-surface megaton-range detonations during Operations Castle (Reference 3) and Redwing (Reference 4) and, to a very-limited extent, during Operation Wigwam (Reference 5) for a deep-underwater detonation, using Liberty ships (YAG's 39 and 40) as the test vehicles.

The experimental results from Operations Castle, Redwing, and Wigwam indicated that attenuation factors inside ships were dependent not only upon the geometries of the ships' structures but also upon: (1) the geometries and relative magnitudes of the various radiation sources, which depend upon detonation conditions and also change with time; and (2) the gamma-energy spectra, which are functions of time and weapon design.

Chapter 2

PROCEDURE

.

2.1 TARGET SHIPS

The positions and orientations of the target destroyers (DD's) were chosen by the Defense Atomic Support Agency (DASA), based upon compromises of requirements from the many projects utilizing the ships (Figures 2.1 and 2.2). The three distances of the ships from surface zero (SZ) were expected to represent regions of moderate shock damage, moderate to light shock damage, and light to no shock damage to the ships of their equipment. The innermost and outermost ships were oriented with their sterns toward surface zero in order to simulate probable escape maneuvers. The middle ship was oriented with its starboard side toward surface zero to meet requirements of other projects.

The ships were located on a line downwind from surface zero in order to maximize the radiological effects for a given distance from surface zero. They were expected to receive varying amounts of radiation contributed by the plume, cloud, and weapon debris trapped in the water near surface zero. In addition, they were expected to be contaminated to varying degrees by the fallout.

The ships were subjected to continual washdown during the dynamic radiological events, because shipboard operations by the various participating projects would have been hampered by the expected high levels of residual contamination. (Washdown is a standard countermeasure aboard naval ships and would normally be used during fallout or other contaminating events.)

Each ship had forced-draft blowers supplying air to one fired boiler in the forward fireroom in order to supply power needed to meet the operational or experimental requirements of various projects. The experimental ingress studies of Project 2.2 aboard DD 592 also required the operation of forced-draft blowers supplying air to one unfired boiler in the aft fireroom and the operation of ventilation systems supplying air to various compartments (Reference 6). The ingress of these air supplies could be expected to create various gamma radiation sources inside the ships and to influence the radiation fields at various stations under investigation by this project.

2.2 INSTRUMENTATION

The gamma-radiation dose rates and doses aboard the three ships were measured with GITR instrumentation and standard Rad-Safe film badges. The shipboard areas selected for investigation represented or simulated major battle stations aboard modern destroyers.

2.2.1 Gamma-Intensity-Time Recorders (GITR's).
Portable, self-contained, battery-powered GITR's were developed as part of NRDL's laboratory program. The GITR consisted of a detector unit and a recorder unit (Appendix A). The detector unit could be mounted inside the recorder unit case, or it could be mounted separately and connected to the recorder unit with a waterproof cable.

The detector unit consisted of two concentric ionization chambers with associated recycling electrometers. Discharge of the initially charged ionization chamber by a predetermined quantity of ionizing radiation, triggered the electrometer circuit, which sent a pulse to the recording unit and recharged the ionization chamber to complete the cycle.

The pulses were recorded as on-off information on magnetic tape in the recorder unit. Three

15

channels of information were recorded on each tape: the equivalent of at least three decades of radiation dose rates could be recorded linearly on each of two channels, and low-frequency timing pulses were recorded on the third channel. The various recorders were started either manually or by the activation of a relay system connected to an Edgerton, Germeshausen and Grier, Inc. (EG&G) radio timing-signal receiver installed on each ship. The recorder shut itself off automatically when the end of the tape was reached.

The nominal dose-rate ranges of various GITR's are presented in Table 2.1.

2.2.2 GITR Installations. Figure 2.3 presents the location and designation of GITR detector stations used by Projects 2.1, 2.2, and 2.3 aboard the ships. Unshielded GITR detector units were mounted on weather decks and in several compartments in order to obtain the total radiation fields at these locations. Each ship also had three specialized GITR stations: (1) Station 14 was directionally shielded against radiation sources aboard the ship, to permit estimation of remote-source radiations; (2) Station 15 was suspended in the water to measure radiation in the nearby water; and (3) Station 16 was modified to a higher dose-rate range to prevent loss of data in case the standard GITR's became saturated. GITR Stations 1 through 16, on all three ships, were of specific concern to this project, although data from other stations was utilized as required.

With the exception of Stations 18 and 21 aboard DD 474 and DD 593 during Shot Umbrella and Stations 15 aboard all three ships during both shots, the detector units were separated from the recorder units. All detector units and all recorder units were spring-mounted to prevent damage from shock. In compartments where temperatures exceeded 120 degrees F (Stations 9, 10, 11, 12, and 13), the detector units were water cooled to prevent damage by heat. Approximately 0.1-inch-thick aluminum was used to: (1) cover each exposed weather-area station as a whole, to provide protection, and (2) jacket the detector itself in the interior stations, to obtain similar energy response characteristics. The centerpoint of each detector's sensitive volume was located 3 feet above the deck on which the station was mounted, except in the specialized GITR Stations 14, 15, and 16.

The modified detector in Station 16 was located 9 feet above the 02 deck to ensure a clear view of all radiation sources, independent of ship orientation. The detector in Station 14 (3.3 feet above the main deck) was encased by 4-inch-thick lead, which shielded against radiation from sources on the ship or in the nearby water but permitted a clear view of surface zero and the sky overhead.

Figures 2.4 and 2.5 show general details of GITR mounting and cooling.

The underwater Station 15 was suspended from a boom extending over the ship's fantail. After the underwater shock waves had passed the ship, the instrument container was meant to be submerged to a depth of 11 feet by means of a winch-release-and-braking mechanism, activated by a delayed relay-closure from the GITR starting circuit. The detector unit was mounted inside the recorder unit case; the whole GITR unit, with detector facing upward, was firmly padded with expanded polystyrene and placed into the instrument container (Figure 2.6).

2.2.3 Gamma-Ionization Decay Unit. This unit consisted of a fallout-sample collector, an acid-wash unit, a delivery tube, a polyethylene sample container, a GITR, and a 6-inch-thick lead cave (Figure 2.7).

The sample collector was a polyethylene tray set inside a Project 2.3 open-close collector (OCC) mounted on the unwashed platform on top of the gun director of DD 592 (Reference 7). A perforated stainless-steel tube was attached to the inside edge of the tray to permit spraying the tray with the acid wash. A $\frac{1}{4}$-inch tygon tube, protected by flexible metal conduit, connected the tray's drain hole with the sample container inside the lead cave, which was mounted on the main deck of the ship.

The GITR detector was installed in the central cavity of the double-walled sample container so that the fallout sample presented at least a $3-\pi$ geometry to the detector. The detector and the sample container were surrounded by foam rubber to prevent damage by shock, and the

16

sample container was provided with an overflow tube to prevent damage by hydrostatic pressure.

An EG&G radio timing signal activated the timing circuit to (1) start the GITR at H−5 minutes; (2) open the cover of the OCC at H−0.5 minute; (3) close the cover of the OCC at H+4 minutes; and (4) wash the tray with 750 cc of concentrated hydrochloric acid at H+5 minutes. The combined acid-and-fallout sample drained into the sample container and remained undisturbed for 53 hours, during which time two 12-hour records of gamma dose rate were obtained. The time period chosen for fallout collection was based upon estimates of the time required to collect a sufficiently large sample of fallout in a short time so as to start decay measurements as early as possible.

2.2.4 GITR Calibration and Maintenance. Primary calibration of the GITR detectors had been performed with an accurately calibrated Co^{60} source at NRDL. At the Eniwetok Proving Ground (EPG), the project used 120 curies of Cs^{137} in a lead-shielded source holder mounted in a trailer for calibration of GITR's. The field calibrations with the Cs^{137} source were related to the primary Co^{60} calibrations by means of Victoreen 70A r-meters (known to be accurate within ±5 percent), which were utilized as transfer standards. The detectors were held in a fixed orientation in the broad-beam radiation field by means of a jig. However, the chosen orientation — which was used in order to insure reproducibility — led to biased calibration, because the directional responses of the detectors were not uniform. The responses to various gamma energies between 0.07 and 1.3 Mev were determined by means of filtered X-ray beams, Cs^{137} sources, and Co^{60} sources. These responses were used to estimate calibration-bias corrections for various assumed radiation-source geometries and gamma spectra. The details are given in Appendix B.

The field maintenance facility consisted of a dehumidified room equipped with tool kits, standard test equipment (oscilloscopes, and the like), and portable beta-radiation sources. The air-conditioned calibration trailer also contained tool kits and standard test equipment in addition to the gamma-calibration range. These facilities were established for use by all projects utilizing the NRDL GITR's.

2.2.5 Film Badges. The GITR gamma-dose measurements were augmented by the use of film badges. Approximately 1,700 standard Rad-Safe film-badge packets were supplied and processed by Task Unit 6 (TU-6).

The standard Rad-Safe film pack consisted of two films: (1) DuPont 502, covering the dose range between 0.1 and 20 r; and (2) DuPont 834, covering the dose range between 10 and 1,200 r. The films were partially covered by lead strips 0.028 ± 0.002 inch thick, to discriminate against beta radiation, thereby permitting determination of gamma dosage. The exposed film was given 5-minute development, with 4.5-minute agitation, in Eastman X-ray film developer at 68 degrees F. The developed film under the lead strip was read with an Eberline-Angus densitometer at the EPG and reread with a Macbeth-Ansco densitometer at NRDL, which permitted scanning the film for damage, pinholes, etc.

The film-badge packets were used in pairs in order to obtain statistical estimates of random errors. Four to eighteen pairs of film-badge packets were either taped to stanchions or suspended with twine 3 feet above deck level in each compartment or area being investigated. Figure 2.8 presents the area locations of the film-badge packets aboard the destroyers. Detailed locations of the packets are presented in Appendix C.

2.3 OPERATIONS

This project participated in Shots Wahoo and Umbrella. The GITR's were checked, repaired if necessary, and calibrated before and after each shot, so far as was practicable.

Project personnel mounted the GITR's on the three ships by D−2 days of each shot. Instrument checkout continued until D−1 day, at which time the system was readied for test participation. Personnel of Task Element 7.3.1.5 were briefed on film-badge locations and recovery

procedures aboard the ships by D−2 days, helped project personnel install the film badges by D−1 day, and helped project personnel recover and process the film badges after shot participation.

The GITR's were started either manually at H−3 hours or by receipt of radio timing signals at H−5 minutes. The majority of the GITR recording units operated for 12 hours, but three GITR recording units per ship operated for 60 hours. As soon afterward as was feasible, the record tapes were recovered and processed for data reduction.

2.4 DATA REQUIREMENTS

As pointed out in Section 1.2, the doses and dose rates presented in this report, in units of r and r/hr, are defined in terms of air ionization and not in terms of biological effects.

2.4.1 Data Obtained by Project 2.1. The data obtained by this project consisted of GITR records from the various stations indicated in Figure 2.3 and of film badges exposed in locations indicated in Figures C.1 through C.19. The measured GITR data consisted of pulses (representing predetermined quantities of air ionization) recorded on magnetic tapes running at constant speed. The observed film-badge data consisted of the optical densities of the developed film areas originally under the lead strips.

2.4.2 Data Reduction. The pulses recorded on the GITR magnetic tapes were initially converted to uncorrected dose or dose-rate data by means of an analog data-reduction apparatus supplied and operated by Project 2.3 (Reference 7); however, the IBM-704 computer at the EPG was eventually utilized for more accurate read-out. In both cases, the conversion to uncorrected dose and dose rates was based upon the biased field-calibration dose increments of 0.243 mr per pulse for the low-range GITR detectors and of 0.243 r per pulse for the high-range GITR detectors.

For the IBM read-out, the pulses from the GITR records (entered via an auxiliary special-purpose magnetic-tape unit and gate chassis connected to the computer) interrupted accumulation of constant-frequency timing signals in a register of the IBM-704. These times between GITR pulses were stored in the computer memory and a simplified computer program was used to convert the stored period information into records of uncorrected dose, uncorrected dose-rate, and time after start of computation. Corrections for GITR recorder speeds, determined by checking the record's timing channel, were applied as part of the IBM computer program. Corrections for GITR calibration shifts and bias, discussed in Appendix B, were applied to the read-out data.

Conversion of time scales from time-after-start-of-computation to time-after-shot was straightforward for data from the radio-started GITR's, because the starting pulse on the record also served to start the IBM computation. That was not the case for the manually started GITR records; therefore, the dose-rate data from these records (plotted on a relative time scale) had to be time-correlated with data from the radio-started GITR's. This was accomplished by lining up times of those prominent curve features (such as maxima, and the like) that should have occurred at the same time for all stations aboard one ship.

Corrected dose and dose-rate data for individual GITR stations were tabulated. The data from the washed weather-deck GITR stations were averaged and tabulated. For the periods during which saturated GITR's created gaps in the data, estimates of average radiation data for the weather-deck areas were approximated by normalizing appropriate data from several unsaturated interior GITR's to fit the actual weather-deck data on both sides of the gap. The averaged weather-deck dose rates were also corrected for decay to serve as a guide in estimating the relative importance of remote-source radiation (Section 3.2). Ratios of dose and dose rate in compartment to average dose and dose rate on washed weather decks were calculated as functions of time. Ratios of the dose rate in the adjacent water to average dose rate

18

on the washed weather decks were calculated. The dose-rate histories from the gamma-ionization decay unit were corrected for background of external radiation and normalized to read 1 r hr at H-1 hour. Slopes of the log-log plot of normalized dose rates versus time were calculated for various periods.

The various estimates of probable error in the results obtained from GITR data were based upon consideration of the following (or combinations thereof): (1) relative accuracies of biased detector calibrations in the field (Section B.1); (2) tolerance intervals for bias-correction factors calculated for a broad range of assumed radiation-source geometries and gamma energies (Section B.2 and Table B.9); (3) estimated effects of timing errors (Appendix D); and (4) the variance of data about the calculated averages, where appropriate.

The film badges were developed by TU-6, but the gross densities were read and converted to gamma-dose values by project personnel. The gamma doses for all film-badge stations in each compartment or area were averaged. Similarly, the doses for stations in each athwart-ship (transverse) third of the various compartments were also averaged. Ratios of average dose in compartment to average dose on washed weather-deck areas were calculated. Film-badge calibrations and estimates of error are discussed in Appendix C.

2.4.3 Data from Other Projects. For both Shots Wahoo and Umbrella, this project required: (1) an approximate total of 1,700 standard Rad-Safe film badges which were supplied and developed by TU-6 — for technical measurements; (2) records of near-surface wind velocities in the vicinity of the target ships — for correlative purposes; (3) access to photographic and other information that helped to define the dynamic radiological phenomena as a function of time and location in the contaminated region; (4) access to all photographs showing the locations and orientations of the ships with respect to surface zero after shot time — for correlative purposes; and (5) film-pack data for the weather-deck areas from Project 2.3 — to augment film-badge data obtained by Project 2.1.

TABLE 2.1 GITR DOSE-RATE RANGES

Detector Type	Record Duration	Gamma Dose-Rate Range
	hr	
Standard	12	9 mr/hr to 87,000 r/hr
Standard	60	9 mr/hr to 17,000 r/hr
Modified	12	10,000 to 2,000,000 r/hr
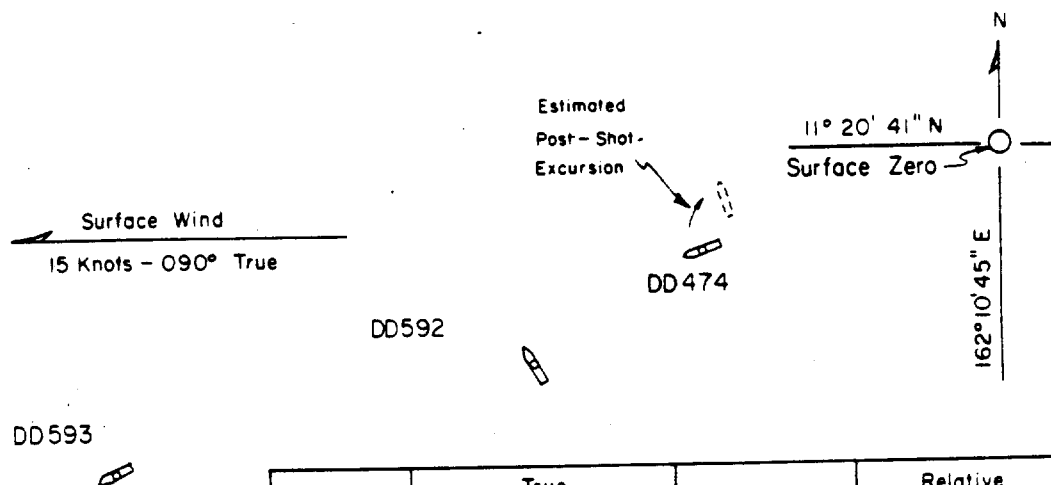
Estimated
Post – Shot –
Excursion

N

11° 20' 41" N
Surface Zero

DD 474

Surface Wind

15 Knots – 090° True

162°10'45" E

DD 592

DD 593

Ship	True Bearing of Ship from SZ	Distance from SZ	Relative Bearing of SZ from Ship
	Degrees	Feet	Degrees
DD 474	251	2900	181.5
DD 592	245	4900	96
DD 593	250	8900	188

Figure 2.1 Target ship array. Shot Wahoo.
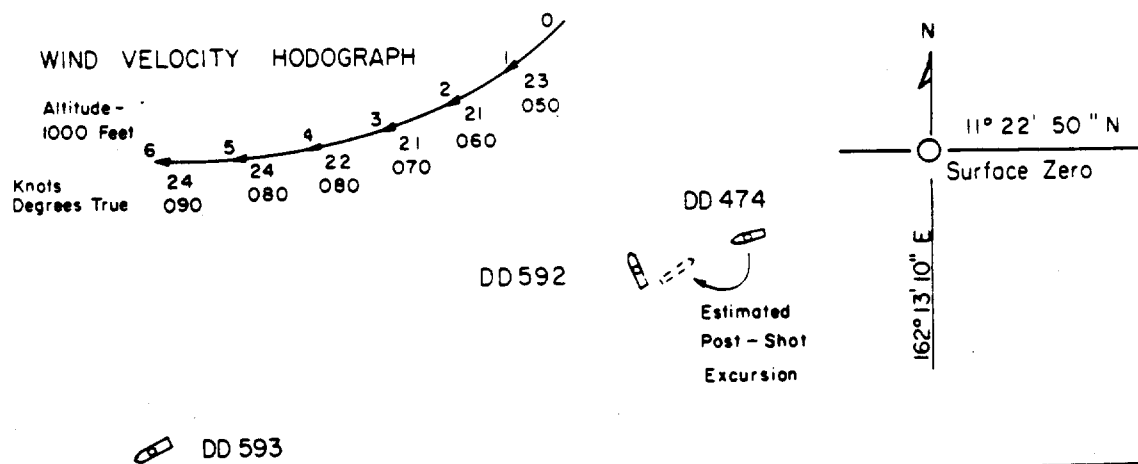
WIND VELOCITY HODOGRAPH

Altitude –
1000 Feet

0

1 23
050

2 21
21 060

3
22 21 070
080

4

5
24 24 080
080

6

Knots
Degrees True   090

N

11° 22' 50 " N
Surface Zero

162° 13'10" E

DD 474

DD 592

Estimated
Post – Shot
Excursion

DD 593

Ship	True Bearing of Ship from SZ	Distance from SZ	Relative Bearing of SZ from Ship
	Degrees	Feet	Degrees
DD 474	245.7	1900	170.6
DD 592	248.5	3000	94.1
DD 593	249.2	7900	186.6

Figure 2.2 Target ship array. Shot Umbrella.

20

SHIELDED STATION, DIRECTION OF VIEW
UNSHIELDED STATION ON ALL DD'S
UNSHIELDED STATION ON DD592 ONLY
DECAY UNIT ON DD592 ONLY
INSTRUMENTED COMPARTMENT

4 ON TOP OF HOUSE

40 MM GUN MOUNT

PILOT HOUSE

O2 LEVEL

GALLEY

MAIN DECK

CREW'S QUARTERS   FIRE ROOM   CREW'S MESS

ENGINE ROOM

FIRST PLATFORM   UPPER LEVEL   SECOND PLATFORM

FIRE ROOM   MAGAZINE

ENGINE ROOM

LOWER LEVEL   THIRD PLATFORM

Figure 2.3 Location and designation of GITR stations on target ships.

21

DD LONGITUDINAL
45°

A

A

$\frac{1}{8}$ IN. Al COVER

DETECTOR

SHOCK MOUNT

SEAL

CABLE TO RECORDER

4 IN. Pb SHIELD

FOUNDATION

DECK

SECTION A-A

SHIELDED GITR STATION

STBD
FANTAIL

DETECTOR

SHOCK MOUNT

Al STRUCTURE

0.1 IN. Al COVER
AND BASE

CABLE TO RECORDER

3 FT

3 FT

COMPARTMENT DECK

WEATHER DECK

UNSHIELDED GITR STATION
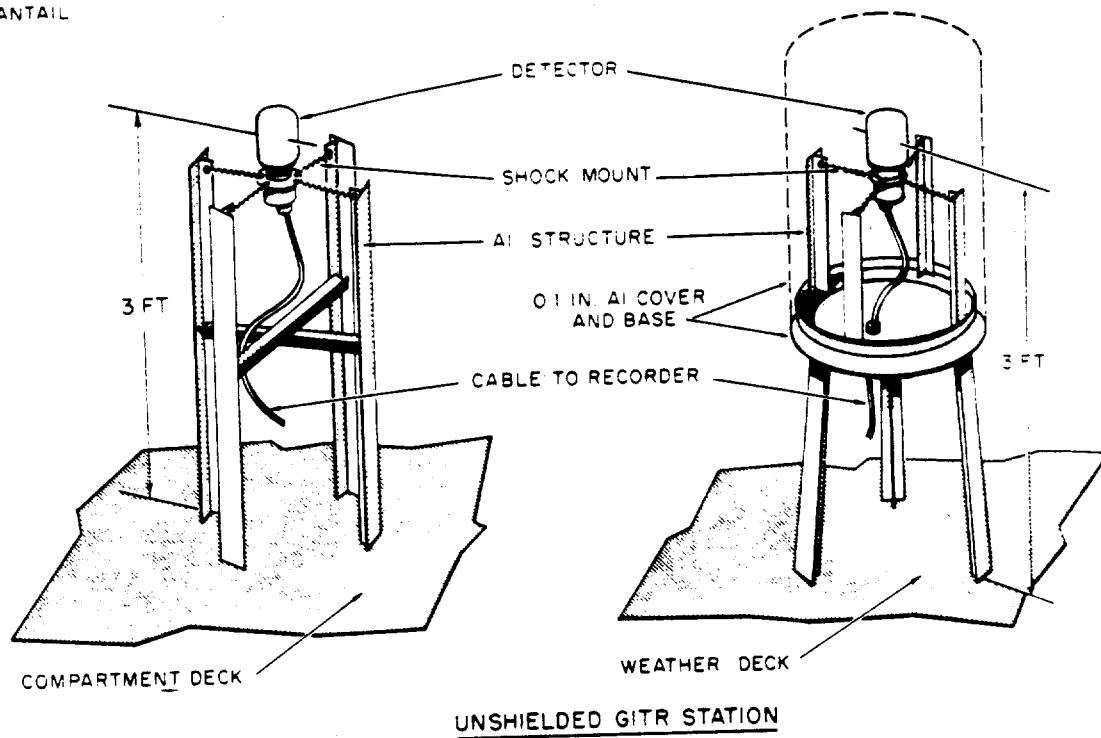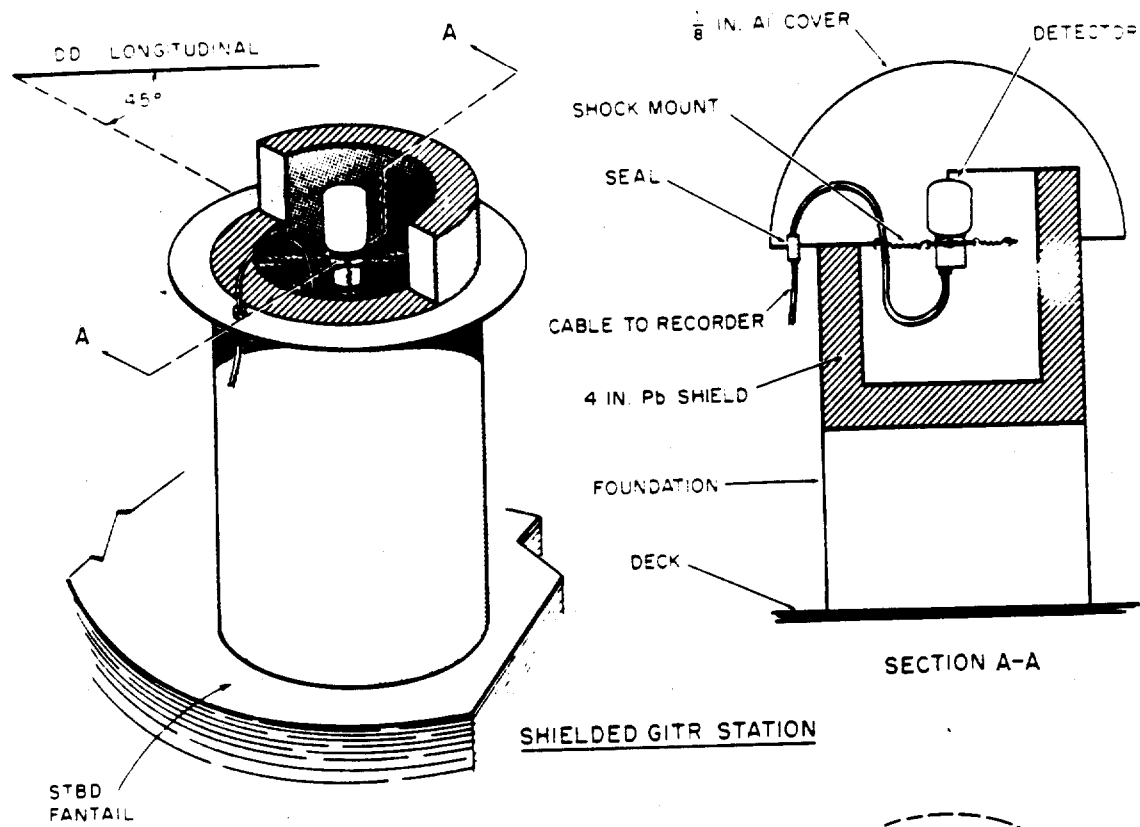
Figure 2.4 GITR detector foundations.

STRAP

RECORDER

DETECTOR CABLE

STARTING SIGNAL CABLE

SHOCK MOUNT FRAMES AND SPRINGS

GITR RECORDER FOUNDATION

RESERVOIR

PUMP

FREON COOLING UNIT

SHOCK MOUNT
FRAME & SPRINGS

DETECTOR

AI COIL

TYGON TUBING
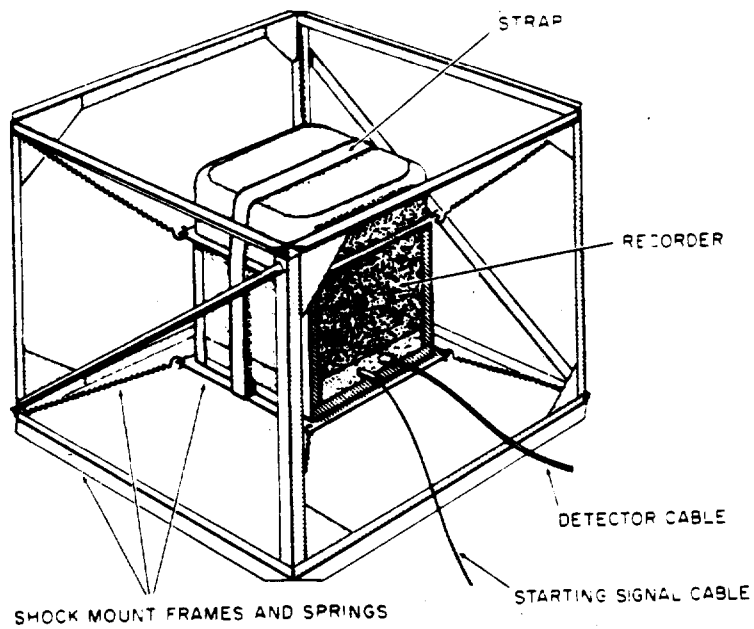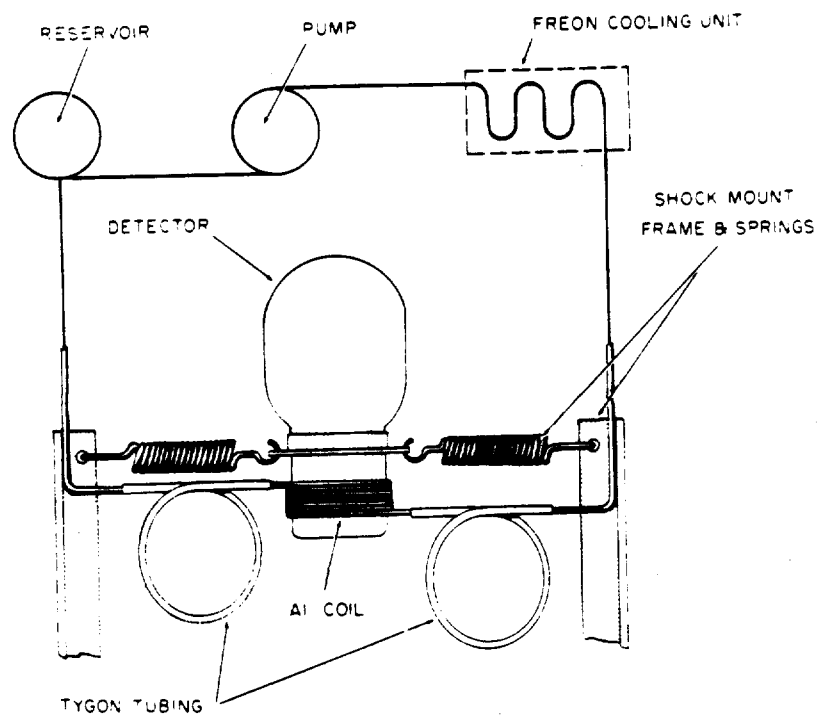
WATER COOLING INSTALLATION FOR GITR

Figure 2.5 GITR recorder and cooling installations.

23

Perforated Stainless Steel Tubing Around Rim

Collecting Tray

Stainless Steel Tubing

MODIFIED NRDL
OPEN-CLOSE COLLECTOR

Starting Signal Cable

Air Supply

Timer

Solenoid Valve

Sliding Lid Shown Open

Air Pressure Line

Steel Container

One Liter Polyethylene Bottle — 750cc of Concentrated HCL

Tygon Tubing

Flexible Conduit Shield

Overflow Tube

Drain in Conduit

GITR Detector Head

Polyethylene Sample Container Surrounding Detector — Shock Mounted

6-INCH-THICK LEAD CAVE

Figure 2.7 Gamma-ionization decay unit.

Winch & Release Mechanism

¼ Inch Diameter Wire Rope

Boom

Starting Signal Cable

Fantail

Instrument Container

Ballast

HOISTING DIAGRAM

Seal

Lid

Starting Signal Cable

GITR Case

Expanded Polystyrene

Detector

Recorder

INSTRUMENT CONTAINER
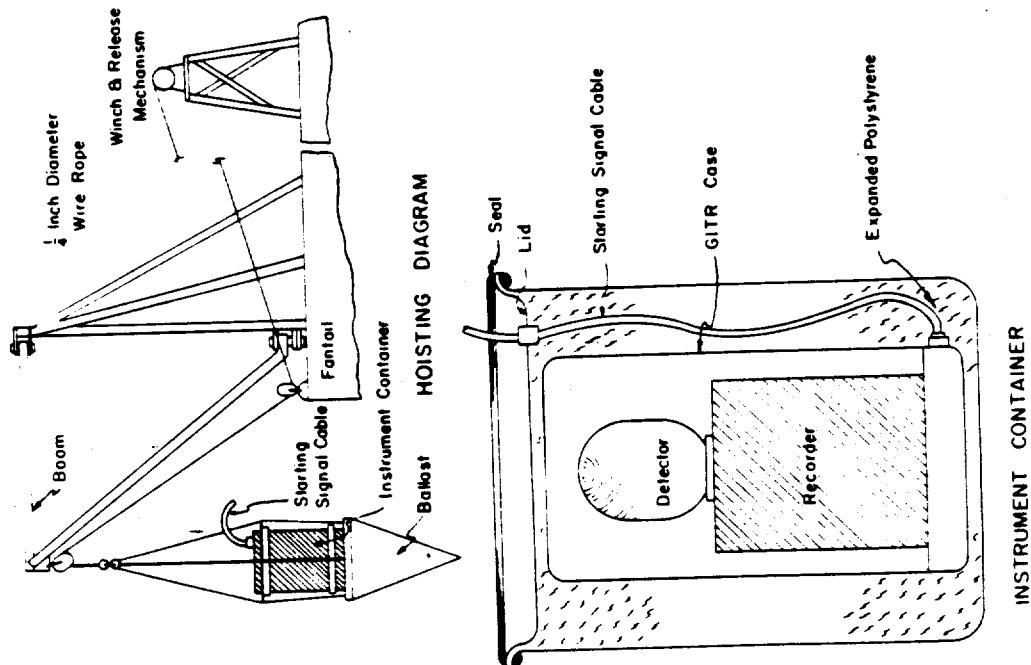
Figure 2.6 Underwater GITR station.

24
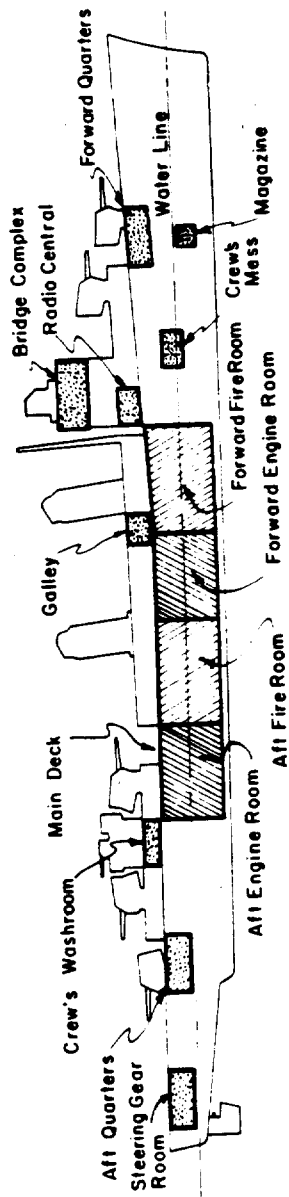
Figure 2.8 Area locations of film badges on target ships.

Chapter 3

RESULTS AND DISCUSSION

After Shot Wahoo, GITR data was obtained only on DD 593, because power failures on the other two ships prevented receipt of the radio timing signals. After Shot Umbrella, GITR data was obtained on all three ships, although some data was lost because of shock damage to several instruments; in addition, the majority of the GITR's were manually started at H−3 hours to circumvent possible repetitions of power failure. The manual starts created some uncertainty in the timing of most records, and as a consequence caused laborious time correlation of dose-rate curves with those few records obtained from radio-started stations.

3.1 TOTAL DOSES AND DOSE RATES ABOARD TARGET SHIPS

Detailed tabulations of film-badge and GITR data are presented in Appendixes C and D.

3.1.1 Weather-Deck GITR Data. After Shot Umbrella, the peak weather-deck dose rates on DD 592 and DD 474 exceeded the normal capacity of the GITR detectors, i.e., the detectors were temporarily saturated. To fill the resulting gaps in the averaged weather-deck data for these saturation periods, data from several unsaturated interior GITR stations were normalized to fit the averaged weather-deck dose-rate curves on both sides of the gap. The interior GITR stations (which supplied the data used for normalization) were selected on the basis of similarity in the shape of the candidate dose-rate curve with that of the averaged weather-deck dose-rate curve in the vicinity of the gap. With this criterion, two sets of normalized data (used consecutively) were required to close the gap in the averaged weather-deck dose-rate curve for DD 474 (Figure 3.1). Estimates of average weather-deck dose were obtained by numerical integration of the filled-in dose-rate curves.

Averaged values of the total dose rates and doses on the washed weather decks of the target ships (and estimates of the standard errors) are presented in Figures 3.2 through 3.5 as functions of time. The averages for DD 593 (both shots) do not include the data from GITR Station 1; the data appeared to be anomalously high when compared to the data from the other weather-deck stations. No reason could be found for this apparent anomaly, although the data and calibrations were rechecked. If the data from Station 1 were included, the average doses and dose rates for the weather-deck areas on DD 593 would be about 1.3 times higher than shown in Figures 3.2 through 3.5.

Figures 3.2 and 3.3 compare the weather-deck radiation histories of the three ships for Shot Umbrella. The dose curves show the rapid buildup of dose aboard the two close-in ships.

Because radiation histories for Shot Wahoo were obtained only on DD 593, the averaged data from the weather-deck stations on DD 593 for both shots are presented in Figures 3.4 and 3.5 to permit comparisons of effects at similar distances from surface zero (i.e., 7,900 feet for Shot Umbrella and 8,900 feet for Shot Wahoo). The curves (Figure 3.5) show that the dose for

26

Shot Wahoo eventually reached a value about four times that for Shot Umbrella even though the dose was accumulated more slowly and the ship was 1,000 feet farther from surface zero.

The very-early dose-rate peaks evident only on the DD 474 and DD 592 curves of Figure 3.2 (during the time period between 0.5 and 6 seconds after Shot Umbrella) occur at the same time for both ships. This indicates the existence of some radiation source which did not move horizontally: however, the shapes of the dose-rate curves do not appear to correlate with the size-versus-time relationships of the plume at surface zero (References 8 and 9). The doses from the above-mentioned very-early radiations were too low to be of any significance; the values observed on the weather decks were approximately 0.13 r on DD 474 and 0.03 r on DD 592. The very-early radiation was not detected on DD 593 for either shot, and there is no data available to indicate whether such radiation was received on DD 474 and DD 592 after Shot Wahoo.

The time sequences of the major dose-rate peaks which follow the very-early peak appear to depend upon the distances of the ships from surface zero (Figure 3.2), thereby indicating that radiation sources were moving horizontally during these later time periods. This is borne out by Reference 7, which suggests that there is a correlation between the shapes of the dose-rate curves and the movements of the visible base surge or cloud for both shots as determined from timed aerial photographs. Such a correlation would be consistent with the results of Section 3.2 in which it is estimated that more than 95 percent of the dose observed on the weather decks was due to remote-source radiation.

3.1.2 Compartment GITR Data. The dose-rate and dose data for the various compartments are tabulated in Appendix D.

Table 3.1 presents gamma doses accumulated within 24 hours after the shots. That part of the dose which was accumulated in the period later than 90 minutes after shot was estimated by: (1) using the dose rates at 90 minutes after shot; (2) assuming that these dose rates would decay as indicated in Figure 3.42; and (3) integrating the resulting dose-rate curves with respect to time. As an estimate of how the average dose in a compartment is related to the GITR dose data, Table 3.1 also presents location-bias factors, which were obtained by averaging all available ratios of average film-badge dose in the compartment to film-badge dose at the GITR station. The locations of the various compartments and stations are shown in Figure 2.3.

The gross relationships, i.e., ratios, of the gamma dose or dose rate in various compartments to the averaged dose or dose rate on the washed weather decks are presented as functions of time in Figures 3.6 through 3.36. It is important to note that these ratios may not necessarily be good measures of the penetrability of ship structures by radiation from exterior radiation-sources for two reasons: (1) the radiation inside some compartments may have been influenced by radiation sources that were inside the ship (Section 2.1, Table 3.2, and Reference 6); and (2) various weather-deck GITR stations may have been shielded by intervening structures whenever remote radiation sources were not directly overhead. This may explain why Figures 3.10, 3.17, 3.18, 3.26, 3.33, and 3.35 show radiation in some compartments to be higher than that on the weather deck during periods preceding possible contaminant ingress. The principal reason for presenting the ratios was to show the variations in the relationship between the radiation inside the ships and the average radiation observed on the weather decks as functions of time.

The ratios of dose in compartment to averaged dose on deck, presented in Figures 3.6 through 3.18, show some fairly consistent trends. There are relatively large variations in the ratios during the time period preceding the major-peak dose rate. This can be attributed principally to the changing radiation-source geometries which probably altered the radiation fields at both interior and exterior GITR stations to an extent depending upon the shielding afforded by structures between the sources and the detectors. For the time period following the major-peak dose rate, by which time most of the dose has been accumulated, most of the dose ratios remain fairly

constant except for a few cases which show significant increases at later times. These increases in dose ratios at late times occur only for stations which are among those listed in Table 3.2 as being probably affected by ingress of contaminants into the ships.

As compared to the ratios of dose shown in Figures 3.6 through 3.18, the ratios of dose rate shown in Figures 3.19 through 3.36 show considerably more variation. This is to be expected because, once most of the dose has already been received, relatively large instantaneous changes in the dose rate may have little effect on the accumulated dose.

For many of the compartments listed in Table 3.2, the dose-rate ratios show significant peaks during the time period following the last major-peak dose rate for both shots and during the time period between the two major-peak dose rates for Shot Umbrella. Most of the above-mentioned effect is attributed to the presence of contaminants inside the ship. Other variations in the dose-rate ratios for all compartments were probably due to changing remote-radiation-source geometries and possibly due to effects from contaminated water surrounding the ships during periods when radiation from other sources was low (see Figure 3.31 for dose-rate ratios based upon the data from the underwater Station 15).

3.1.3 Film-Badge Data.

Averages of the 24-hour gamma doses aboard the target ships are shown in Table 3.3. Film-pack data from Project 2.3 (Reference 7) are included in the table. The locations of the various compartments are shown in Figure 2.8. The locations and data from individual film-badge stations are presented in Appendix C. In general, the Project 2.3 film-pack doses are significantly lower than the Project 2.1 film-badge doses for the weather-deck areas. This may be due to differences in film, in processing control, and possibly in calibration and read-out technique. Some of the Project 2.1 film-badge data from Shot Umbrella for the DD 474 appears to be anomalously low when compared to the data for DD 592; the GITR data indicates that the doses on DD 474 should be significantly higher than the doses on DD 592. The data was rechecked and the badges were reexamined, but no reasons for the anomalies could be determined.

For Shot Wahoo, most of the film-badge stations were exposed to doses in excess of 500 r aboard DD 474, 200 r aboard DD 592, and 90 r aboard DD 593. For Shot Umbrella, the doses were lower although the ships were from 1,000 to 2,000 feet closer to surface zero; but DD 474 and DD 592 were still exposed to doses in excess of 200 r in many compartments, whereas aboard DD 593 the doses in all compartments were less than 45 r.

Ratios of averaged gamma dose in various compartments to the averaged dose on the weather decks of DD 592 and DD 593 are presented in Table 3.4. Ratios for DD 474 are not presented, because the average dose on the weather decks could not be determined for Shot Wahoo, and because the film-badge data for Shot Umbrella was considered to be unreliable. For each compartment, the several dose ratios are in very good agreement so that reliable averages could be determined. The film-badge dose ratios range between 0.36 and 0.56 for compartments on or above the main deck, 0.14 and 0.46 for nonmachinery compartments below the main deck, 0.11 and 0.20 for machinery spaces above the waterline, and 0.019 and 0.068 for machinery spaces below the waterline. Note that the possible limitations of the GITR dose ratios that were discussed in Section 3.1.2 should also apply to the film-badge dose ratios.

As a rough indication of dose distribution, the doses observed in each athwartship, i.e., transverse, third of various compartments were averaged and presented in Tables 3.5 through 3.7. In wide compartments there was a tendency to have lower doses in the center, presumably because of shielding afforded by the superstructure. Another indication of nonuniform dose distribution in some compartments is the location-bias factor presented in Table 3.1 and discussed in Section 3.1.2.

The available comparisons of GITR and film-badge doses at the GITR stations are presented in Table 3.8. The ratios of GITR dose to film-badge dose range between 0.72 and 1.46 and have an average value of 0.96 with a standard deviation of 0.14. Comparisons of GITR and film-badge ratios of dose at GITR stations to average dose on the weather decks are presented in Table 3.9. The ratios of GITR dose ratio to film-badge dose ratio range between 0.76 and 1.21 and have an

28

average value of 1.02 with a standard deviation of 0.11. These comparisons show that, with few exceptions, there is good agreement and apparently no bias between results obtained from GITR and film-badge dose data.

3.2 REMOTE-SOURCE GAMMA RADIATION

The directionally shielded GITR Station 14 was designed to permit discrimination between remote-source radiation and high backgrounds of radiation from deposited contaminants. However, examination of the data indicated that the background of radiation from contaminants on the washed weather decks was so low that the differences between remote-source and total radiation were smaller than the probable errors in the radiation measurements. This led to the following approach for estimation of the remote-source-radiation contribution to the total radiation observed on the washed weather decks.

The basis for the estimation technique was examination of the decay-corrected plots of the average total dose rates on the weather decks, which are presented in Figures 3.37 through 3.40. Measured decay data were available for the period later than 6 minutes after Shot Umbrella (Section 3.4). For Shot Wahoo and for the period earlier than 6 minutes after Shot Umbrella, estimated probable limits for the unknown decay curve were based upon: (1) the calculations of gamma dose-rate decay for unfractionated fission products (Reference 10); and (2) straight-line extrapolation on the log-log plot of the measured gamma dose-rate decay shown in Figure 3.42. The following discussion requires the assumptions that some undetermined decay-corrected dose-rate curve can represent the buildup of contaminants on the ships' weather surfaces; and that this unknown curve always had either zero or positive slopes during the period of interest, even though the decks were continuously washed (Reference 3 indicates that the major value of washdown is the continuous suppression of contaminant buildup). Consider the above assumptions and refer to Figures 3.37 through 3.40. The minima between the two major peaks of the Shot Umbrella curves can certainly be considered to be upper limits of the decay-corrected dose rate from fallout deposited on the weather surfaces of the ships at the indicated times, because even if no radiation was contributed by airborne radioactivity (which may not have been the case) the contribution from deposited fallout could not be greater than the total. For similar reasons, those portions of the curves which tend to level off after the last major peak for either shot can also be considered upper limits of decay-corrected dose rates from deposited radioactivity, especially if there was a significant drop in the decay-corrected dose rate after the nearly horizontal portion of the curve. Therefore, if the assumption of a continuously increasing buildup of contaminants is valid, it follows that overestimates of the contribution by deposited contaminants to the decay-corrected dose rates can be represented by the horizontal lines labeled as such in Figures 3.37 through 3.40. These decay-corrected estimates were converted to dose rates that were integrated to obtain upper limits of the estimated dose contributed by deposited contaminants for each assumed decay curve.

The estimated doses contributed by remote-source radiation to the total doses observed on the washed weather decks of the three target ships, based upon the above-mentioned approach, are presented in Table 3.10. These values indicate that at least 95 and 98 percent of the total dose observed on the washed decks was due to remote-source radiation resulting from Shots Umbrella and Wahoo, respectively. As a consequence, the observed total-radiation data can adequately represent the remote-source radiation for the washed weather-deck areas during the first 10 minutes after shot. Unfortunately, there was no data available from which it would have been feasible to estimate the percent contribution of the remote-source radiation to the total dose for unwashed weather decks.

3.3 TOTAL GAMMA RADIATION IN ADJACENT WATER

The attempt to measure the radiation in the water adjacent to the target ships was not succussful. No data was obtained for Shot Wahoo, because the starting signals were not received

on the only two target ships that were instrumented (the instrument on DD 593 had been canni-balized at the last minute to replace a burned out solenoid on one of the closer ships). Because the dropping mechanism for GITR Station 15 proved unreliable, the underwater radiation de-tectors were submerged in the water prior to Shot Umbrella in the hope that some data would be obtained; however, the instruments on DD 474 and DD 592 were damaged by shock. Conse-quently, the only data obtained was from DD 593 after Shot Umbrella.

The tabulated radiation data obtained from the underwater GITR on DD 593 for Shot Umbrella is presented in Appendix D. During the period when the ship was enveloped by the base surge, the peak dose rates   are attributed to contaminants depositing in the water and possibly to con-taminants washed off the ship. Following this period, the underwater dose rates were very low until   6.4 hours after shot,   This late resurgence of underwater radiation is attributed to a patch of contaminated water (detonation debris originally upwelling at surface zero) drifting down upon DD 593.

Figure 3.41 presents ratios of dose rate in the water to average dose rate on the washed weather decks of DD 593 after Shot Umbrella. Three curves were constructed because of a possible uncertainty of 30 seconds in the timing. The results for all three possibilities show that the underwater dose rates were less than 0.2 percent of the washed-weather-deck dose rates during the periods when the ship was enveloped by the base surge and were no more than 20 percent of the washed-weather-deck dose rates during the later periods when the deck dose rates were very low. Therefore, although the contaminated water did not contribute signifi-cantly to the gamma dose observed on DD 593 after Shot Umbrella, the radiation from the water may have influenced the dose-rate ratios to a significant degree at later times.

3.4 GAMMA-IONIZATION DECAY

No data on gamma-ionization decay was obtained for Shot Wahoo, because the starting signal was not received. The gamma dose-rate data from the decay unit (GITR Station 22) aboard DD 592 after Shot Umbrella is presented in Appendix D.

Logarithms of the relative gamma dose rates are plotted as a function of logarithms of the time-after-shot in Figure 3.42. The decay curve was also separated into segments fitted to an equation of the form

$$\text{Dose rate} = \text{constant} \times (\text{time})^n$$

The exponents n were evaluated for various time intervals and are represented by the slopes of the log-log curve shown in the figure. Standard regression techniques were applied to the logarithmic variables to obtain the slopes and their 95-percent confidence limits.

The background of external radiation affecting the dose rates inside the 6-inch-thick lead cave was estimated to be negligible for the time periods under consideration. The estimate was based upon use of: (1) gamma energy variations listed in Reference 10; (2) gamma-radiation ab-sorption coefficients and buildup factors from Reference 11; and (3) monodirectional attenuation equations applied to the average deck-dose rates.

TABLE 3.1 TWENTY-FOUR-HOUR GAMMA DOSES AT GITR STATIONS, BASED UPON GITR DATA

Dose in roentgens.

Compartment	GITR Station	Shot Wahoo DD 593	Shot Umbrella DD 474	DD 592	DD 593	Location-Bias Factor *
Weather decks †	1 through 4					0.99
Pilot house	5					1.15
Crew's mess	6					0.82
	7					0.98
Magazine	8					0.95
Galley	9					1.54
Forward fireroom	10					0.82
	11					1.35
Forward engine room	12					0.80
	13					1.38
Aft fireroom	17					0.77
	18					1.13
Aft engine room	19					1.23
	20					1.12
Aft quarters	21					

* The location-bias factor is the mean ratio of average film-badge dose in compartment to film-badge dose at GITR station.
† Doses for washed weather decks are averaged values.

TABLE 3.2 COMPARTMENTS PROBABLY INFLUENCED BY INGRESS OF RADIOACTIVE CONTAMINANTS

Compartment	GITR Station	Ship	Shot	Probable Source of Ingress
Galley	9	DD 592	Umbrella	Ventilation air
Forward fireroom	10 and 11	All	Umbrella and Wahoo	Boiler air (fired boiler)
Forward engine room	13	DD 474 DD 592	Umbrella	Condenser water (?)
Aft fireroom	17 and 18	DD 592	Umbrella	Boiler air (unfired boiler)
Aft engine room	19 and 20	DD 592	Umbrella	Ventilation air
Aft quarters	21	DD 592	Umbrella	Ventilation air

Page 32 deleted.

TABLE 3.16 ESTIMATED DOSE CONTRIBUTED BY REMOTE-SOURCE
RADIATION OBSERVED ON WASHED WEATHER DECKS
OF THE TARGET SHIPS

Ship	Shot	Remote-Source Contribution to Total Dose on Deck	
		At 15 min After Shot	At 2 hrs After Shot
		pct	pct
DD 474	Umbrella	97.2 *	96.6 *
		94.8 †	94.3 †
DD 592	Umbrella	97.5 *	97.0 *
		96.0 †	95.5 †
DD 593	Umbrella	96.5 *	96.1 *
		96.3 †	94.9 †
DD 593	Wahoo	99.4 *	98.1 *
		98.9 †	97.6 †

* Estimate based upon use of decay curve (Reference 10).
† Estimate based upon use of extrapolated measured-decay curve.

Figure 3.1 **Example of estimating average dose rates on deck**
of DD 474 for period of GITR saturation, Shot Umbrella.

36

Pages 37 through 40
deleted.

Figure 3.6 Ratios of dose in compartments to average dose on weather decks of DD 474, Shot Umbrella. Vertical bars indicate estimates of probable error.

41

Figure 3.7 Ratios of dose in compartments to average dose on weather decks of DD 474, Shot Umbrella. Vertical bars indicate estimates of probable error.

Figure 3.8 Ratios of dose in compartments to average dose on weather decks of DD 592, Shot Umbrella. Vertical bars indicate estimates of probable error.

43

Figure 3.9 Ratios of dose in compartments to average dose on weather decks of DD 592, Shot Umbrella. Vertical bars indicate estimates of probable error.

44

Figure 3.10 Ratios of dose in compartments to average dose on weather decks of DD 592, Shot Umbrella. Vertical bars indicate estimates of probable error.

45

Figure 3.11 Ratios of dose in compartments to average dose on weather decks
of DD 592, Shot Umbrella. Vertical bars indicate estimates of probable error.

Figure 3.12 Ratios of dose in compartments to average dose on weather decks of DD 592, Shot Umbrella. Vertical bars indicate estimates of probable error.

Figure 3.13 Ratios of dose in compartments to average dose on weather decks of DD 592, Shot Umbrella. Vertical bars indicate estimates of probable error.

48

Figure 3.14 Ratios of dose in compartments to average dose on weather decks of DD 592, Shot Umbrella. Vertical bars indicate estimates of probable error.

49

Figure 3.15 Ratios of dose in compartments to average dose on weather decks of DD 593, Shot Umbrella. Vertical bars indicate estimates of probable error.

Figure 3.16 Ratios of dose in compartments to average dose on weather decks of DD 593, Shot Umbrella. Vertical bars indicate estimates of probable error.
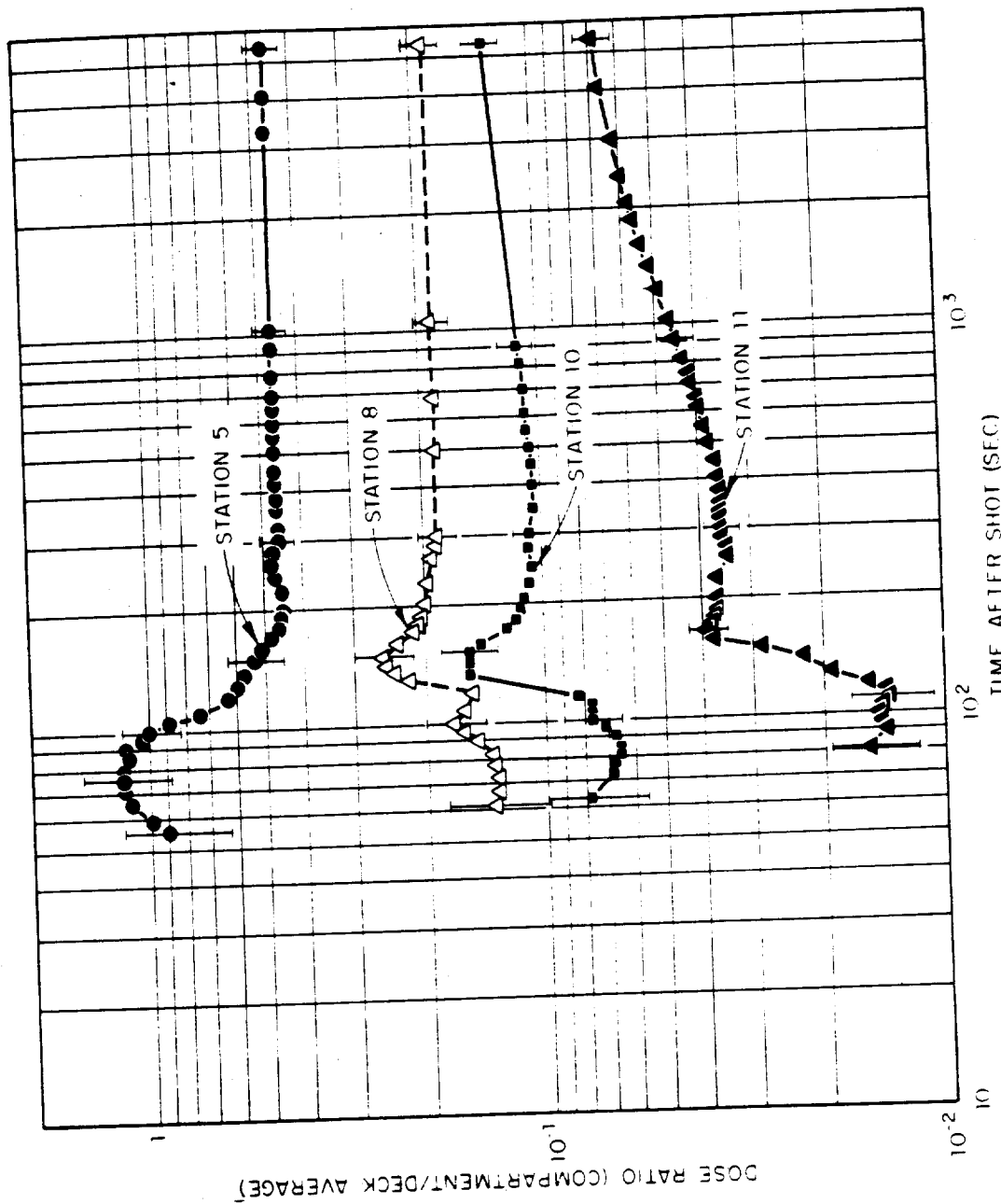
Figure 3.17 Ratios of dose in compartments to average dose on weather decks of DD 593, Shot Wahoo. Vertical bars indicate estimates of probable error.

52
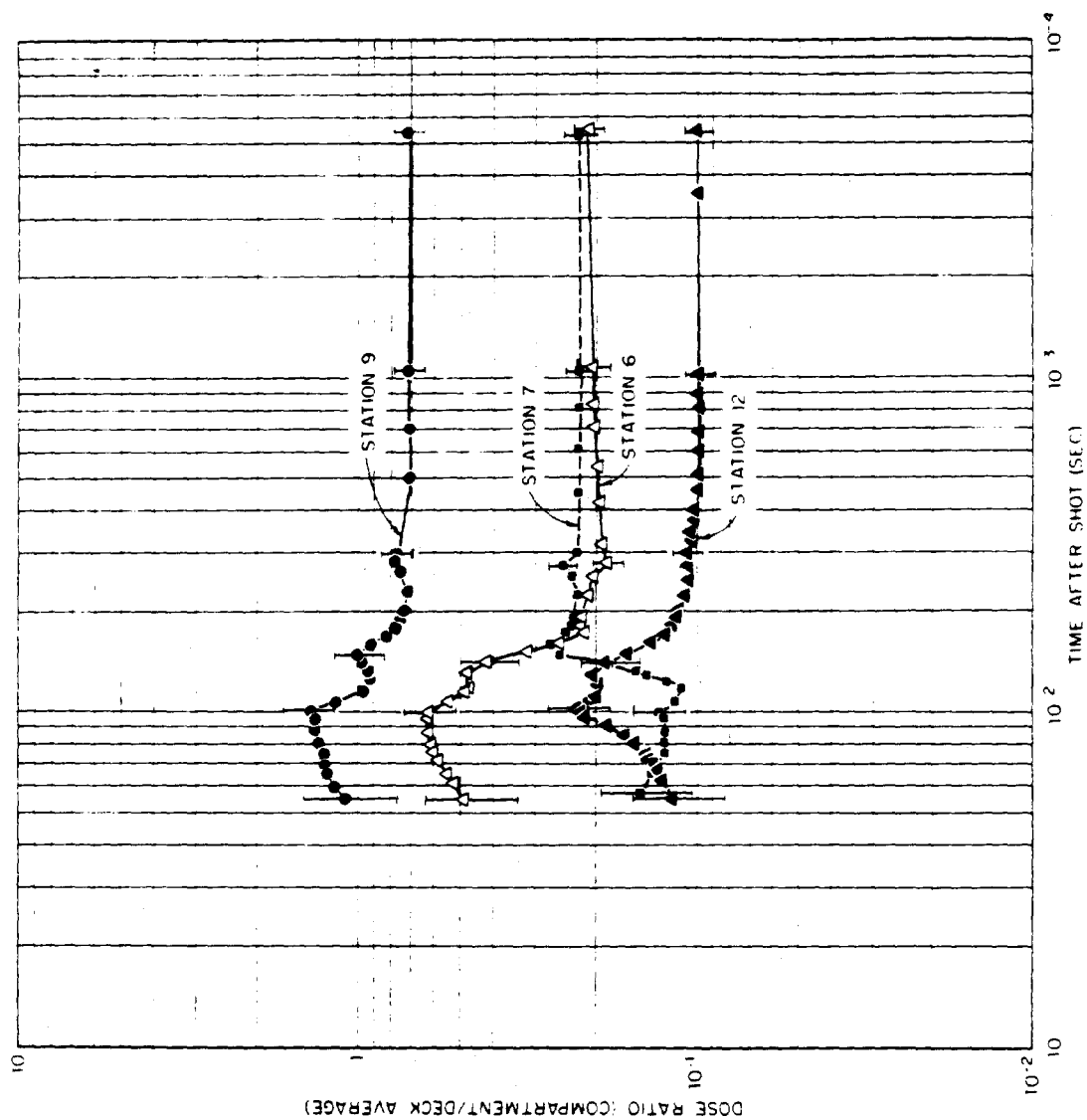
Figure 3.18 Ratios of dose in compartments to average dose on weather decks of DD 593, Shot Wahoo. Vertical bars indicate estimates of probable error.
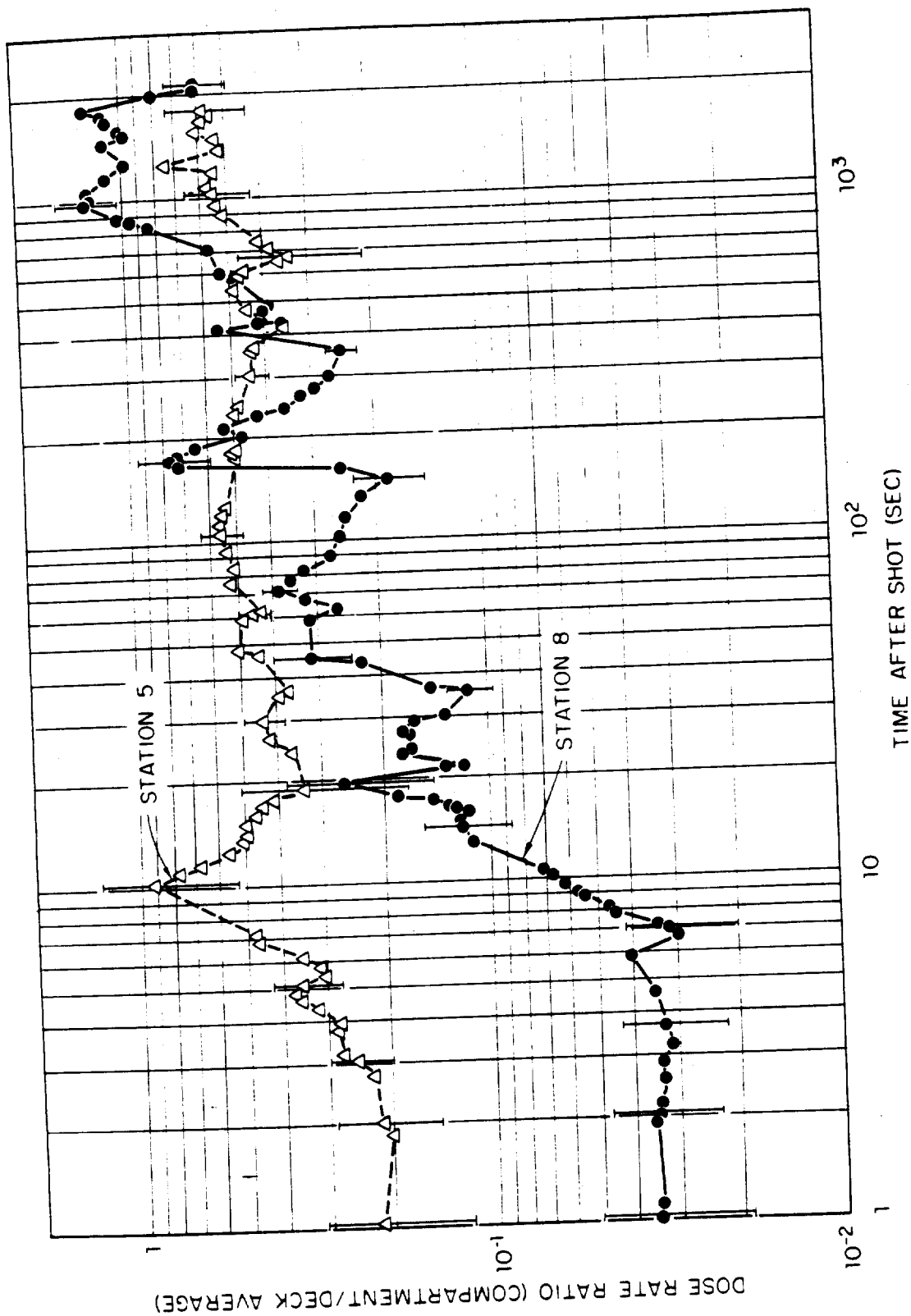
Figure 3.19 Ratios of dose rate in compartments to average dose rate on weather decks of DD 474, Shot Umbrella. Vertical bars indicate estimates of probable error.

54
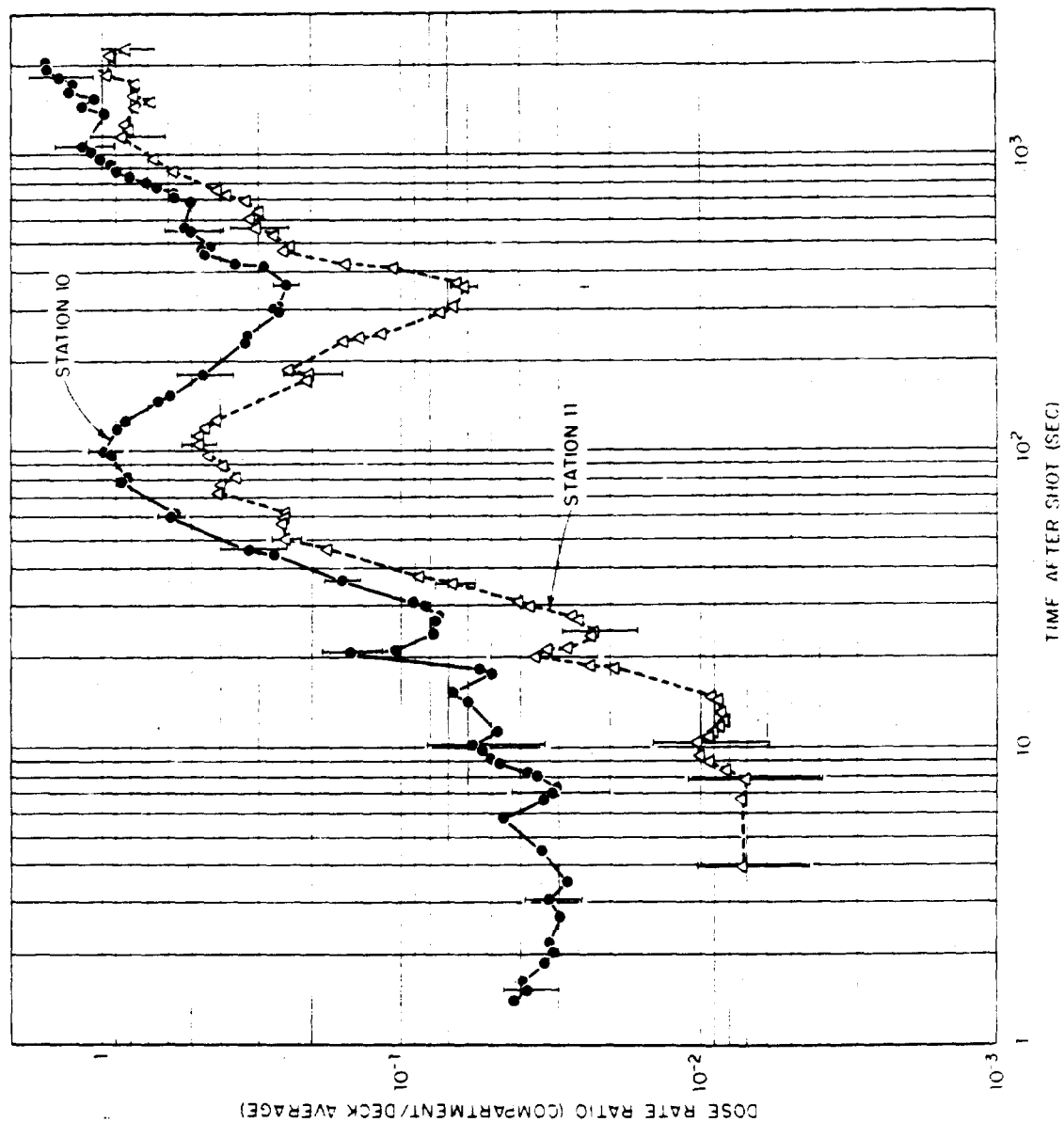
Figure 3.20 Ratios of dose rate in compartments to average dose rate on weather
decks of DD 474, Shot Umbrella. Vertical bars indicate estimates of probable error.

55
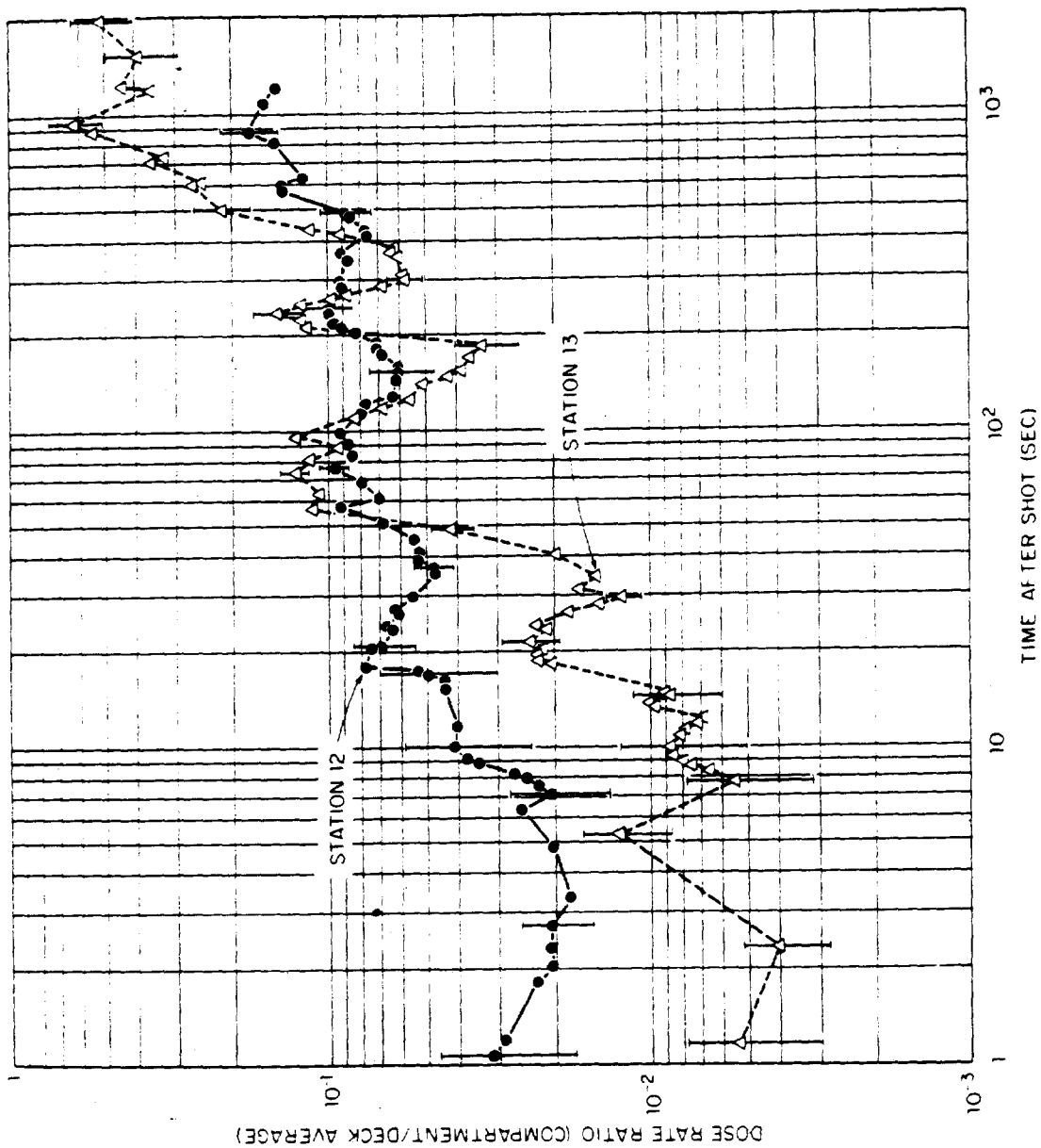
Figure 3.21 Ratios of dose rate in compartments to average dose rate on weather decks of DD 474, Shot Umbrella. Vertical bars indicate estimates of probable error.

56
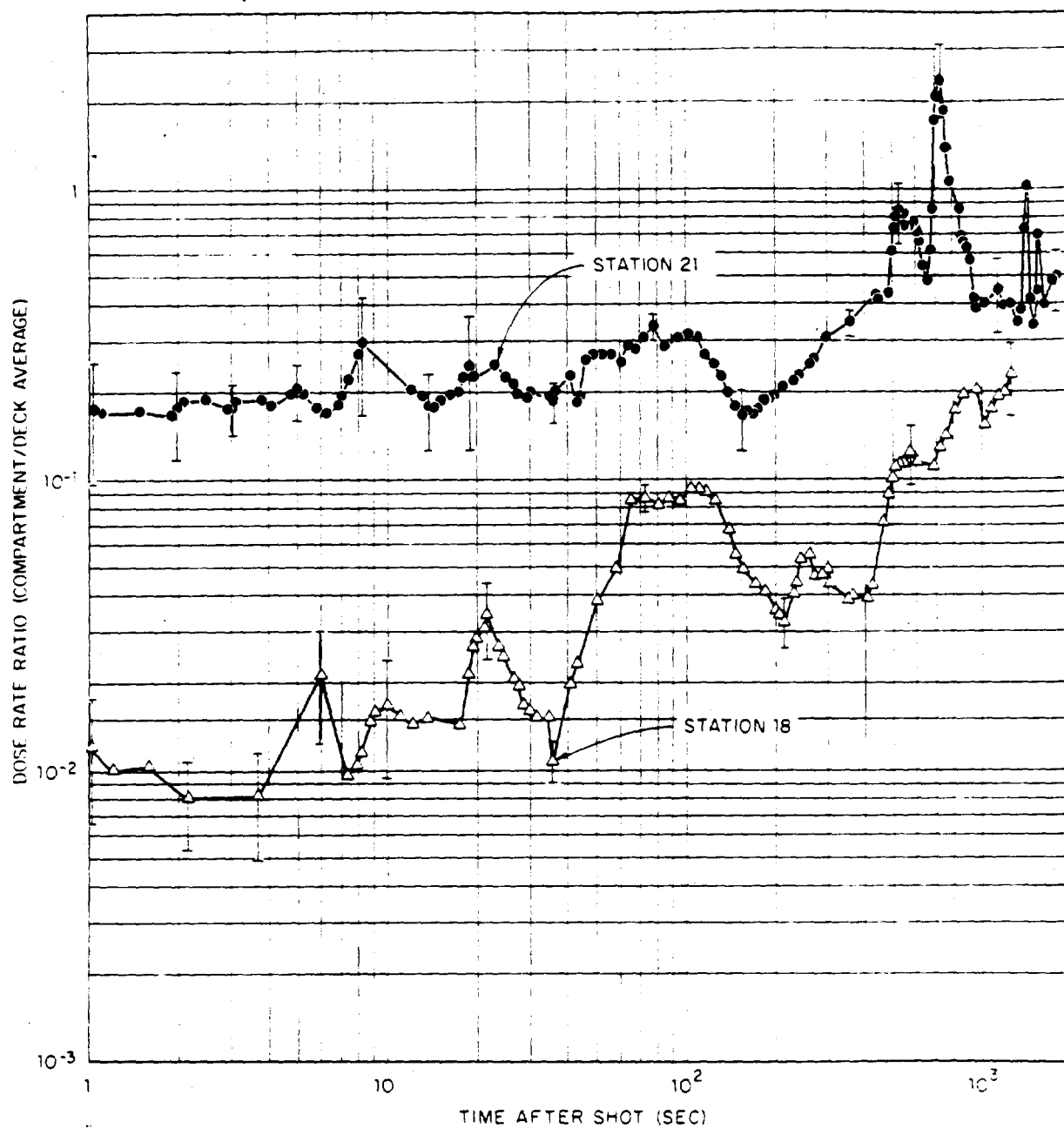
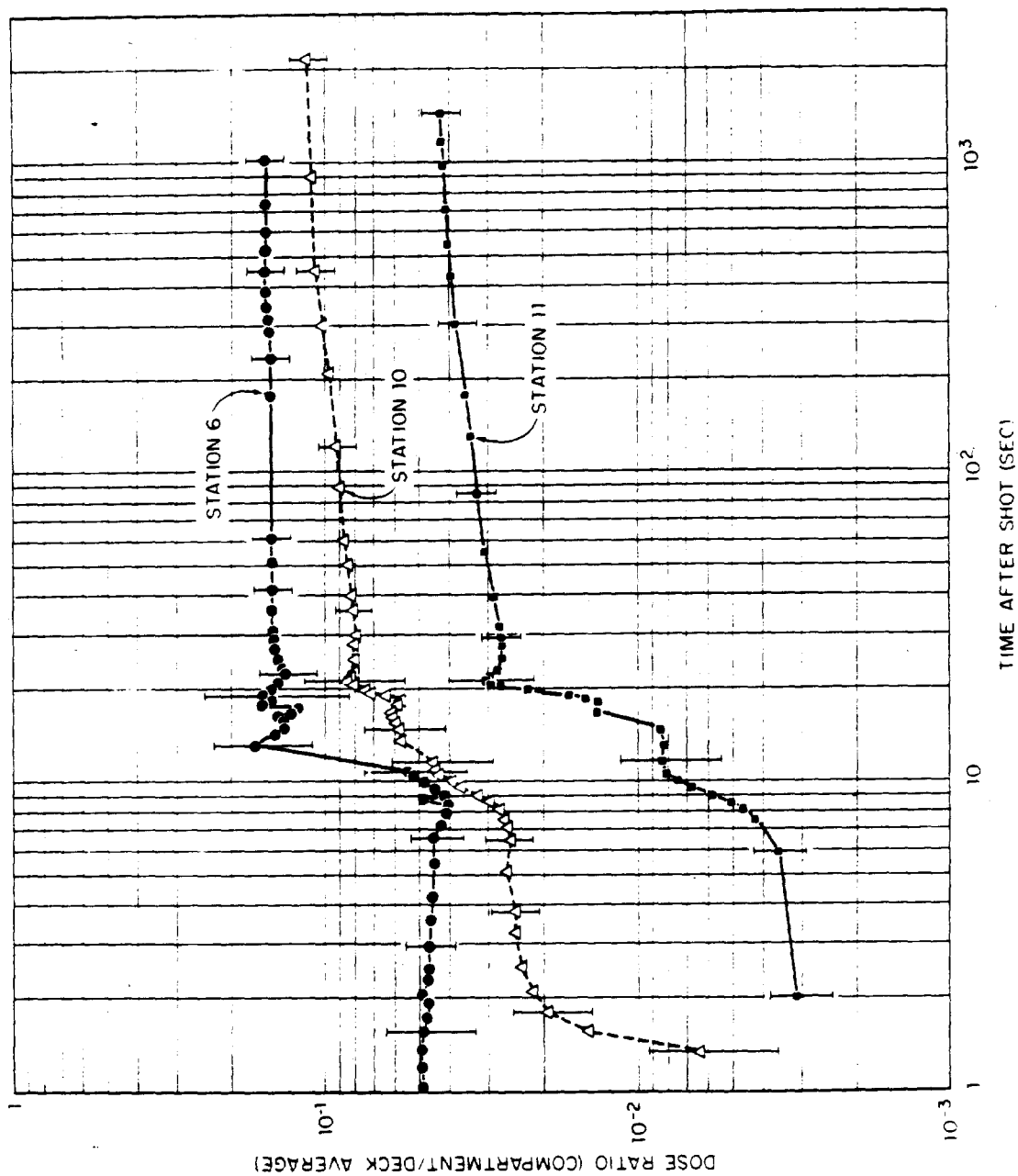Figure 3.22 Ratios of dose rate in compartments to average dose rate on weather decks of DD 474, Shot Umbrella. Vertical bars indicate estimates of probable error.
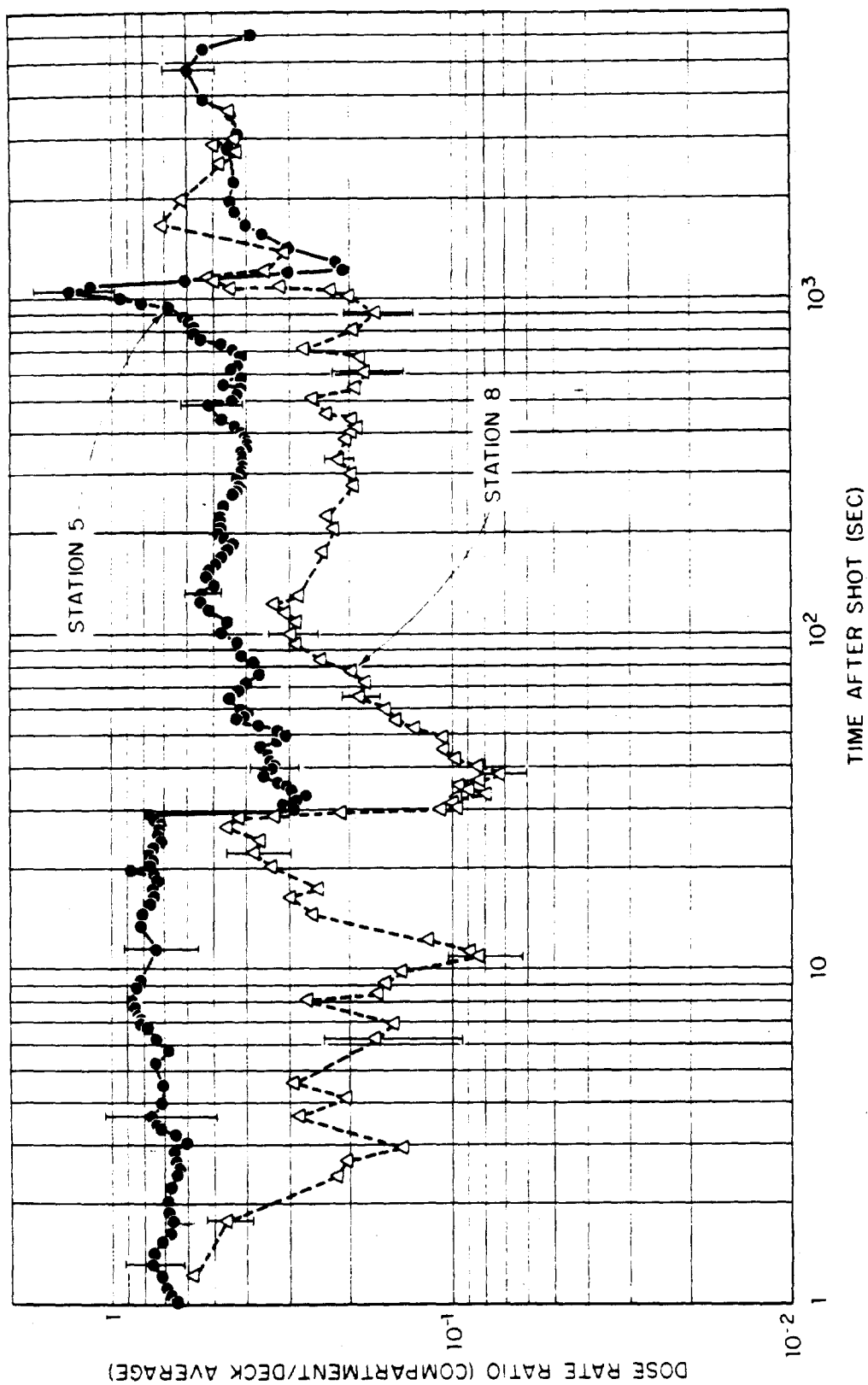
Figure 3.23 Ratios of dose rate in compartments to average dose rate on weather decks of DD 592, Shot Umbrella. Vertical bars indicate estimates of probable error.
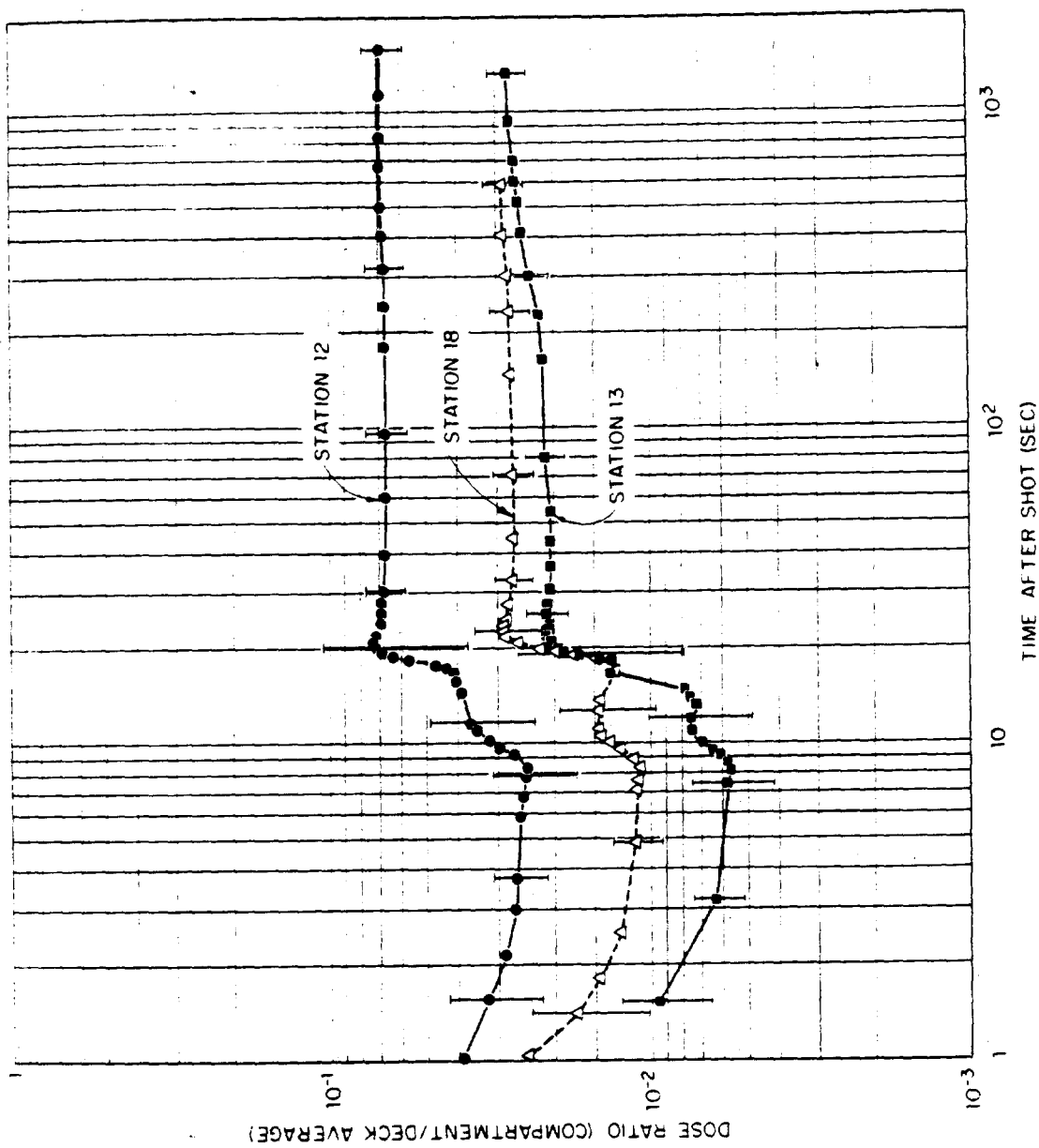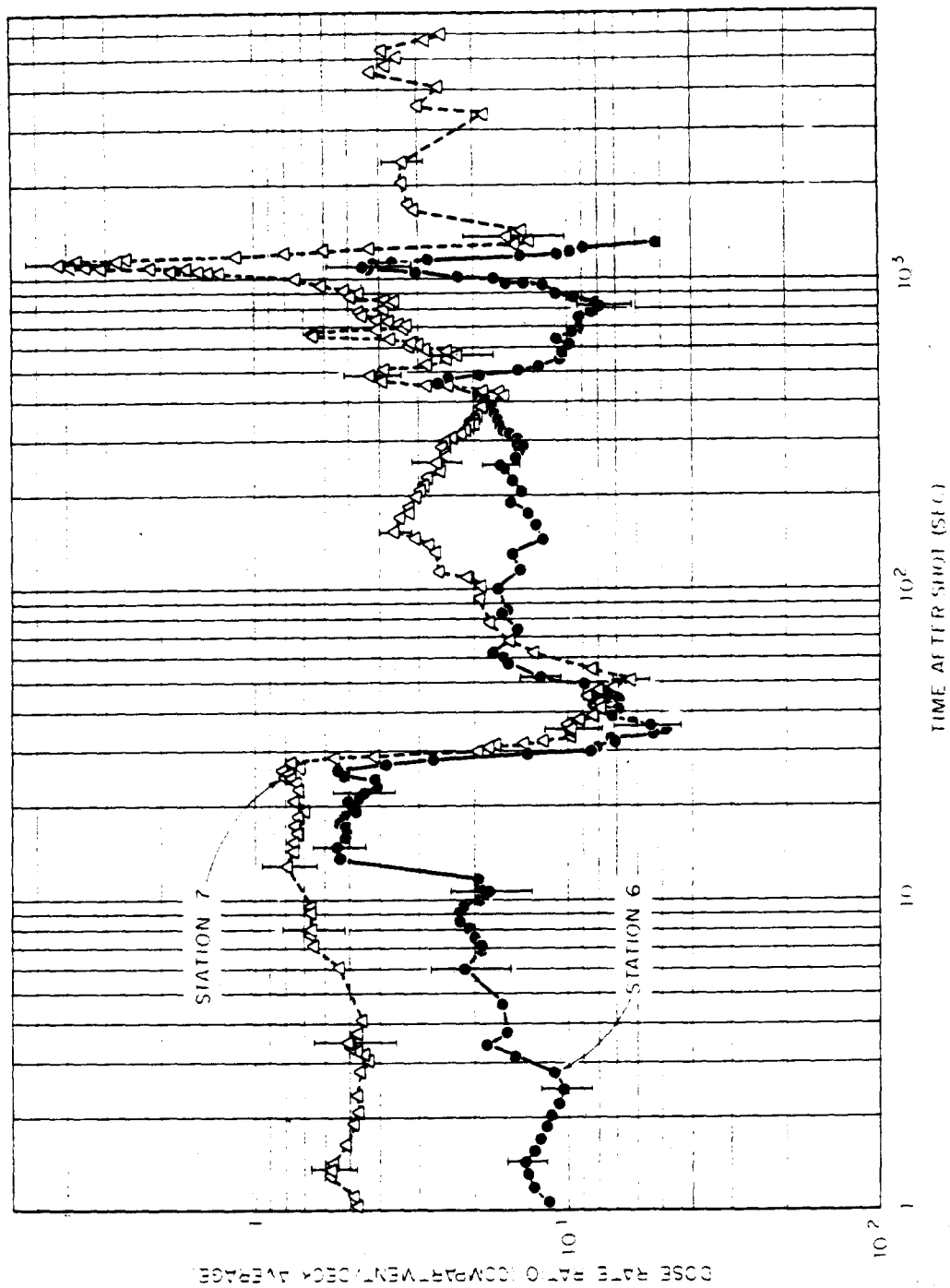
Figure 3.24 Ratios of dose rate in compartments to average dose rate on weather decks of DD 592, Shot Umbrella. Vertical bars indicate estimates of probable error.
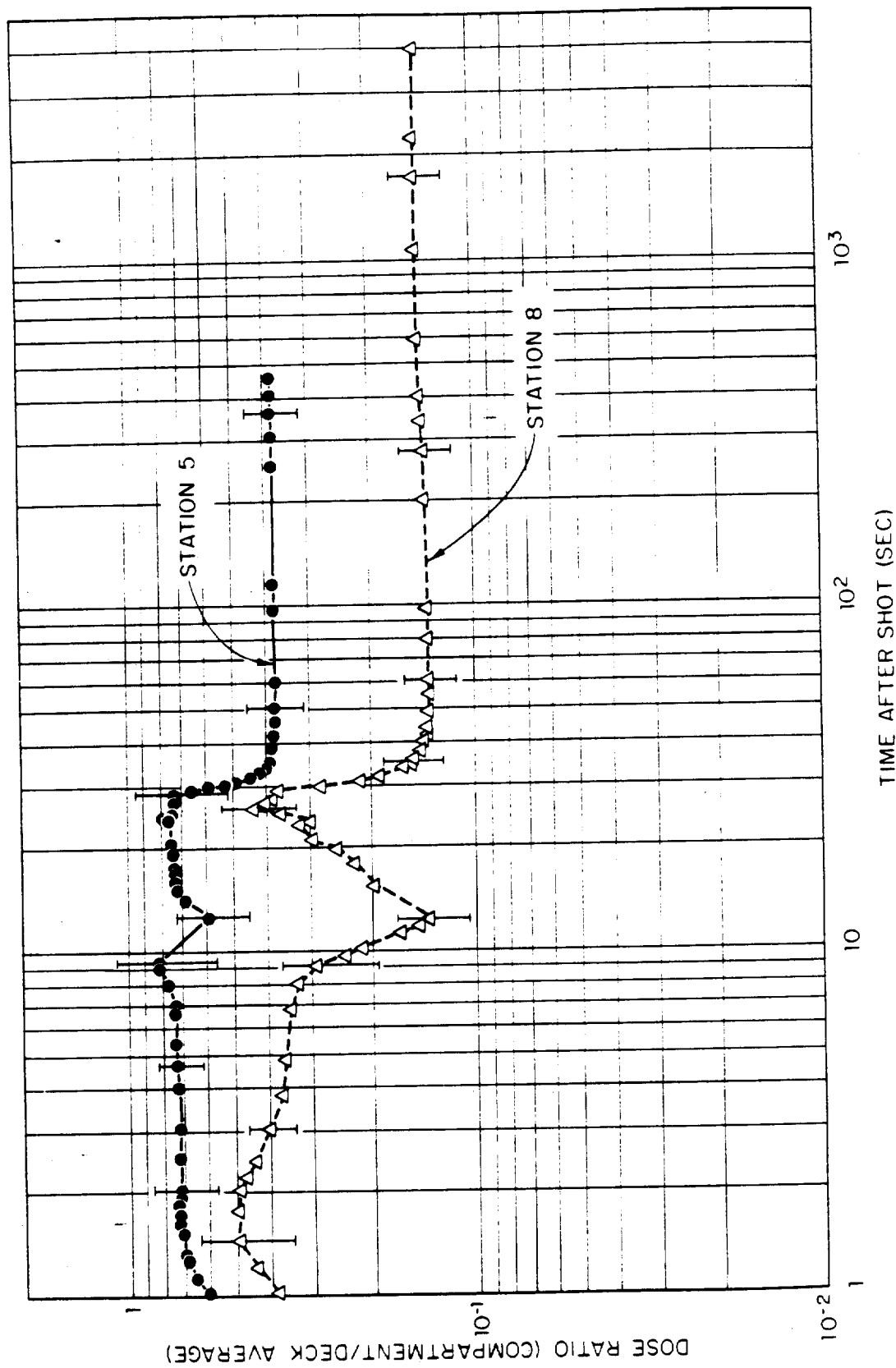
59
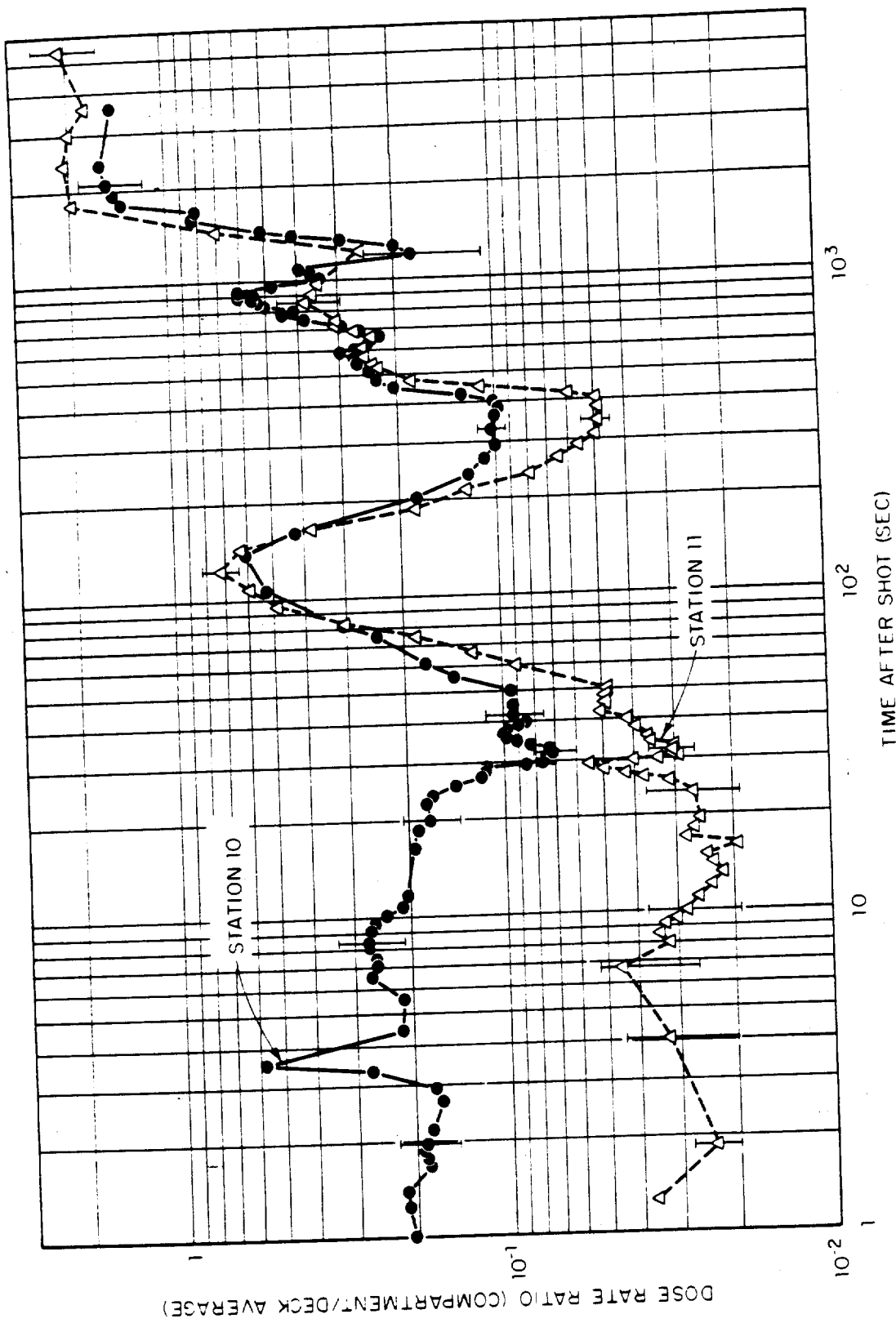
Figure 3.25 Ratios of dose rate in compartments to average dose rate on weather decks of DD 592, Shot Umbrella. Vertical bars indicate estimates of probable error.
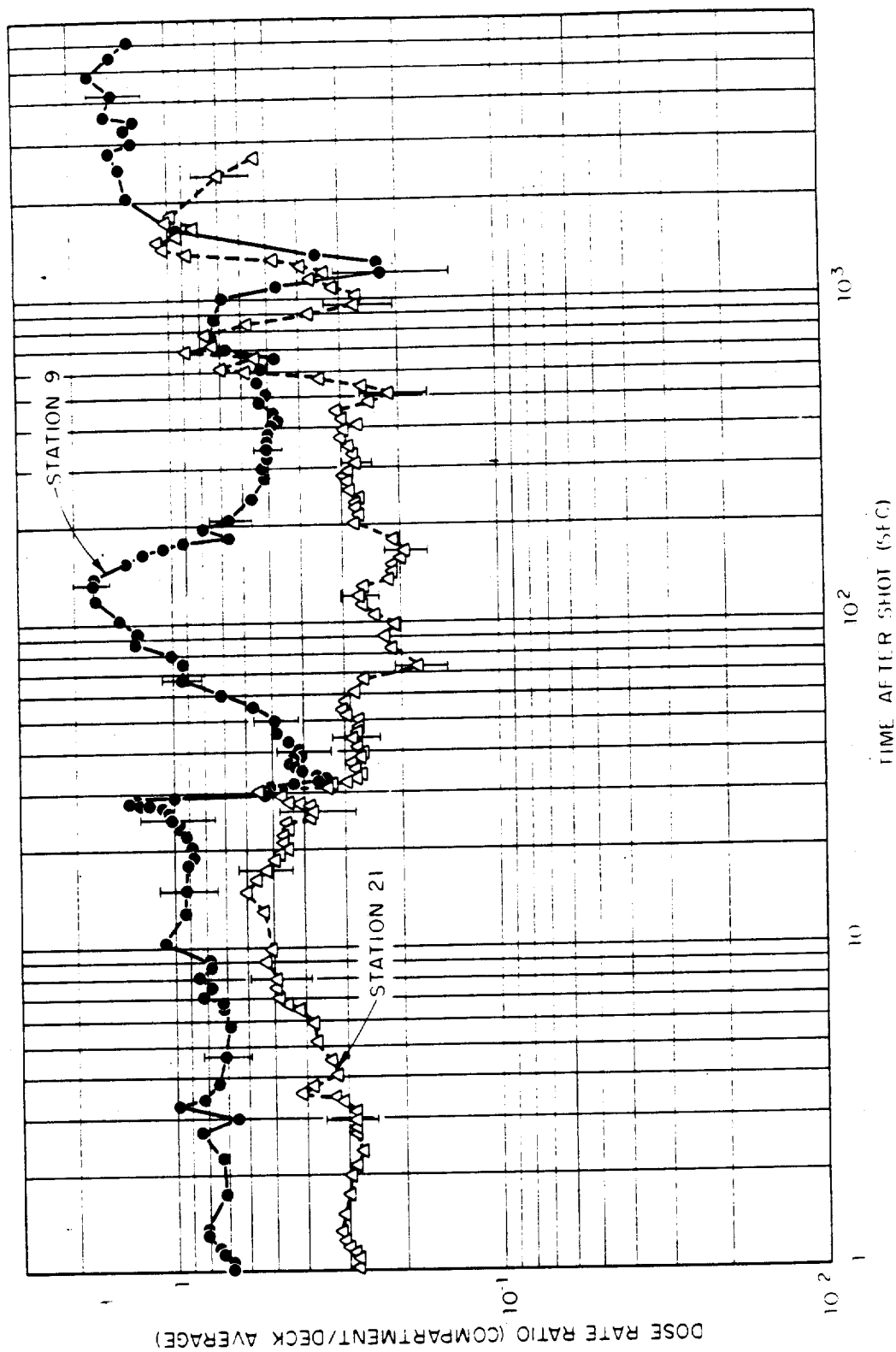
Figure 3.26 Ratios of dose rate in compartments to average dose rate on weather decks of DD 592, Shot Umbrella. Vertical bars indicate estimates of probable error.
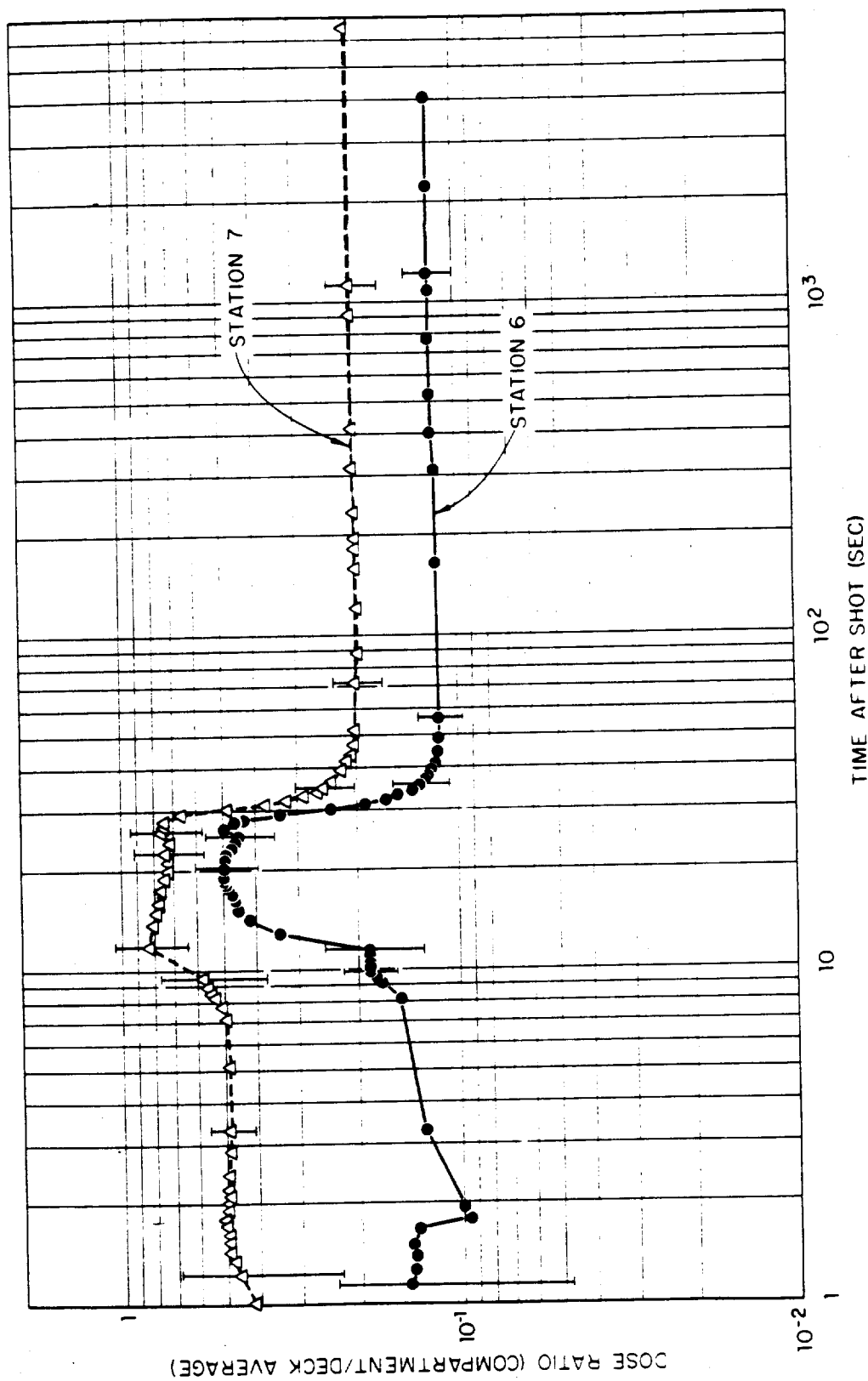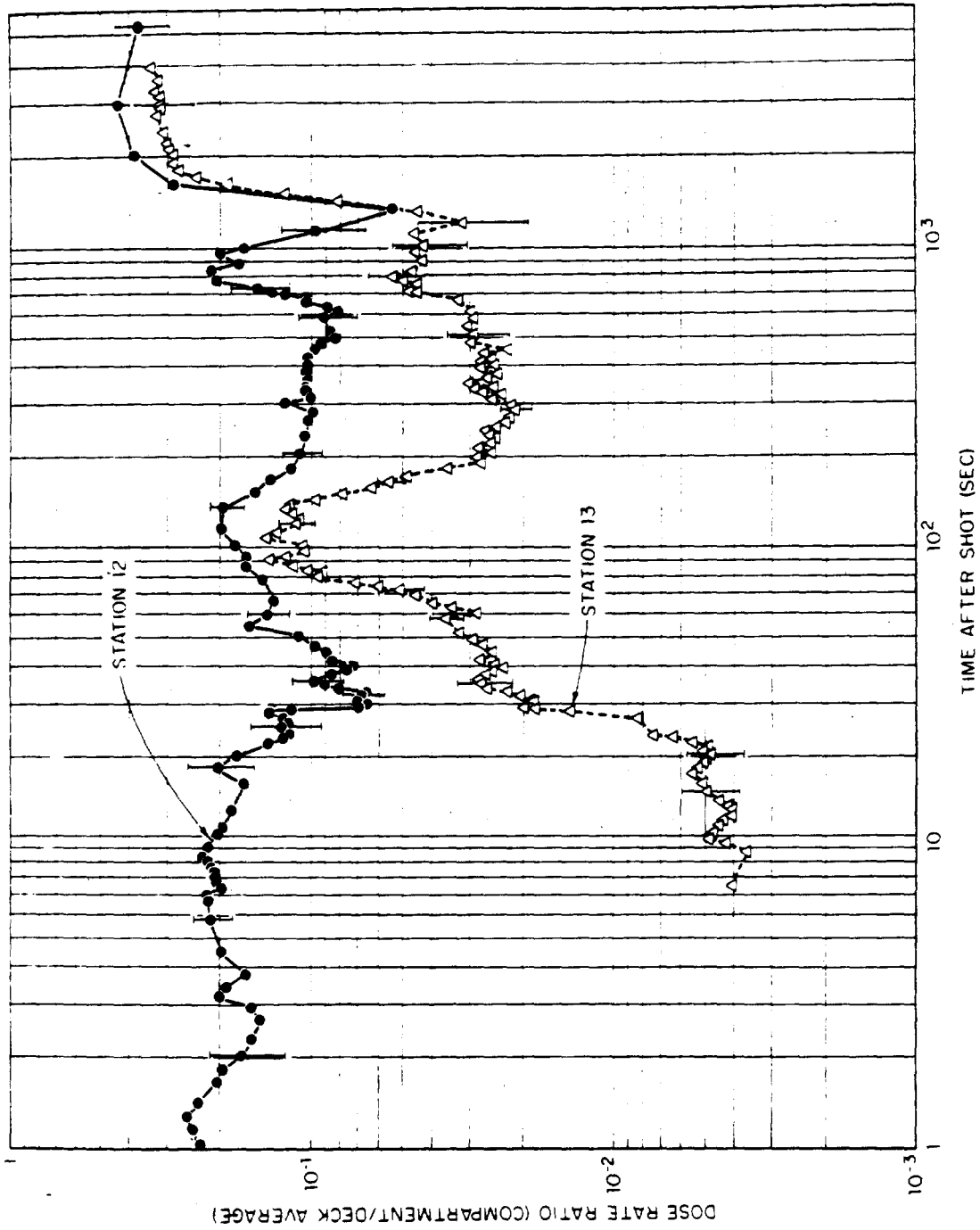
Figure 3.27 Ratios of dose rate in compartments to average dose rate on weather decks of DD 592, Shot Umbrella. Vertical bars indicate estimates of probable error.
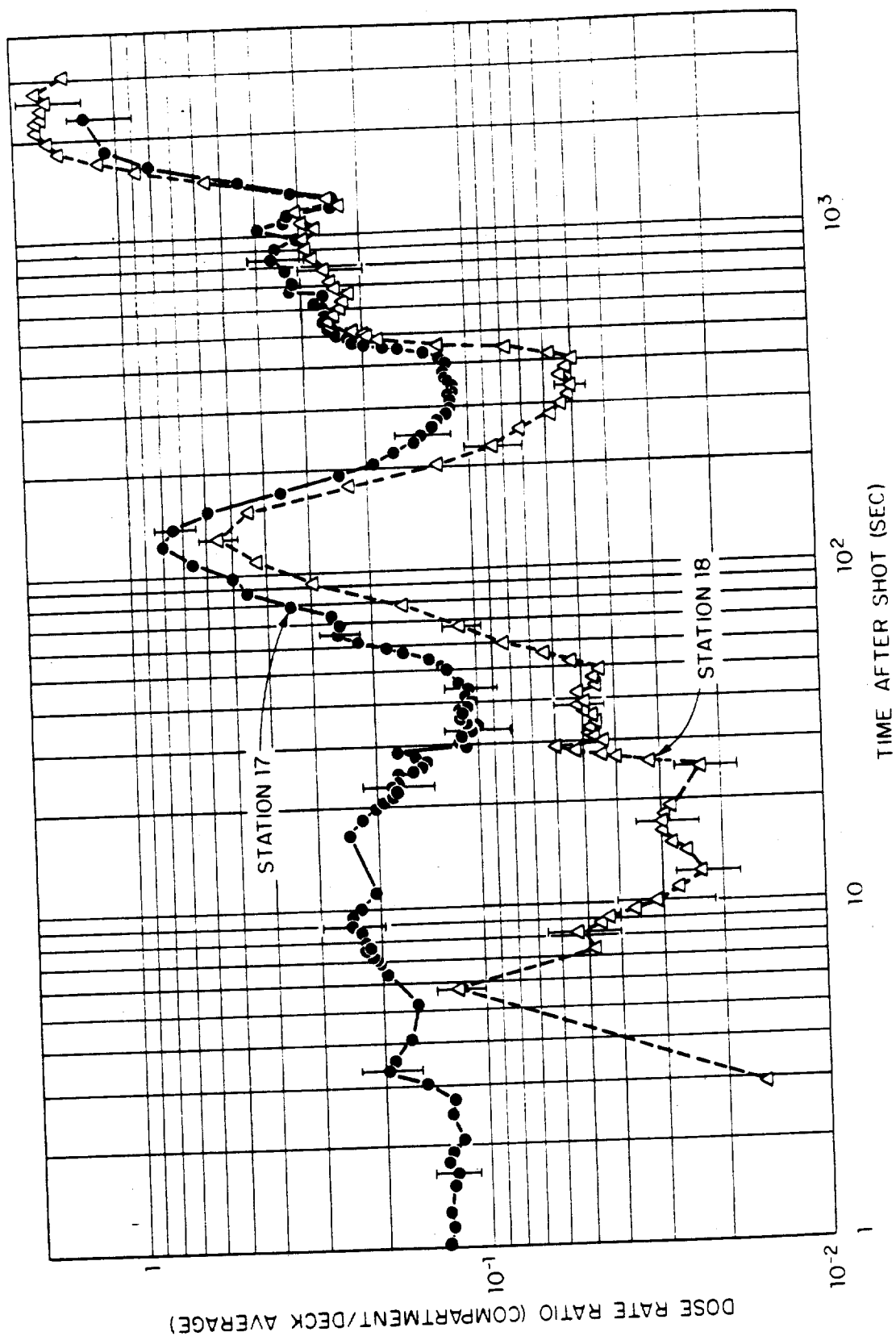
Figure 3.28 Ratios of dose rate in compartments to average dose rate on weather decks of DD 592, Shot Umbrella. Vertical bars indicate estimates of probable error.

63
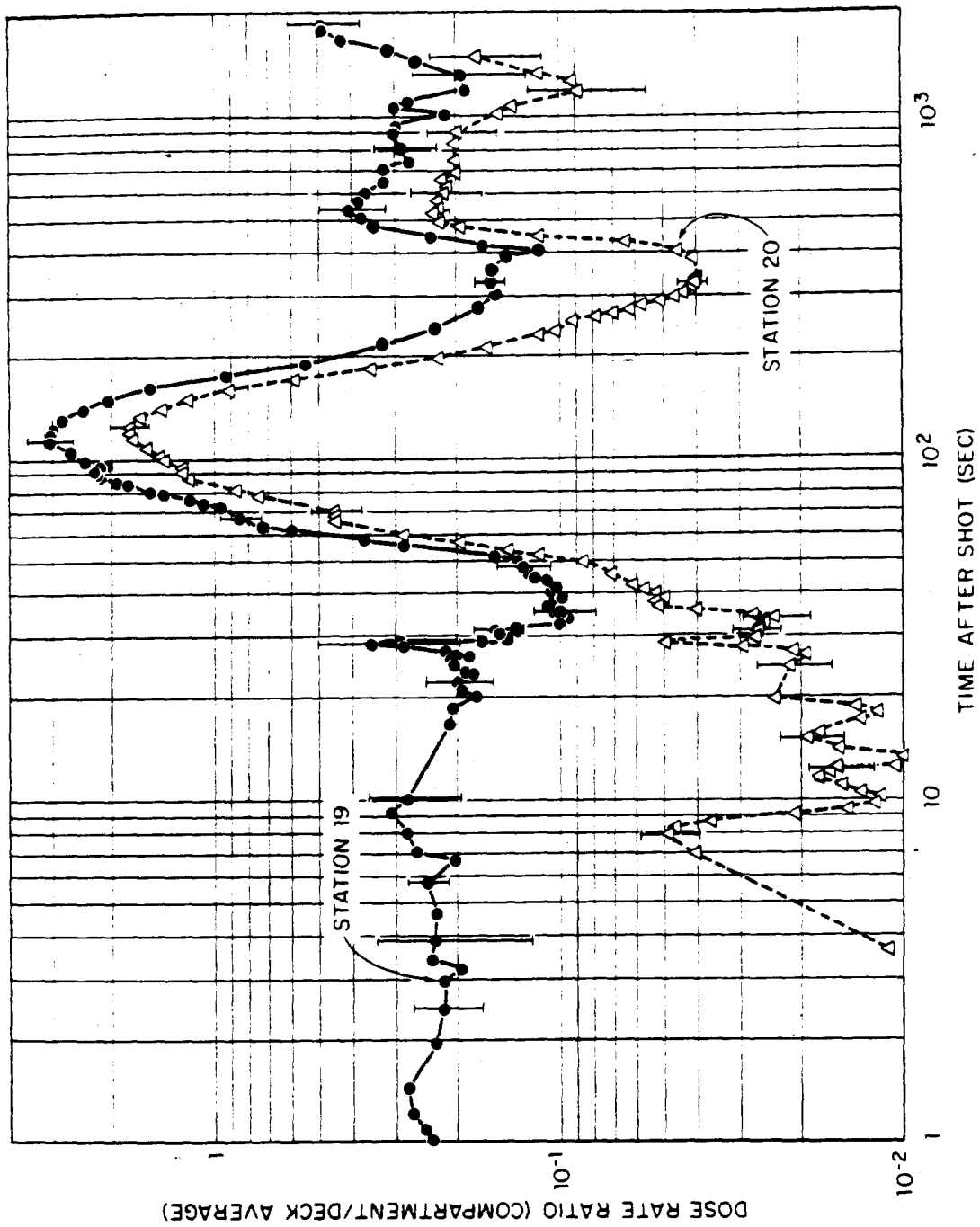
Figure 3.29 Ratios of dose rate in compartments to average dose rate on weather decks of DD 592, Shot Umbrella. Vertical bars indicate estimates of probable error.
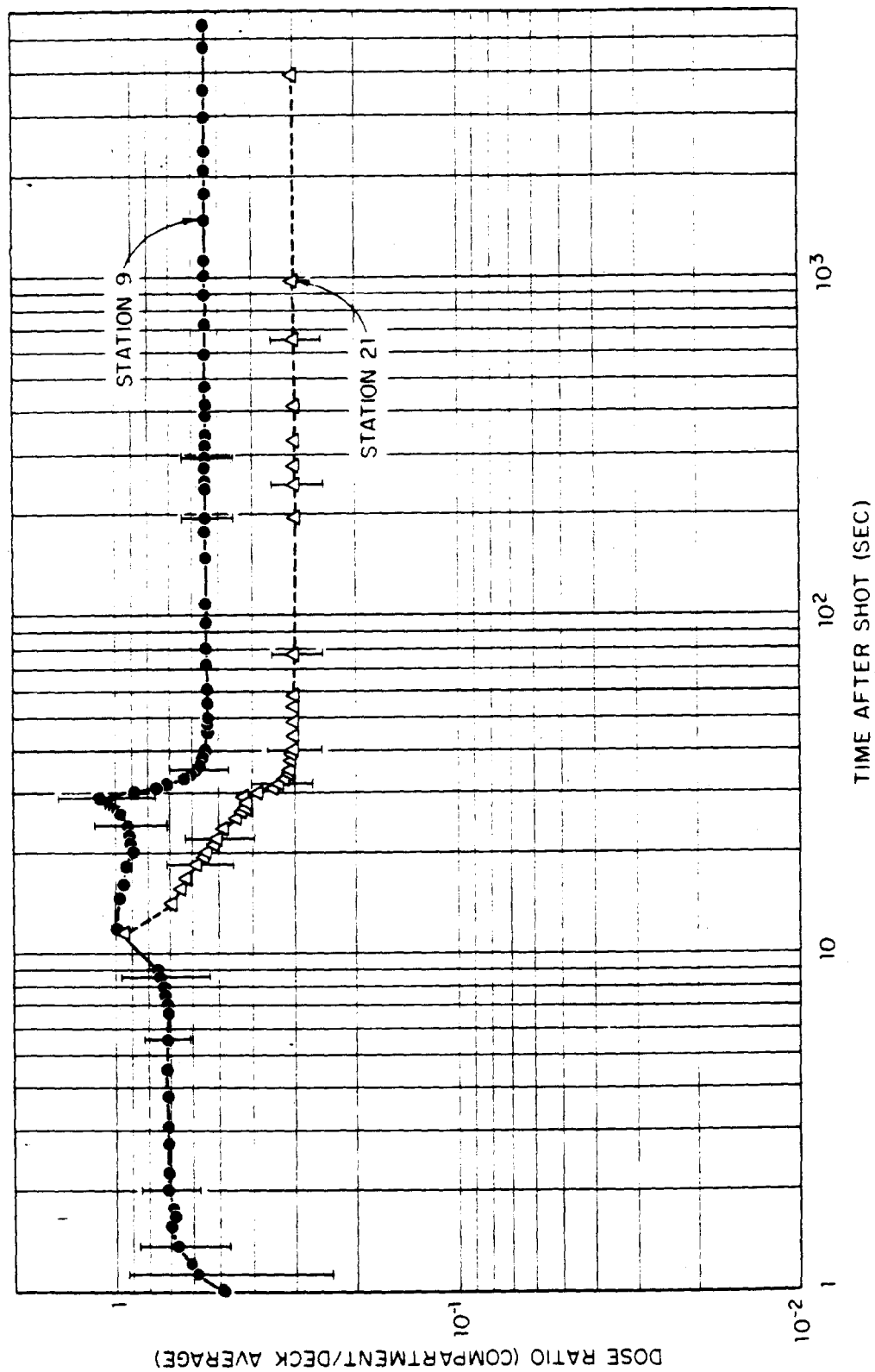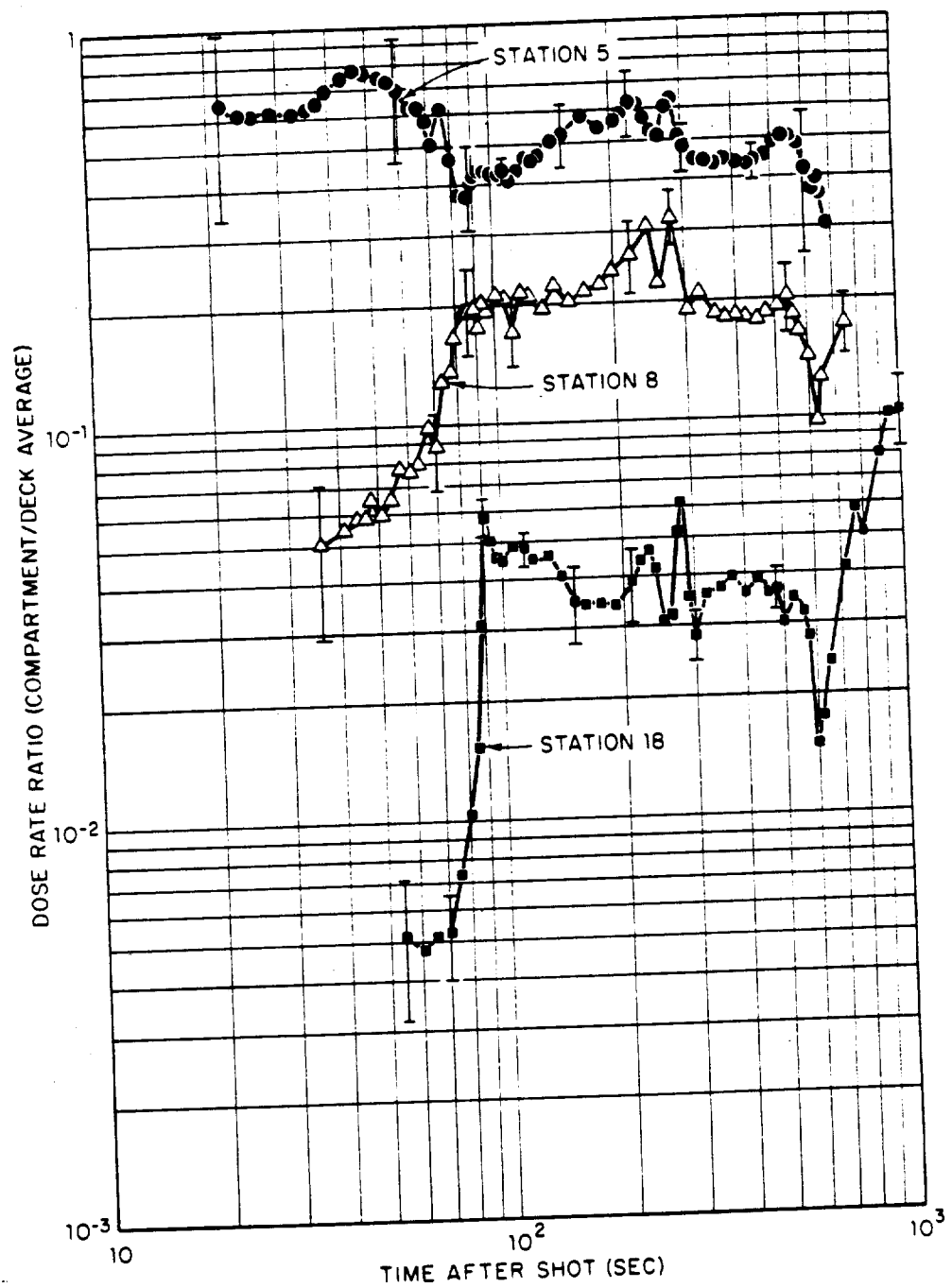
Figure 3.30 Ratios of dose rate in compartments to average dose rate on weather decks of DD 593, Shot Umbrella. Vertical bars indicate estimates of probable error.
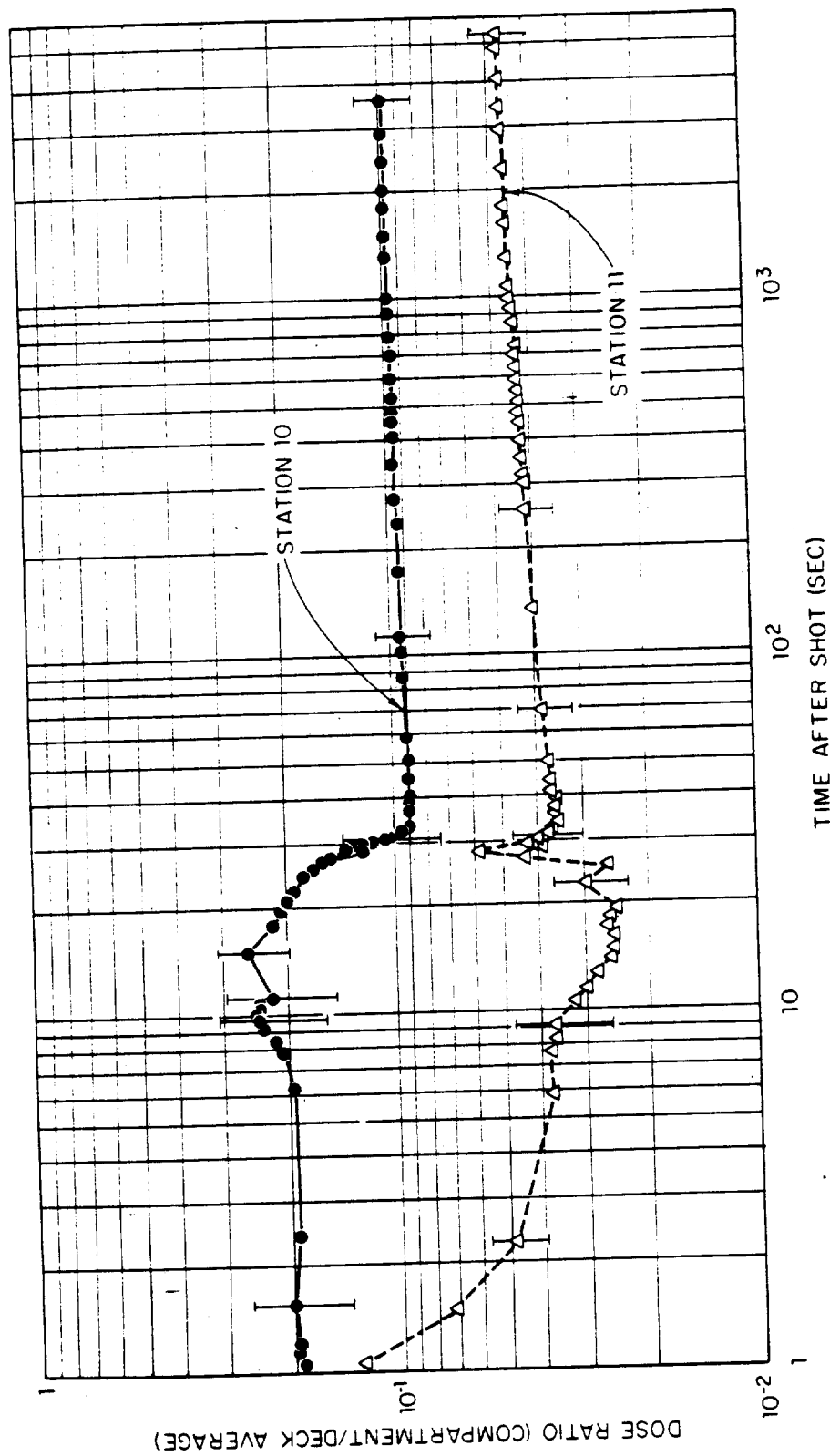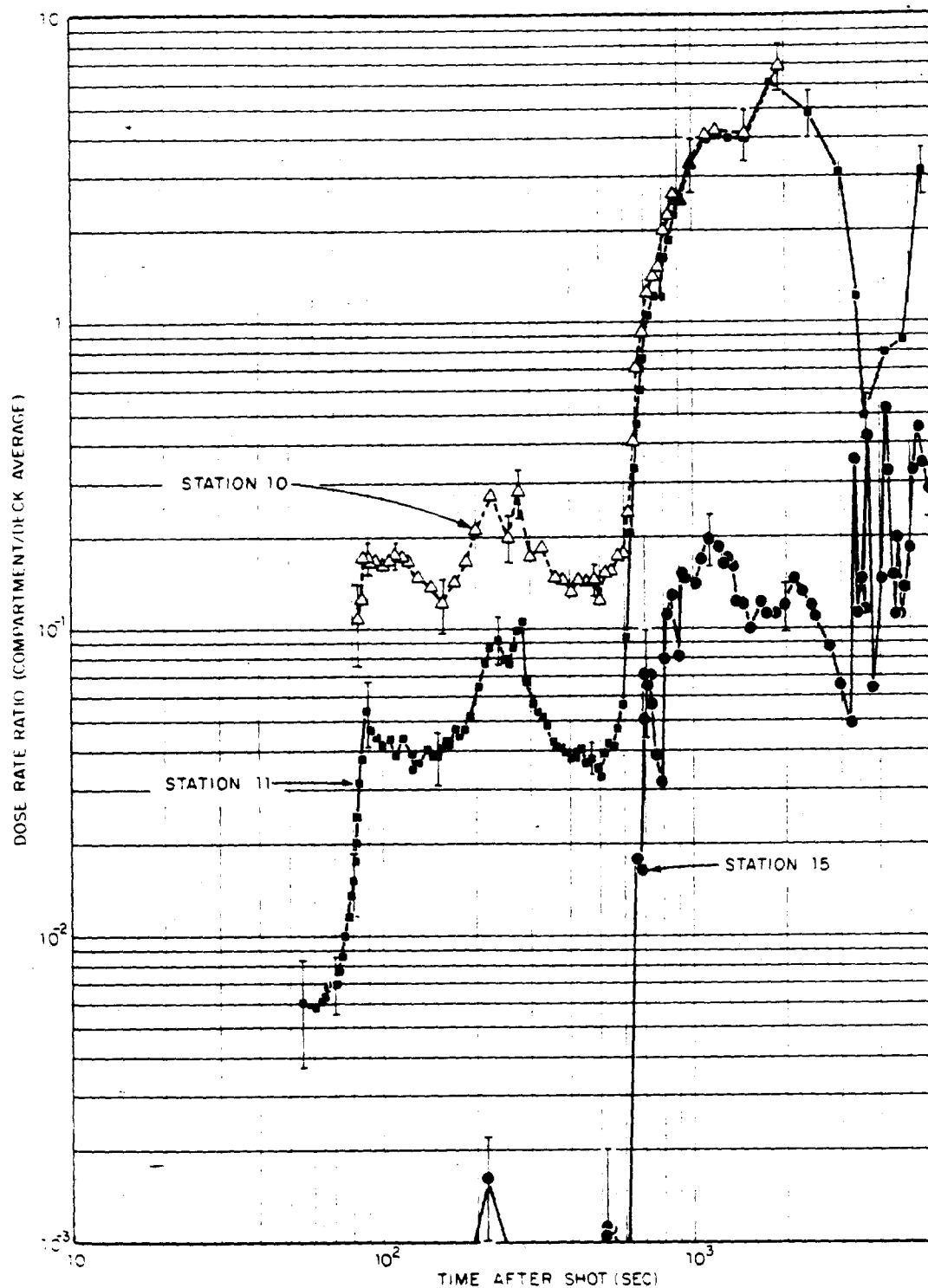
Figure 3.31 Ratios of dose rate in compartments to average dose rate on weather decks of DD 593, Shot Umbrella. Vertical bars indicate estimates of probable error.
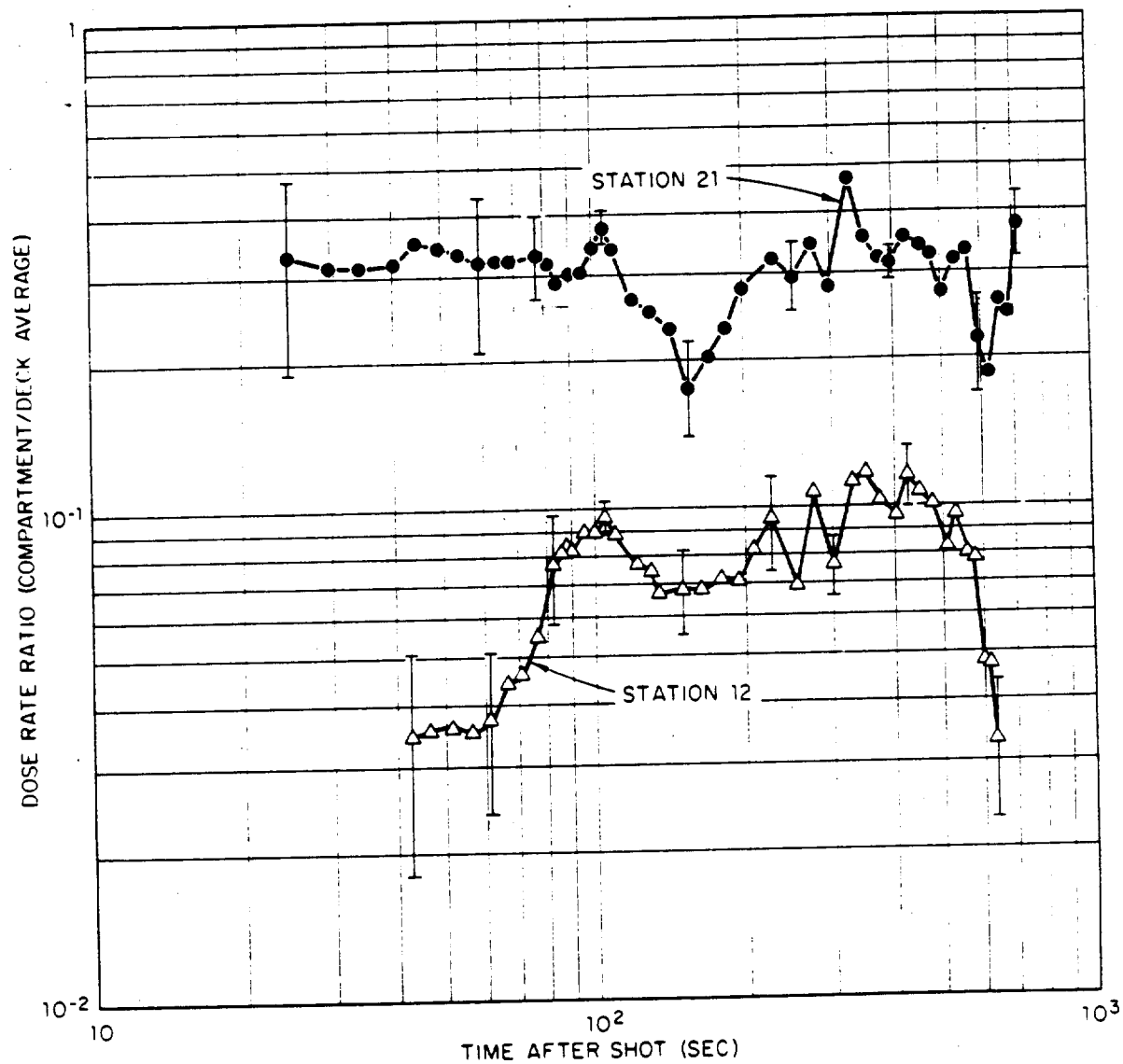
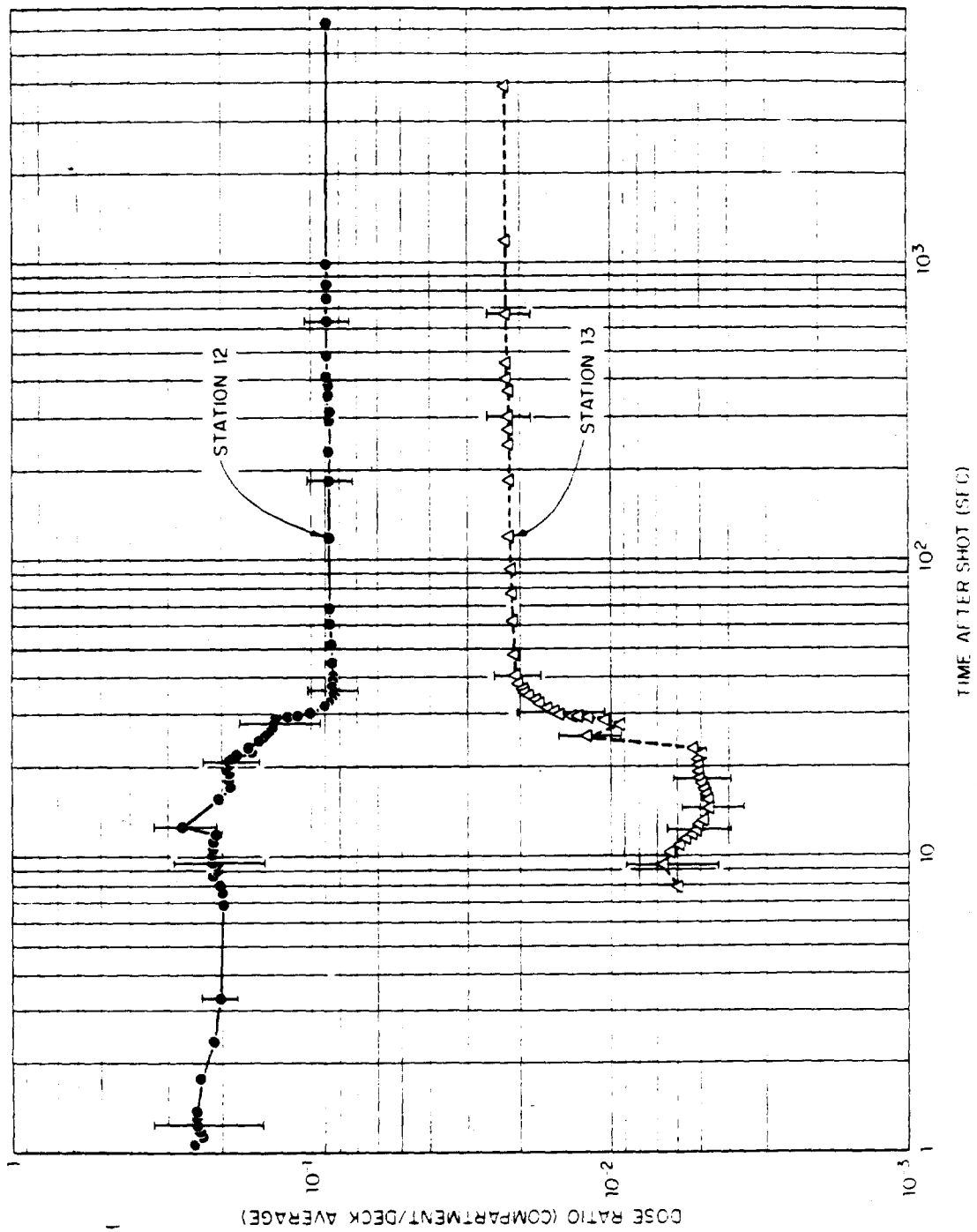Figure 3.32 Ratios of dose rate in compartments to average dose rate on weather
decks of DD 593, Shot Umbrella. Vertical bars indicate estimates of probable error.

67
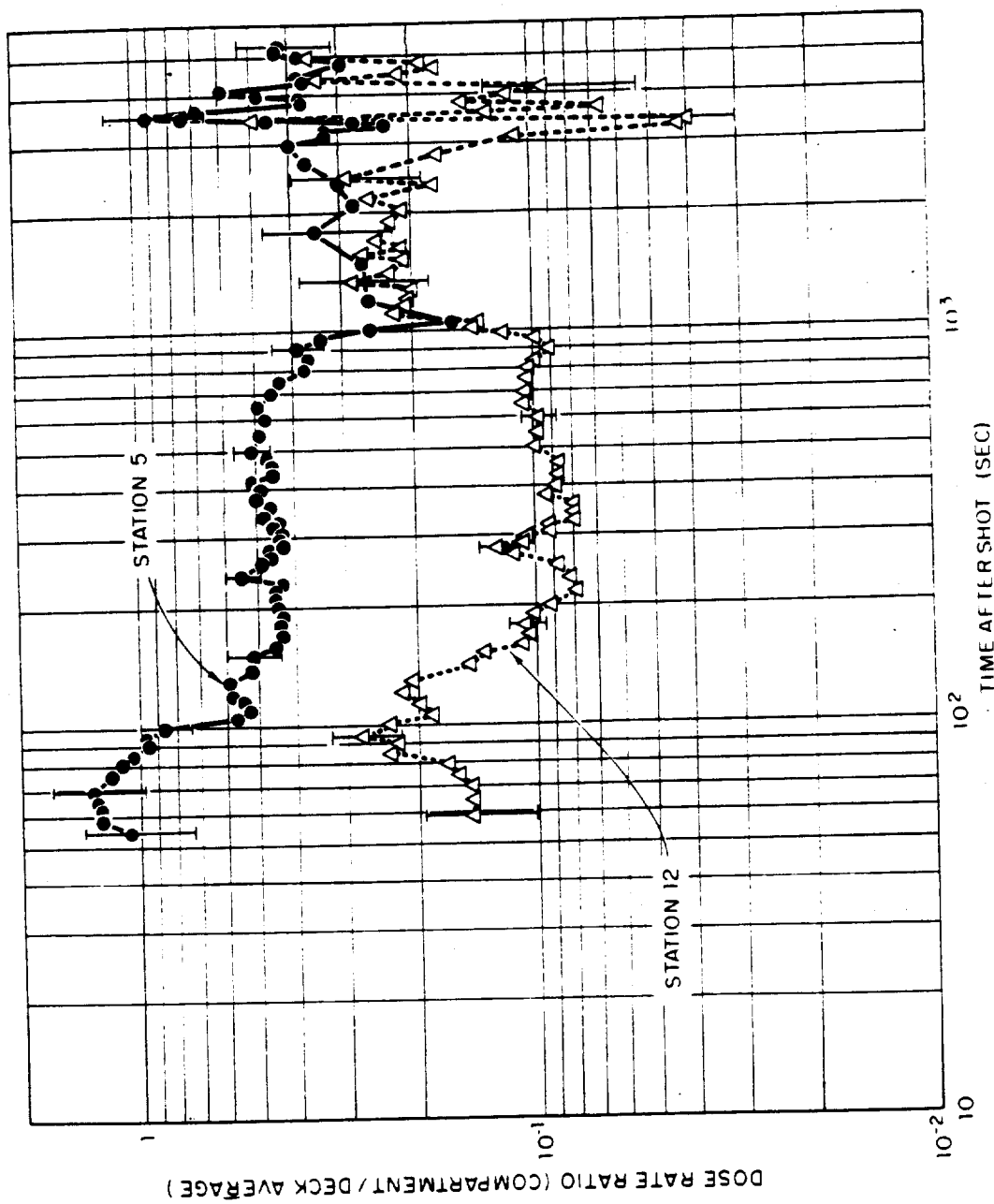
Figure 3.33 Ratios of dose rate in compartments to average dose rate on weather decks of DD 593, Shot Wahoo. Vertical bars indicate estimates of probable error.

68
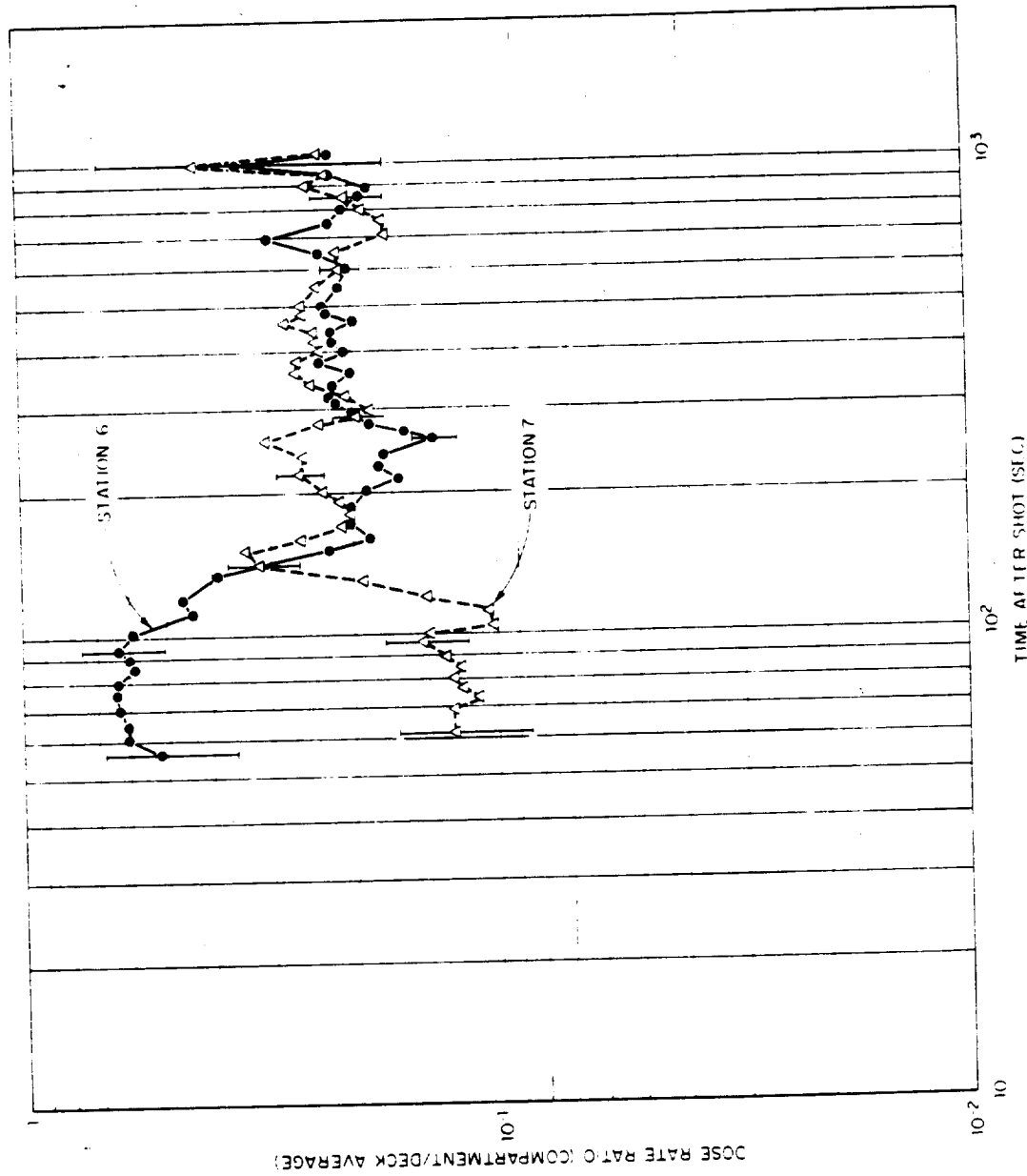
Figure 3.34 Ratios of dose rate in compartments to average dose rate on weather decks of DD 593, Shot Wahoo. Vertical bars indicate estimates of probable error.
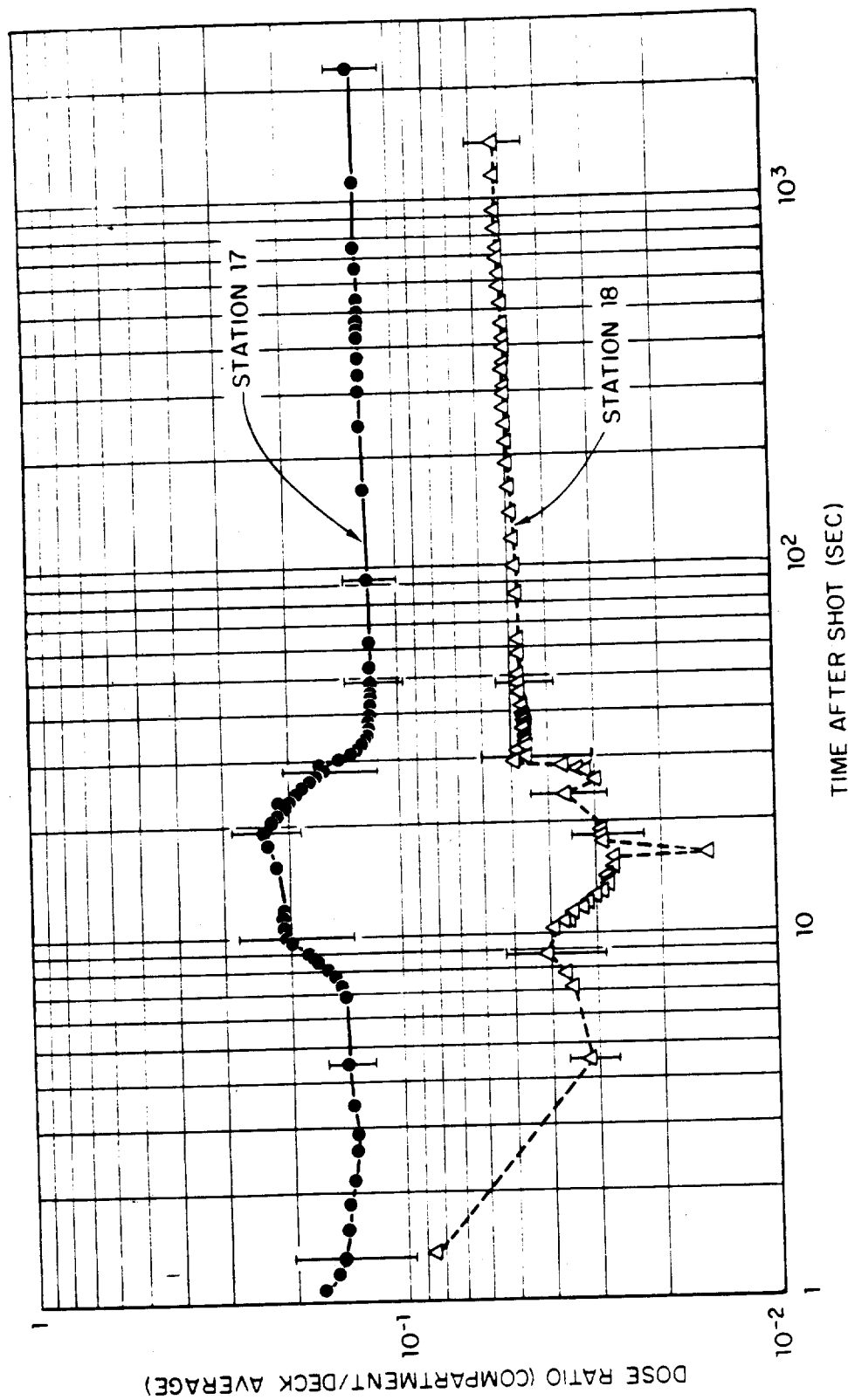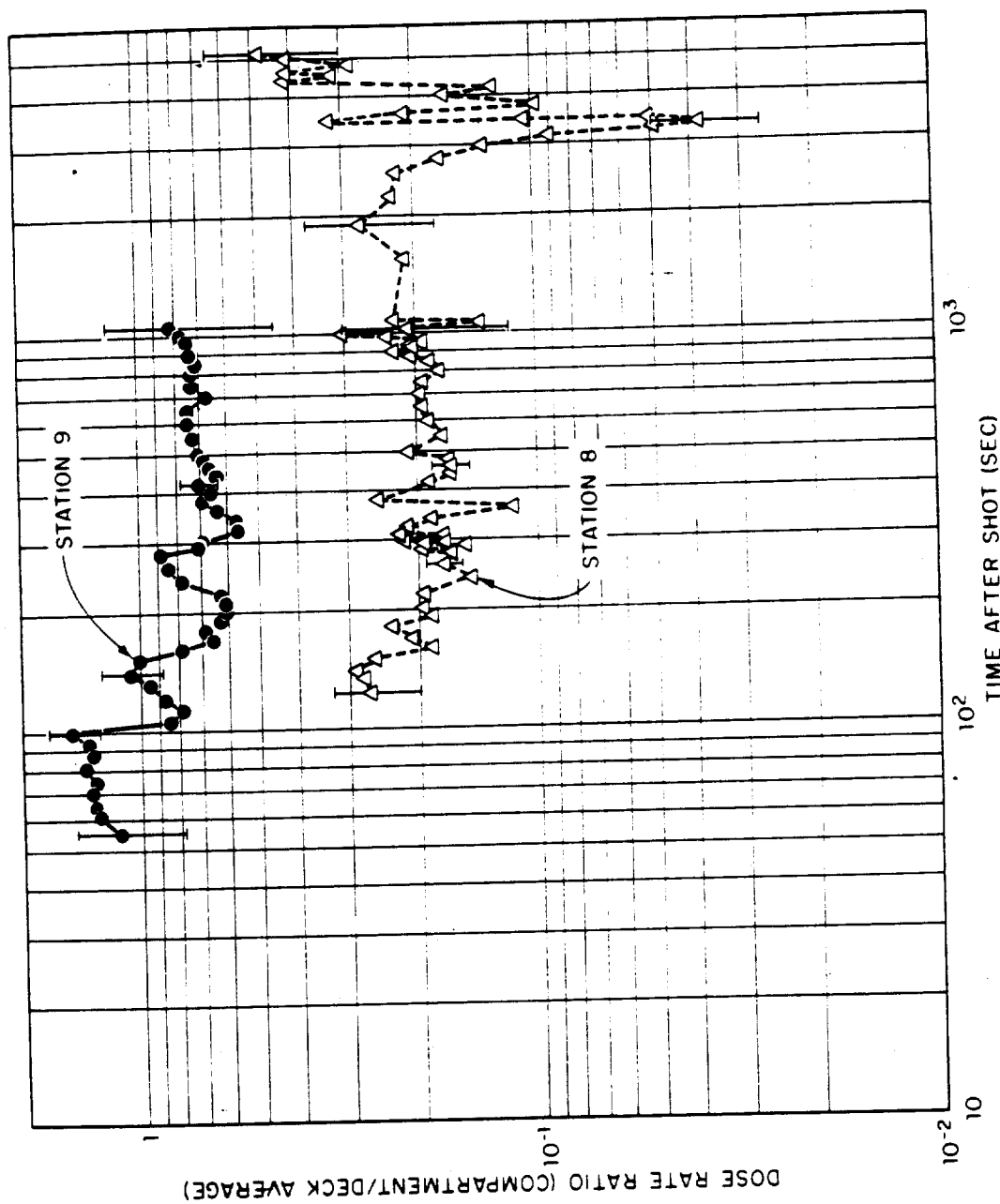
Figure 3.35 Ratios of dose rate in compartments to average dose rate on weather decks of DD 593, Shot Wahoo. Vertical bars indicate estimates of probable error.
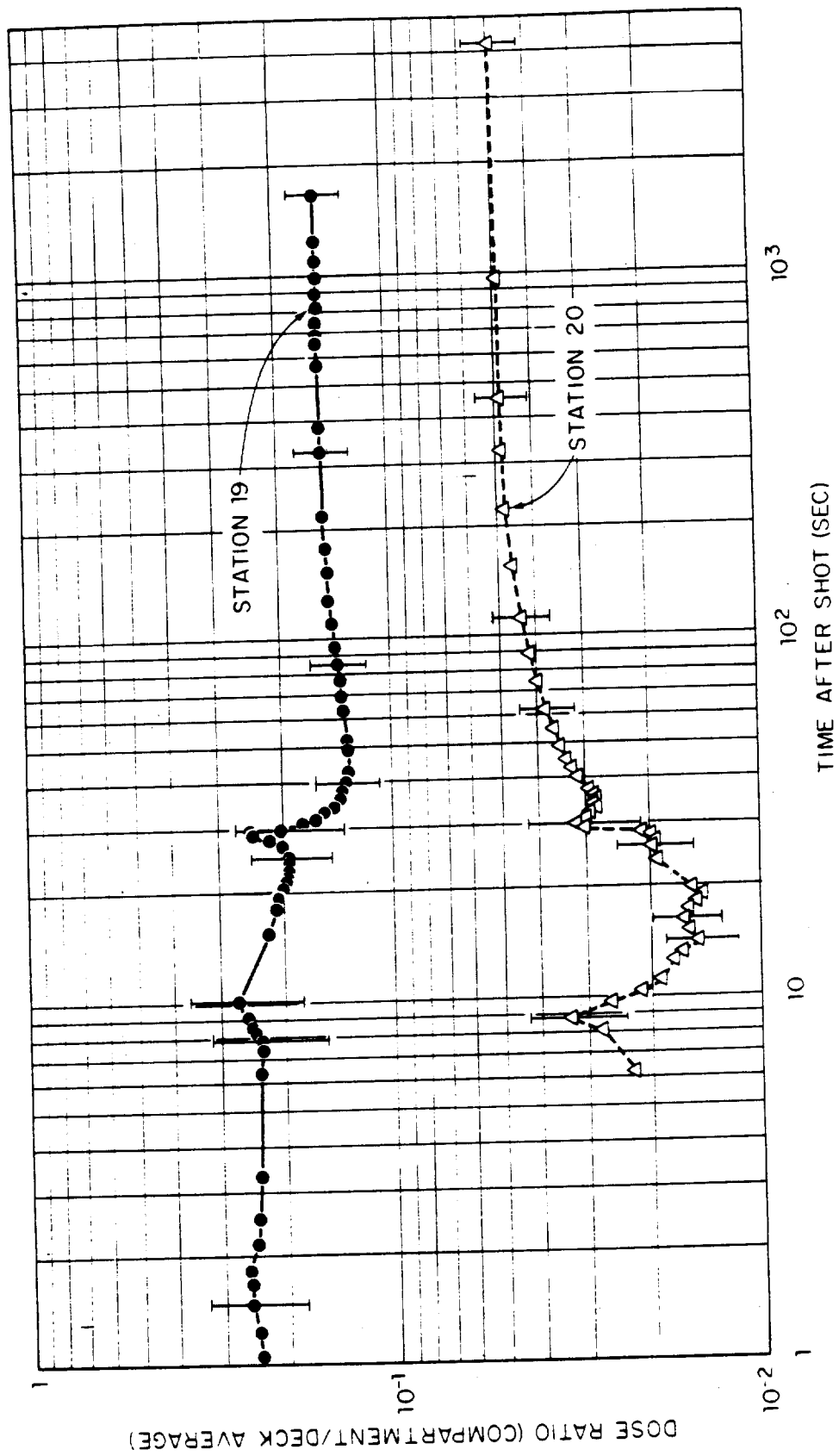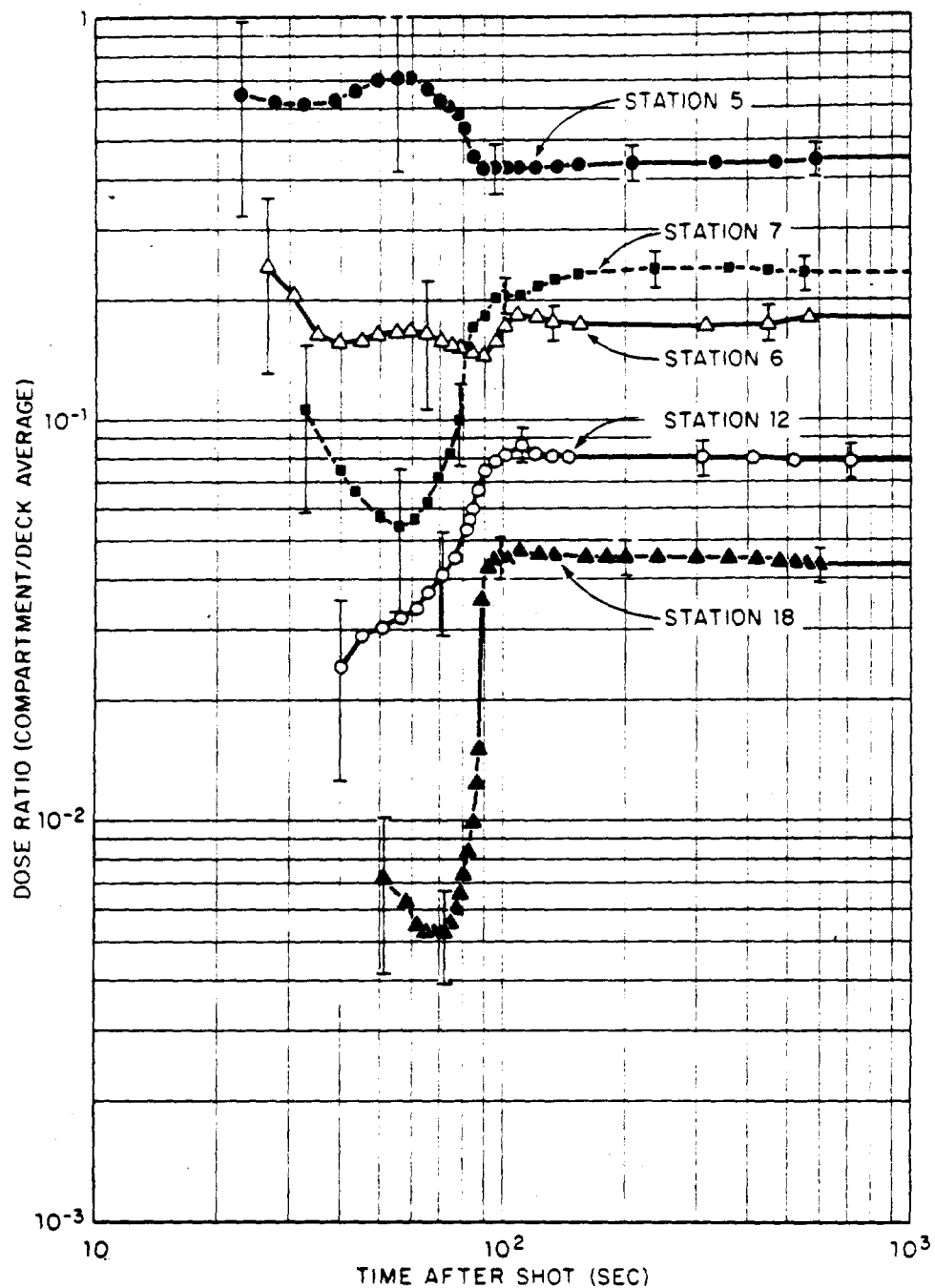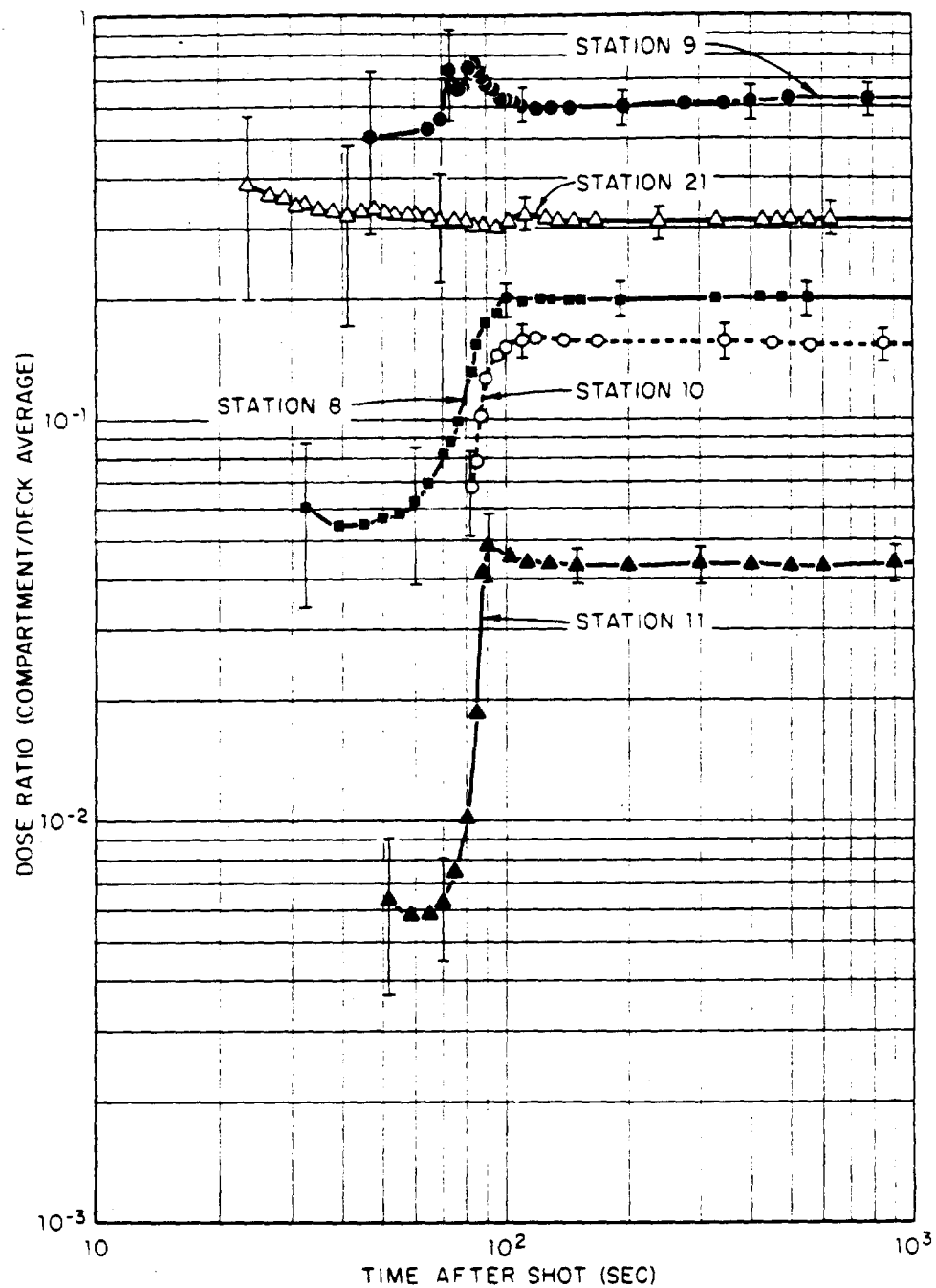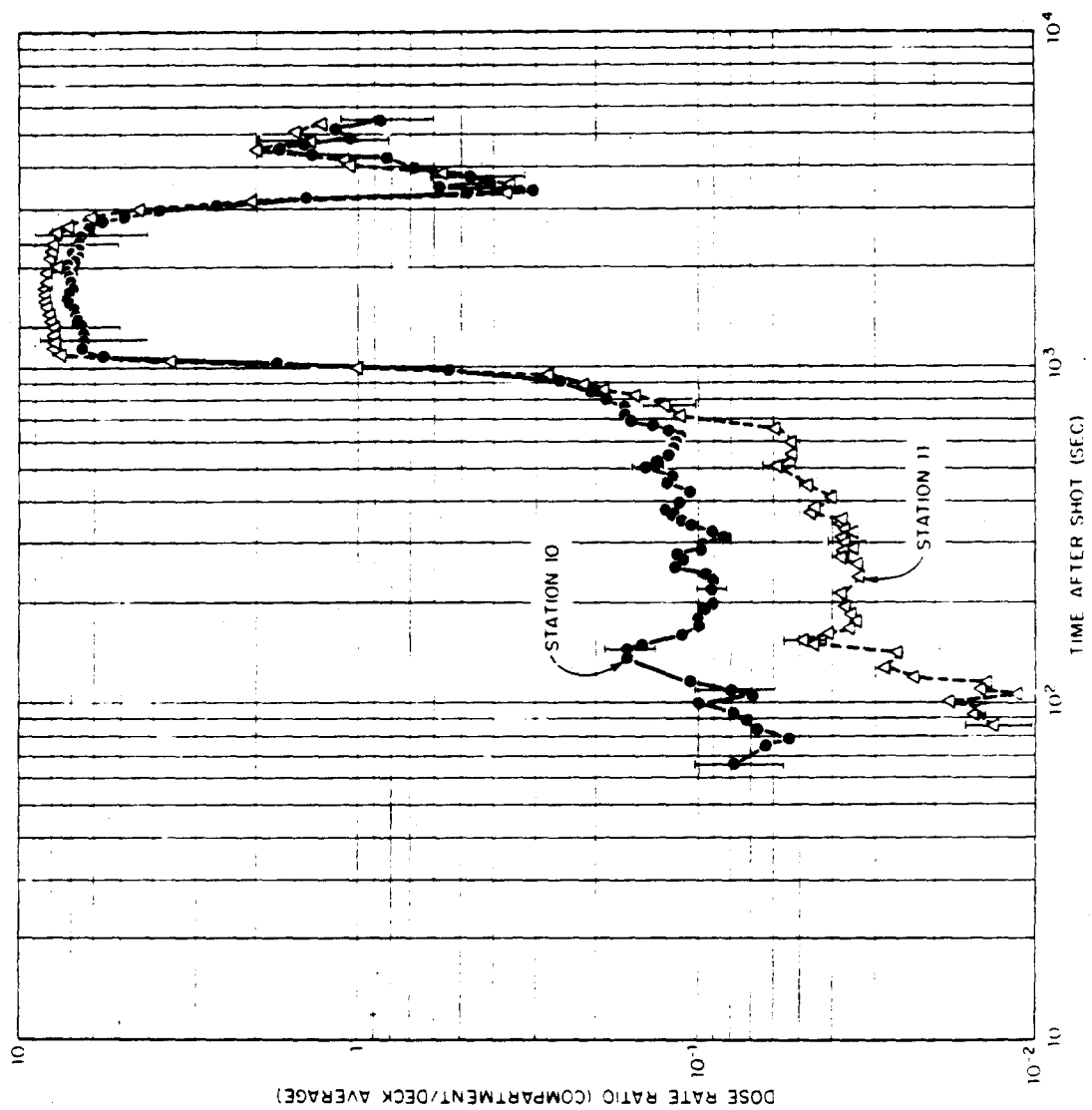
Figure 3.36 Ratios of dose rate in compartments to average dose rate on weather decks of DD 593, Shot Wahoo. Vertical bars indicate estimates of probable error.

71

Pages 72 through 75 deleted.
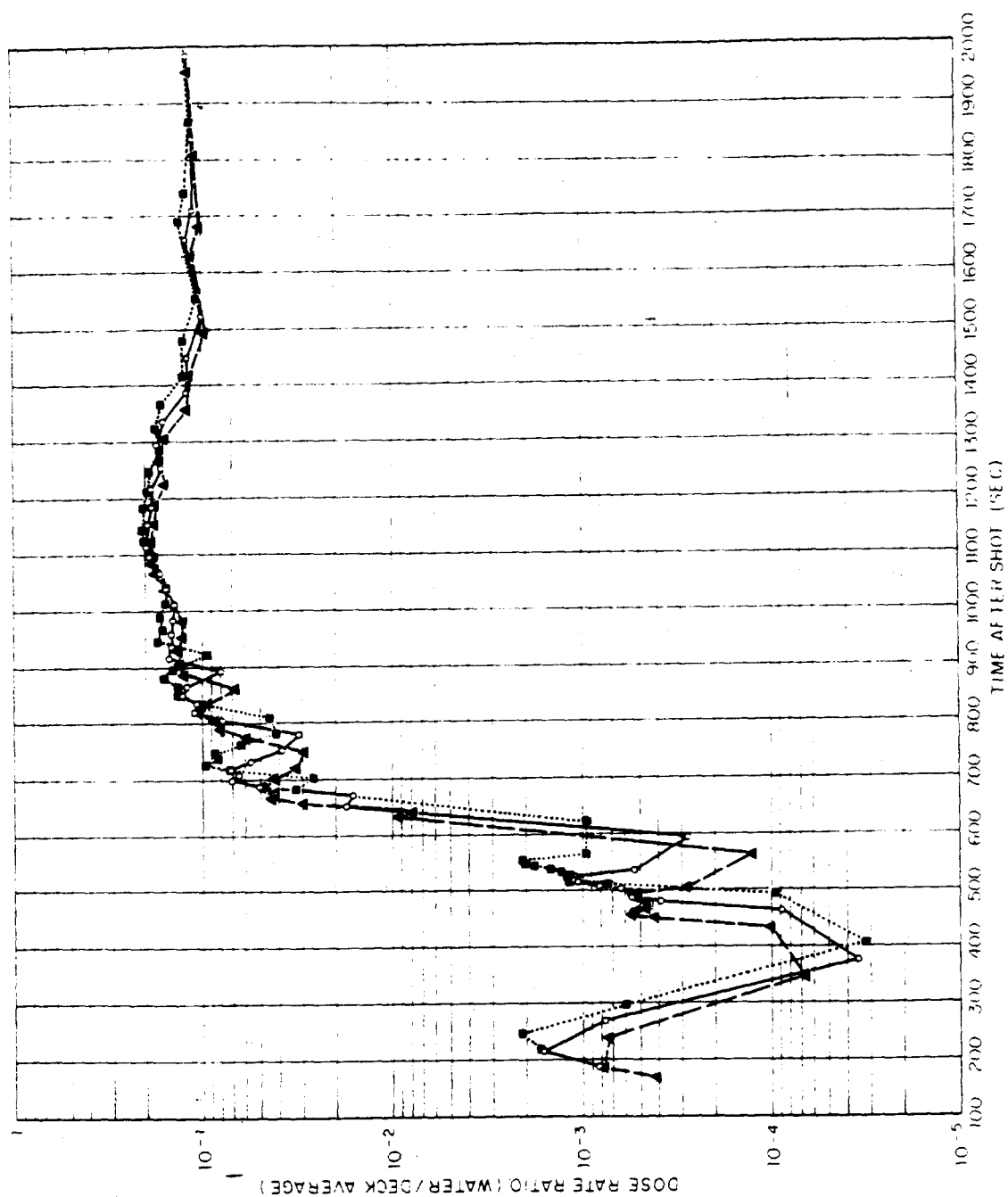
Figure 3.41 Ratios of dose rate in adjacent water to average dose rate on weather decks of DD 593, Shot Umbrella. Effects of possible 30-second timing errors are indicated by the two broken-line curves.
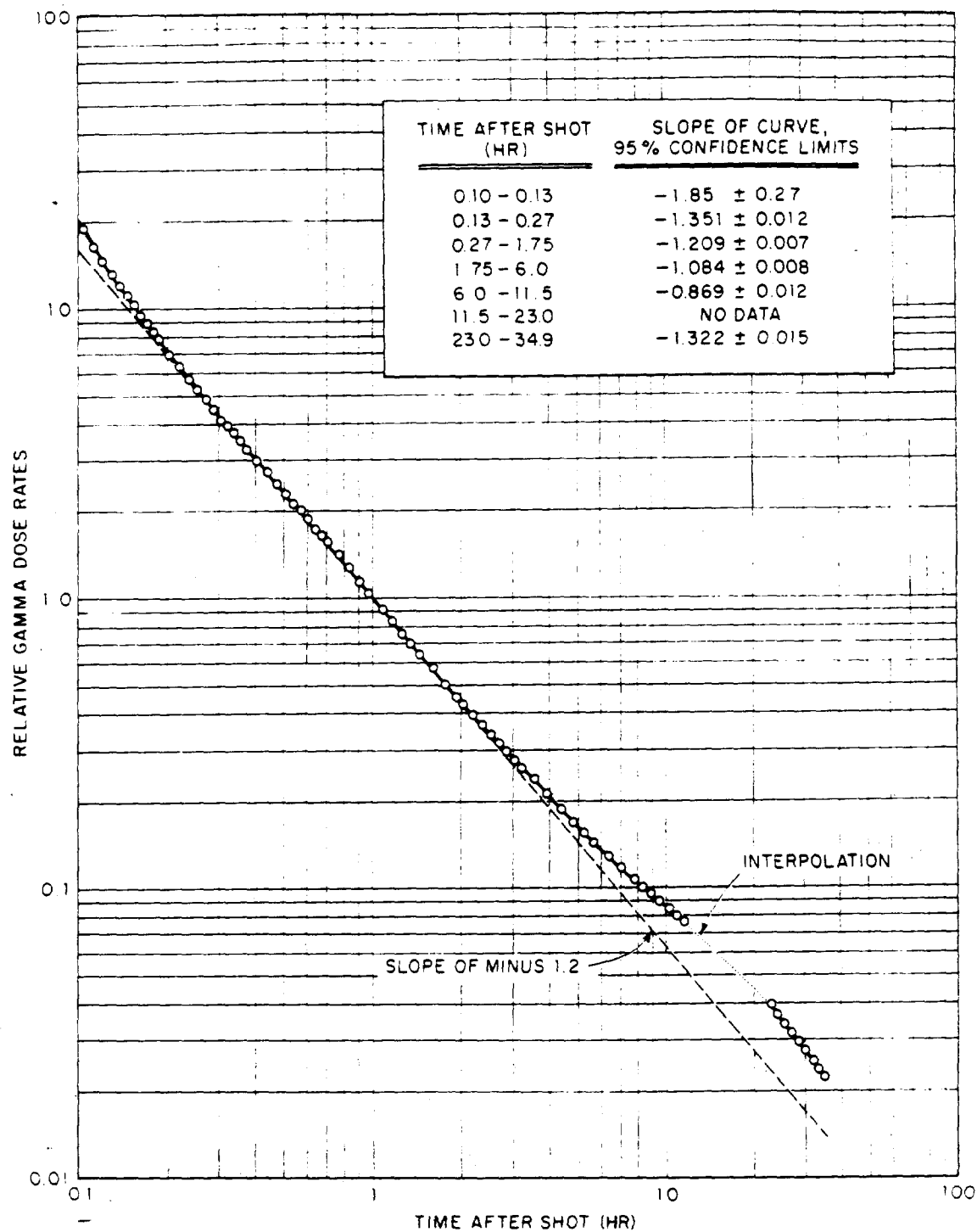
Figure 3.42 Gamma-ionization decay of contaminant collected
in 6-inch-thick lead cave on DD 592, Shot Umbrella.

77

Chapter 4

CONCLUSIONS AND RECOMMENDATIONS

4.1 CONCLUSIONS

The project had only limited success in meeting its objectives for Shot Wahoo, but met most of its objectives for Shot Umbrella. The conclusions are meant to apply only to the specific test conditions and radiological environments encountered aboard the moored and washed target ships.

4.1.1 Total Gamma Radiation Aboard Target Ships. The gamma radiation data indicated rapid rates of change with time after burst, and dependence upon distance from surface zero. These characteristics are summarized in Table 4.1 for the washed weather-deck areas. After Shot Wahoo, the weather-deck doses accumulated more slowly but eventually reached values on the order of 300 r higher than for Shot Umbrella, even though the ships were from 1,000 to 2,000 feet farther from surface zero.

For nuclear-weapon-delivery situations simulated by the two closer-in ships, temporary immobilization could result in lethal or near-lethal doses. After Shot Wahoo, the majority of compartments received doses in excess of 500 r aboard DD 474 and in excess of 200 r aboard DD 592. After Shot Umbrella, the two ships received doses in excess of 200 r in many compartments.

Ratios of dose or dose rate in compartments to dose or dose rate on the weather decks were dependent upon changes in radiation-source geometries and upon the presence of contaminants inside the ships. In one instance a dose-rate ratio changed by a factor of 1,000 within 28 minutes. The long-term dose ratios ranged between 0.36 and 0.63 for nonmachinery compartments on or above the main deck, between 0.14 and 0.46 for other nonmachinery compartments, between 0.08 and 0.20 for machinery spaces above the waterline, and between 0.02 and 0.07 for machinery spaces below the waterline.

4.1.2 Remote-Source Gamma Radiation. For the washed weather-deck areas, the observed total radiation can adequately represent the remote-source radiation during the first 10 minutes after the shots. At least 95 and 98 percent of the total dose on the washed decks was attributed to radiation from airborne radioactivity for Shots Umbrella and Wahoo, respectively.

On DD 474 and DD 592, a very-early radiation peak was observed between 0.5 and 6 seconds after Shot Umbrella but the dose from this effect was negligible, i.e., less than 0.13 r. No data was available to indicate whether similar very-early radiation was received after Shot Wahoo. There was apparently no correlation of dose-rate data with the size-versus-time relationship of the plume.

4.1.3 Total Gamma Radiation in Adjacent Water. Determination of underwater gamma radiation was not successful; data was obtained only for DD 593 after Shot Umbrella.

Contaminated water adjacent to the ship did not contribute significantly to the total radiation observed aboard DD 593 after Shot Umbrella. Indirect evidence suggests that, although radiation from the water may have affected the compartment/deck dose-rate ratios to a considerable degree at later times, the contribution of contaminated water to the total dose observed aboard the target ships was probably of little significance.

4.2 RECOMMENDATIONS

1. It is recommended that the data from all Operatio⁻ Hardtack Program 2 projects be analyzed and correlated. This is required to serve as a ⊥sis for an operational analysis to determine safe standoff distance for antisubmarine warfare delivery of nuclear weapons under Operation Hardtack underwater-detonation conditions.

2. It is further recommended that additional high-explosive or nuclear detonations be studied under other detonation conditions. This is required to estimate radiological effects for other possible weapon detonation conditions.

REFERENCES

1. C. F. Ksanda and others; "Gamma Radiation from Contaminated Planes and Slabs"; USNRDL TM-27, 15 February 1955; U. S. Naval Radiological Defense Laboratory, San Francisco 24, California; Unclassified.

2. R. W. Shnider; "Personnel Radiation Hazards Associated with Ships Immobilized by an Underwater Atomic Burst"; USNRDL-TR-5, 8 February 1954; U. S. Naval Radiological Defense Laboratory, San Francisco 24, California; Secret Restricted Data.

3. G. G. Molumphy and M. M. Bigger; "Proof Testing of Atomic Weapons Ship Countermeasures"; Project 6.4, Operation Castle, WT-927, October 1957; U. S. Naval Radiological Defense Laboratory, San Francisco 24, California; Confidential Formerly Restricted Data.

4. H. R. Rinnert; "Ship-Shielding Studies"; Project 2.71, Operation Redwing, WT-1321, July 1959; U. S. Naval Radiological Defense Laboratory, San Francisco 24, California; Confidential Formerly Restricted Data.

5. M. B. Hawkins and others; "Determination of Radiological Hazard to Personnel"; Project 2.4, Operation Wigwam, WT-1012, May 1957; U. S. Naval Radiological Defense Laboratory, San Francisco 24, California; Official Use Only.

6. M. M. Bigger and others; "Shipboard Contaminant Ingress from Underwater Bursts"; Project 2.2, Operation Hardtack, WT-1620, draft manuscript; U. S. Naval Radiological Defense Laboratory, San Francisco 24, California; Confidential.

7. E. C. Evans and others; "Characteristics of the Radioactive Cloud from Underwater Bursts"; Project 2.3, Operation Hardtack, WT-1621, draft manuscript; U. S. Naval Radiological Defense Laboratory, San Francisco 24, California; Confidential Formerly Restricted Data.

8. E. Swift, Jr. and others; "Surface Phenomena from Underwater Bursts"; Project 1.3, Operation Hardtack, ITR-1608, January 1959; U. S. Naval Ordnance Laboratory, White Oak, Silver Spring, Maryland; Confidential Formerly Restricted Data.

9. D. J. Barnes; Edgerton, Germeshausen and Grier, Inc., Boston, Massachusetts; Letter and enclosure to: R. Willey, U. S. Naval Ordnance Laboratory, White Oak, Silver Spring, Maryland; Registry Numbers 854785/854786, Subject: "Up-to-date Summary of Analysis of Wahoo and Umbrella Records," 27 May 1959; Confidential Formerly Restricted Data.

10. P. D. LaRiviere; "Early-Time Gamma Ray Properties of U^{235} Gross Fission Products"; USNRDL TM-89, 9 July 1958; U. S. Naval Radiological Defense Laboratory, San Francisco 24, California; Unclassified.

11. H. Goldstein and J. E. Wilkins, Jr.; "Calculations of the Penetration of Gamma Rays"; NYO-3075, 30 June 1954; Nuclear Development Associates, Inc., White Plains, New York; Unclassified.

12. A. T. Nelms and J. W. Cooper; "U^{235} Fission Product Decay Spectra at Various Times After Fission"; NBS-5853, 11 April 1958; National Bureau of Standards, Washington, D. C.; Unclassified.

13. E. Laumets and C. F. Ksanda; "Technique for Estimating Gamma Dose Rate Spectra from Field Attenuation Measurements and Comparison of Results for Operation Castle";

USNRDL TR-308, 7 April 1959; U. S. Naval Radiological Defense Laboratory, San Francisco 24, California; Secret Restricted Data.

14. L. A. Webb and others; "Analysis of Gamma Radiation from Fallout from Operation Teapot"; USNRDL TR-106, 27 August 1956; U. S. Naval Radiological Defense Laboratory, San Francisco 24, California; Confidential Restricted Data.

15. "Reactor Shielding Design Manual"; TID-7004, March 1956; Naval Reactors Branch, Division of Reactor Development, U. S. Atomic Energy Commission, Washington, D. C.; Unclassified.

16. R. Golden and E. Tochilin; "Characteristic Curves from Different Ionizing Radiations and Their Significance in Photographic Dosimetry"; USNRDL-TR-248, 23 June 1958; U. S. Naval Radiological Defense Laboratory, San Francisco 24, California; Unclassified.

Appendix A

GITR INSTRUMENT

Instruments to record gamma radiation as a function of time had been developed and used during previous field operations (References 3 and 4). However, this earlier instrumentation was entirely unsuitable for use during Operation Hardtack, wherein high time resolution, wide radiation-intensity ranges, improved detector geometry, simplified and unattended operation, rugged watertight performance, and improved capability for data reduction were required. These requirements were the basis for the development of the GITR Model 103 (Figures A.1 and A.2).

The instrument developed was a dose-increment recorder consisting of: (1) two concentric ionization chambers with recycling electrometers, (2) magnetic-tape recorder, (3) mechanical timer, and (4) control circuit and battery power supply (Figure A.3). These components were packaged in a watertight aluminum case 21 by 16 by 13 inches in size and had an overall weight of 55 pounds. The externally mounted detector unit was connected to the main instrument assembly by means of a watertight cable. Optionally, the detector could be plugged into the main instrument assembly within the case itself.

A.1 DETECTOR UNIT

The detector consisted of a low-range ionization chamber constructed around a high-range ionization chamber, with each chamber connected to a recycling electrometer circuit (Figure A.4). The recycling electrometer consisted of a CK 5886 electrometer tube connected as a cathode-coupled blocking oscillator with the interelectrode capacity of the ionization chamber in the first grid. Initially, the ionization chamber was charged, and the voltage on the first grid was below the predetermined triggering level of the electrometer. Ionizing radiation discharged the chamber and caused a positive voltage shift on the first grid. When a predetermined voltage level was reached, the circuit was triggered and generated a pulse of fixed amplitude at the cathode. The pulse caused the first grid to conduct and to transfer a constant, predetermined charge to the chamber. Simultaneously, the pulse was recorded on magnetic tape. The pulse terminated at the cathode in approximately 500 μsec, and the tube was left nonconducting with a negative voltage on the first grid, thus completing the cycle.

The gamma-dose increment required to discharge the ionization chamber was directly proportional to the amount of charge transferred to the chamber (Figures B.1 and B.2, Appendix B). The charge transferred during each cycle was constant but dependent upon the triggering level of the electrometer, which was controlled by the adjustable bias voltage of the second grid. Calibration of detectors was achieved by adjustment of the bias voltage until a predetermined dose increment caused the electrometer to cycle (Appendix B). The calibration control for each chamber was located on the moistureproof electrometer housing attached to the base of the chamber assembly.

The ionization chambers were constructed of thin-walled aluminum spinnings mounted concentrically. Cylindrical and hemispherical surfaces were used wherever possible to establish optimum voltage gradients for efficient charge collection. The chambers were filled with pure argon at 7.5 psi and sealed by soft-soldering techniques over nickel-plated surfaces. The volumes of the two chambers were 1.475 cc and 14.0 cc for the low-range and high-range chambers, respectively. The sensitivity ratio of 1.000 between the two ranges was achieved by the design value of the input capacity of the electrometer circuits. A lead-tin filter over the entire outer surface of the detector provided reasonably uniform energy response from about 100 kev to 2 Mev (Figure B.3).

A.2 RECORDER SYSTEM

The recording medium was 900-foot lengths of instrumentation-quality magnetic tape spooled on standard 5-inch reels. The tape was 0.25 inch wide and had a polyester backing 0.001 inch thick. A Brush Electronics Company BK 1303-1 three-channel recording head, driven to tape saturation, recorded unidirectional pulses on the tape. The maximum usable pulse packing was 400 bits per inch of tape. Re-

cording intervals of 12 hours and 60 hours were used, with tape transport speeds of 0.25 and 0.05 in/sec. respectively. These speeds were accurate to ±2 percent for the entire recording interval. Both recorders were of identical construction with the exception of the drive motors. A single 6.7-volt mercury-battery stack having a capacity of 14,000 ma-hr powered each recorder. The 12-hour recorder was driven by a 2-watt motor operating at a speed of 6,000 rpm and regulated by a centrifugal governor. A 0.75-watt, chronometrically governed motor rotating at 900 rpm operated the 60-hour recorder. Both recorders utilized gear reduction and worm-gear drive. The tape was guided in the conventional manner. Metal friction plates on the feed spindle established an average tape tension of about 4 ounces. Contacts on the recorder turned off the instrument when a conductive section of tape at the end of the reel passed over them to cause a circuit closure. Both recorders were developed at U.S. Naval Radiological Defense Laboratory (NRDL) in conjunction with the Precision Instruments Company, San Carlos, California.

The dose increments chosen for the low- and high-range ionization chambers were 0.243 mr and 0.243 r, respectively. At the maximum intensity of each range, the maximum-usable pulse packing on the tape limited the recycling rate of the electrometer to 100 cps (87,500 r/hr) for the 12-hour recording interval and to 20 cps (17,500 r/hr) for the 60-hour interval. These dose increment and dose-rate values apply only to the particular detector orientation and gamma energy chosen for the calibration (Appendix B).

As radiation data was recorded on the two channels of the three-channel tape, bits were recorded on the third channel at 3.75-second intervals to establish a time reference for data reduction. The time bits were generated by a cam-operated switch driven by a low-power, 6-volt, direct-current, chronometrically governed motor. The accuracy of these pulses was ±0.5 percent. The timer was manufactured by the Haydon Company and was used because of its known accuracy and high reliability.

The function of the control circuit was to start and to turn off the instrument. Power to all the motors and to the filaments was controlled by means of a latching relay. This relay could be activated locally by a switch on the instrument or remotely by a contact closure through a cable into the instrument. The instrument could be turned off by deactivation of the relay with the switch on the instrument or by the tape-actuated turnoff switch on the recorder.

Mercury batteries were used to power the motors and the filaments in order to take advantage of the high current capacity and flat-discharge characteristics these batteries offer. In addition, a mercury battery with very-low current drain was used in the electrometer-calibration circuit to restrict calibration shift to less than ±1 percent during the expected life of the battery. Chamber bias and transistor bias were supplied by carbon batteries. With the exception of the motor battery, the minimum battery life was in excess of 250 hours. However, the 12-hour recorder could be operated in excess of 26 hours and the 60-hour recorder in excess of 80 hours without a battery change.

A.3 DESIGN LIMITS FOR OPERATION

All components were designed to operate under the following maximum conditions: (1) a shock of 15 g at 11 msec in all planes, (2) vibrations of 12 g at frequencies up to 45 cps in all planes, (3) temperature within the detector of 120 degrees F, (4) temperature within the main instrument assembly at 155 degrees F, (5) ambient relative humidity of 100 percent, and (6) a static overpressure of 5 psi. During the operation, satisfactory performance beyond these limits was frequently observed.

A.4 SHOCK MOUNTING

The GITR instruments were installed throughout the three target ships. Because of the high shock expected on these platforms, all instruments were shock mounted for approximately 6 inches of deflection. An eight-point suspension from steel springs in lines through the center of gravity of the instrument was used to support the main instrument assembly. The natural frequency of the suspension was about 5 cps. The detector unit was supported from four springs in a horizontal plane through the center of gravity of the unit. The suspension had a natural frequency of 7 cps and allowed 5 inches of deflection.

A.5 REMOTE-STARTING CIRCUIT

The limited recording time of the instruments and the requirement for unattended operation necessitated remote triggering of the instrument installations. A shipboard system was designed to meet this requirement (Figure A.5). The system consisted of the EG&G tone receiver and minus-5-minute relay, which was connected to the project control panel and relay system. The relay system consisted of latching relays, which were spaced throughout the ship. When activated by the timing signal, each latching relay started

as many as four GITR instruments. The project control panel recorded the receipt of all H−5-minute signals and could manually be set to lock out the EG&G signal or arm the project relay system and to reset all project relays. The triggering systems were similar on the three target ships.

Figure A.2 GITR Model 103 instrument with watertight case.
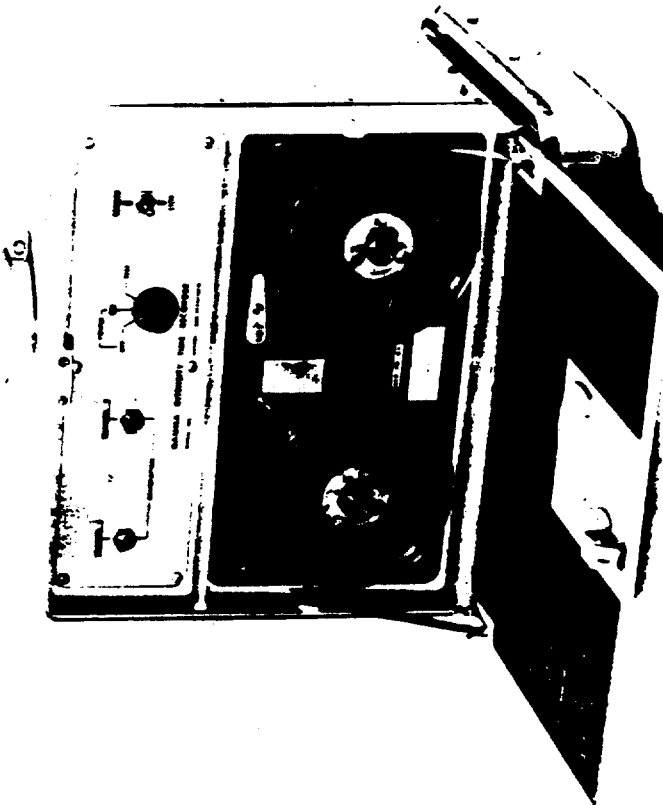
Figure A.1 GITR Model 103 instrument with the outer watertight case cover removed. The detector is shown mounted on main instrument assembly.

85

Figure A.3 Block diagram of GITR Model 103 with remote detector: a, low-range channel; b, high-range channel; c, time.

Figure A.4 Simplified schematic diagram of GITR Model 103 recycling electrometer.

Figure A.5 Block diagram of GITR triggering system for target ships. Each relay starts four GITR instruments (reference LBNS drawing No. 474-401-1586967 for details).

86

Appendix B

GITR CALIBRATION

B.1 BIASED-FIELD CALIBRATIONS

All instruments were initially calibrated at NRDL with Co^{60} sources accurate to within 3 percent. All calibrations were made with a standard orientation; the longitudinal axes of the detector and the radiation beam were parallel, and the electrometer housing faced away from the source. In this orientation, dose increments of 0.243 mr and 0.243 r were established for the low- and high-range chambers, respectively. The linearity of the detector had been checked over a wide range of gamma intensities and is shown in Figures B.1 and B.2.

To assure optimum reliability and accuracy in the data, each detector was recalibrated in the field, before and after each shot, with the 120-curie Cs^{137} source installed in the project's instrumentation trailer. This source was standardized to the Co^{60} sources by means of the Victoreen 70-A r-meter and various calibrated chambers. To assure maximum reproducibility of calibration, a jig was fabricated to control positioning of all detectors in the radiation beam. For personnel protection, the beam was directed vertically through the roof of the trailer. A calibration radiation field of 56.4 r/hr was used for the adjustment of the detector output-pulse periods to 0.016 and 15.5 seconds for the low-range and the high-range channels, respectively. The low-range-channel pulse period of 0.016 second (instead of the expected value of 0.0155 second to give 0.243 mr) compensated for the 0.0005-second recycling time of the circuit. The calibration radiation field was too low to require a similar compensation for the high-range chamber.

It was estimated that all field calibrations were made with a precision of about ±2 percent. Upon recalibration following an event, the random shifts in calibration were noted to be about ±3 percent. Evaluation of all phases of instrument operation indicated that the relative precision of almost all detectors was about ±7 percent throughout an event. However, it was known that the detector orientation used for calibration, and chosen because it assured reproducibility, biased the results because of the nonuniform directional response of the detectors. Figures B.3 and B.4 show the results of pretest studies of energy response and directional response characteristics.

B.2 CORRECTIONS FOR CALIBRATION BIAS

After Operation Hardtack, a more-extensive investigation of GITR directional characteristics as a function of energy was undertaken at NRDL for three conditions: (1) detector in the aluminum jacket, representing interior GITR stations; (2) detector inside the aluminum drum, representing exterior GITR stations; and (3) detector mounted inside the recorder case. Figure B.5 and Tables B.1 through B.6 show the results in relationship to the biased field-calibration condition. The actual responses of the shielded detectors (simulating the station mountings) to the several monoenergetic gamma-radiation beams for various detector orientations were divided by the responses of the unshielded detectors to Cs^{137} radiation beamed at the top of the detector (the biased field-calibration responses).

The directional responses indicated above were used to calculate integrated responses to four idealized radiation-source geometries: (1) horizontal radiation incidence, simulating remote pretransit radiation; (2) hemispherical radiation source above station, simulating the transit phase; (3) spherical radiation source around station, simulating interior stations affected by radiation from both the overhead decks and adjacent water; and (4) radiation source presenting solid angle of $1.7-\pi$ steradians below station, simulating exterior stations exposed only to contaminated decks and/or adjacent water. Figures B.6 through B.9 show these integrated responses in relationship to the biased field-calibration condition. However, these values apply only for monoenergetic radiation sources.

In the absence of measured gamma-energy spectra for these shots, the sensitivity of calculated correction factors to various assumed spectra was investigated. Six un-degraded energy spectra for various times after fission were considered: 9-second and 6.8-minute spectra from Reference 10; a 31-minute spectrum from Reference 12; 1.1- and 5.2-hour spectra from Reference 13; and a 9-hour spectrum from

Reference 14. Degradation of these six spectra by penetration of about 1 inch of steel was also estimated as follows.

An unattenuated gamma-energy spectrum (broken into n energy intervals) has an average energy flux of U Mev cm²-sec for the jth energy interval D_j Mev wide. After attenuation by x-cm of steel the energy flux from the jth energy interval has been reduced to $U_j B_j \exp(-ux)$, assuming plane monodirectional radiation for simplicity, where B_j is an energy-buildup factor determined by cross-interpolation in Reference 11, and u is the total absorption coefficient per centimeter of steel (at the energy representative of the jth interval) determined from Reference 15. To reduce the computational complexity, it was assumed that for energy originating in the jth energy interval, the attenuated energy flux per unit energy interval became uniformly distributed over the interval $\sum_1^j D_i$. This assumption biases the results somewhat by over-emphasizing the low energies (Figure B.10). The energy flux for the pth intervals ($p \leq j$), originating from the jth interval, is represented by

$$\left(D_p \Big/ \sum_1^j D_i \right) U_j B_j \exp(-ux) \tag{B.1}$$

Summing all of the attenuated and degraded energy flux (A_p) for the pth energy interval, originating from all intervals that can contribute to it, results in

$$A_p = D_p \sum_{j=p}^{j=n} \left\{ \left[U_j B_j \exp(-ux) \right] \Big/ \sum_1^j D_i \right\} \tag{B.2}$$

An example of the effect of this assumed degradation on one of the assumed gamma-energy spectra is presented in Figure B.11.

The energy flux for each of the energy intervals of the twelve energy spectra (six original and six degraded) was converted to an equivalent dose rate by using conversion factors determined from Reference 15. These dose rates were used to calculate percent dose-rate contributions from energy intervals representative of the energies at which the integrated detector responses had been calculated (Tables B.7 and B.8). These percentages were used as weighting factors applied to the data of Figures B.6 through B.9, thereby obtaining the overall responses to the assumed spectra in relationship to the biased-field-calibration. GITR bias-correction factors were obtained by averaging the reciprocals of the weighted integrated responses to the assumed energy spectra for the various idealized radiation-source geometries (Table B.9).

TABLE B.1 DIRECTIONAL RESPONSE OF LOW-RANGE
GITR DETECTOR (INSIDE 0.13-INCH ALUMINUM
DRUM) TO BEAMS OF VARIOUS RADIATIONS

Values are comparisons to response of unshielded detector to
Cs^{137} radiation beamed at top of detector (0 degree orientation).
Detector and drum were rotated in longitudinal plane about cen-
ter of detector. Response is symmetrical about longitudinal
axis of detector.

Detector Orientation deg	70-kev X-rays	120-kev X-rays	180-kev X-rays	Cs^{137}	Co^{60}
0	1.071	0.894	0.911	0.949	1.091
22	1.039	0.930	0.950	0.958	1.124
45	1.064	0.992	0.993	0.953	1.129
67	1.211	1.095	1.046	0.956	1.128
90	1.265	1.124	1.057	0.947	1.132
101	1.242	1.114	1.040	0.936	1.126
112	1.170	1.058	1.003	0.912	1.107
123	1.011	0.965	0.937	0.892	1.087
135	0.834	0.840	0.856	0.854	1.051
146	0.609	0.693	0.701	0.796	0.988
157	0.473	0.317	0.571	0.507	0.666
180	0.212	0.292	0.368	0.561	0.751

TABLE B.2 DIRECTIONAL RESPONSE OF HIGH-RANGE
GITR DETECTOR (INSIDE 0.13-INCH ALUMINUM
DRUM) TO BEAMS OF VARIOUS RADIATIONS

Values are comparisons to response of unshielded detector to
Cs^{137} radiation beamed at top of detector (0 degree orientation).
Detector and drum were rotated in longitudinal plane about cen-
ter of detector. Response is symmetrical about longitudinal
axis of detector.

Detector Orientation deg	70-kev X-rays	120-kev X-rays	180-kev X-rays	Cs^{137}	Co^{60}
0	0.985	0.828	1.000	1.056	1.132
22	0.987	0.912	1.110	1.144	1.262
45	0.988	0.972	1.152	1.146	1.281
67	1.197	1.142	1.259	1.163	1.314
90	1.289	1.217	1.309	1.171	1.336
101	1.245	1.222	1.296	1.167	1.344
112	1.189	1.199	1.277	1.162	1.350
123	1.034	1.089	1.173	1.117	1.303
135	0.823	0.954	1.041	1.042	1.255
146	0.684	0.826	0.893	0.943	1.182
157	0.444	0.774	0.763	0.848	0.720
180	0.125	0.228	0.252	0.297	0.530

TABLE B.3 DIRECTIONAL RESPONSE OF LOW-RANGE GITR DETECTOR
(WITH 0.13-INCH ALUMINUM JACKET) TO BEAMS OF
VARIOUS RADIATIONS

Values are comparisons to response of unshielded detector to Cs^{137} radiation
beamed at top of detector (0 degree orientation). Detector was rotated about
its center in longitudinal plane. Response is symmetrical about longitudinal
axis of detector.

Detector Orientation	70-kev X-rays	120-kev X-rays	180-kev X-rays	Co^{60}	Detector Orientation	Cs^{137}
deg					deg	
0	1.012	0.902	0.854	1.068	0	0.958
					10	0.958
22	0.969	0.940	0.907	1.102	20	0.964
					30	0.982
45	1.030	1.006	0.957	1.115	40	0.994
					50	1.000
					60	1.019
67	1.156	1.106	1.005	1.123	70	1.013
					80	1.013
90	1.211	1.137	1.018	1.120	90	1.019
101	1.180	1.112	1.005	1.112	100	1.013
112	1.122	1.082	0.974	1.102	110	1.006
123	1.041	1.016	0.934	1.093	120	0.994
135	0.918	0.923	0.872	1.070	130	0.976
146	0.750	0.795	0.805	1.027	140	0.941
					150	0.884
157	0.582	0.639	0.666	0.953	160	0.788
					170	0.648
180	0.264	0.357	0.415	0.819	180	0.637

TABLE B.4 DIRECTIONAL RESPONSE OF HIGH-RANGE GITR DETECTOR
(WITH 0.13-INCH ALUMINUM JACKET) TO BEAMS OF
VARIOUS RADIATIONS

Values are comparisons to response of unshielded detector to Cs^{137} radiation
beamed at top of detector (0 degree orientation). Detector was rotated about
its center in longitudinal plane. Response is symmetrical about longitudinal
axis of detector.

Detector Orientation	70-kev X-rays	120-kev X-rays	180-kev X-rays	Co^{60}	Detector Orientation	Cs^{137}
deg					deg	
0	0.907	0.826	0.952	1.090	0	0.965
					10	1.103
22	1.038	0.947	1.103	1.223	20	1.152
					30	1.176
45	1.023	0.976	1.145	1.250	40	1.192
					50	1.204
					60	1.226
67	1.210	1.139	1.245	1.281	70	1.240
					80	1.257
90	1.295	1.213	1.283	1.301	90	1.264
101	1.198	1.159	1.253	1.302	100	1.272
112	1.161	1.164	1.253	1.314	110	1.288
123	1.138	1.153	1.199	1.308	120	1.276
135	0.940	1.023	1.093	1.289	130	1.249
146	0.781	0.919	0.985	1.250	140	1.209
					150	1.111
157	0.709	0.814	0.854	1.133	160	0.911
					170	0.590
180	0.164	0.282	0.298	0.467	180	0.274

TABLE B.5 DIRECTIONAL RESPONSE OF LOW-RANGE
DETECTOR (MOUNTED INSIDE GITR CASE)
TO BEAMS OF VARIOUS RADIATIONS

Detector and case were rotated in three longitudinal planes (45
degrees apart) about center of detector. The three responses
for each latitudinal angle were averaged and compared to response
of unshielded detector to Cs^{137} radiation beamed at top of detector
(0 degree orientation).

Detector Orientation deg	70-kev X-rays	120-kev X-rays	180-kev X-rays	Cs^{137}	Co^{60}
0	1.055	0.830	0.769	0.936	1.095
22	0.982	0.823	0.767	0.963	1.115
45	0.977	0.861	0.783	0.979	1.115
67	1.080	0.933	0.807	0.992	1.113
90	1.189	0.973	0.830	1.019	1.136
101	1.165	0.959	0.821	1.009	1.131
112	0.974	0.826	0.737	0.947	1.083
123	0.703	0.633	0.624	0.869	1.021
135	0.421	0.486	0.506	0.783	0.955
146	0.240	0.224	0.324	0.641	0.846
157	0.057	0.085	0.139	0.401	0.579
180	0.031	0.080	0.105	0.324	0.490

TABLE B.6 DIRECTIONAL RESPONSE OF HIGH-RANGE
DETECTOR (MOUNTED INSIDE GITR CASE)
TO BEAMS OF VARIOUS RADIATIONS

Detector and case were rotated in three longitudinal planes (45
degrees apart) about center of detector. The three responses
for each latitudinal angle were averaged and compared to response
of unshielded detector to Cs^{137} radiation beamed at top of detector
(0 degree orientation).

Detector Orientation deg	70-kev X-rays	120-kev X-rays	180-kev X-rays	Cs^{137}	Co^{60}
0	0.955	0.857	0.926	0.964	1.079
22	1.034	0.948	1.024	1.137	1.208
45	0.945	0.924	1.011	1.163	1.223
67	1.165	1.082	1.103	1.219	1.265
90	1.274	1.179	1.147	1.255	1.290
101	1.196	1.124	1.111	1.250	1.316
112	0.996	0.994	1.015	1.182	1.292
123	0.615	0.745	0.796	1.024	1.159
135	0.358	0.552	0.638	0.910	1.076
146	0.221	0.393	0.495	0.735	0.936
157	0.053	0.153	0.235	0.455	0.646
180	0.024	0.067	0.084	0.252	0.286

TABLE B.7 GAMMA DOSE RATES CONTRIBUTED BY VARIOUS INTERVALS OF
ASSUMED GAMMA-ENERGY SPECTRA

See Section B.2 for details.

Energy Interval	Class Mark	Dose Rate from Energy Interval					
		9 sec After Fission		7 min After Fission		0.5 hr After Fission	
		Original Spectrum	Degraded Spectrum	Original Spectrum	Degraded Spectrum	Original Spectrum	Degraded Spectrum
Mev	Mev	pct	pct	pct	pct	pct	pct
0 to 0.09	0.07	0	34.1	0	35.5	0.7	20.7
0.09 to 0.15	0.12	0	2.4	0	2.5	0.3	3.5
0.15 to 0.37	0.18	0	5.9	0	6.1	4.8	14.7
0.37 to 0.93	0.66	36.9	34.8	45.3	36.6	22.7	32.2
0.93 to 5.0	1.25	63.1	22.8	54.7	19.3	71.5	28.9

TABLE B.8 GAMMA DOSE RATES CONTRIBUTED BY VARIOUS INTERVALS OF
ASSUMED GAMMA-ENERGY SPECTRA

See Section B.2 for details.

Energy Interval	Class Mark	Dose Rate from Energy Interval					
		1.1 hr After Fission		5.2 hr After Fission		9 hr After Fission	
		Original Spectrum	Degraded Spectrum	Original Spectrum	Degraded Spectrum	Original Spectrum	Degraded Spectrum
Mev	Mev	pct	pct	pct	pct	pct	pct
0 to 0.09	0.07	12.9	33.0	30.1	37.4	0.6	48.4
0.09 to 0.15	0.12	0.4	3.2	1.1	3.6	2.6	3.4
0.15 to 0.37	0.18	3.9	13.4	5.3	14.7	5.6	17.6
0.37 to 0.93	0.66	28.5	28.1	34.5	29.4	60.1	23.8
0.93 to 5.0	1.25	54.3	22.3	30.0	14.9	31.1	6.8

TABLE B.9 GITR BIAS-CORRECTION FACTORS

Tolerance half-intervals, covering 95 percent of the population with 95 per-
cent confidence, are shown in parentheses as percentages of the factors.

| Type of GITR Installation | Appropriate Period of Application Relative to Envelopment of Ship by Base Surge | | |
	Before	During	Afterward
Low-Range Chamber:			
Standard exterior station	0.94 (14%)	0.94 (11%)	1.03 (13%)
Standard interior station	0.91 (5.5%)	0.94 (3.3%)	0.97 (4.7%)
Detector inside recorder case	0.93 (4.9%)	0.97 (7.8%)	1.07 (15%)
Combined average	0.92 (5.6%)	0.95 (6.1%)	—
High-Range Chamber:			
Standard exterior station	0.79 (7.7%)	0.81 (9.4%)	0.86 (12%)
Standard interior station	0.78 (1.0%)	0.82 (5.9%)	0.84 (9.2%)
Detector inside recorder case	0.79 (2.8%)	0.84 (8.5%)	0.94 (18%)
Combined average	0.79 (3.2%)	0.83 (6.9%)	—
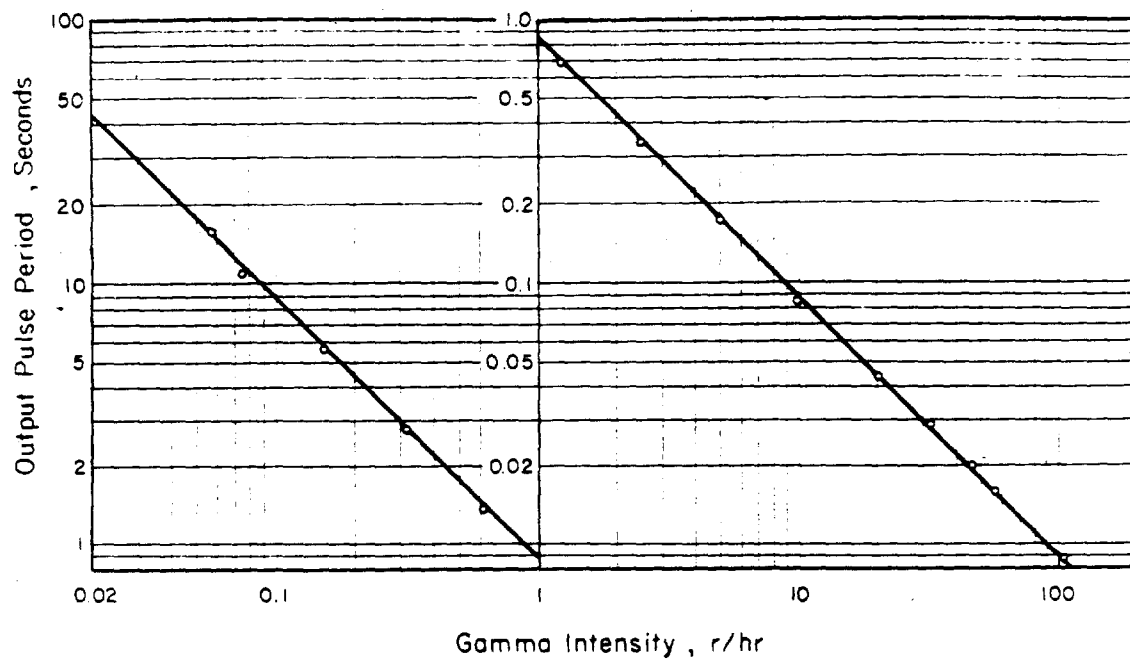
Figure B.1 GITR Model 103 low-range detector output pulse period as a function of gamma intensity for Co[60] and Cs[137]. The longitudinal axes of the detector and the beam were parallel. and the electronics housing was directed away from the source.
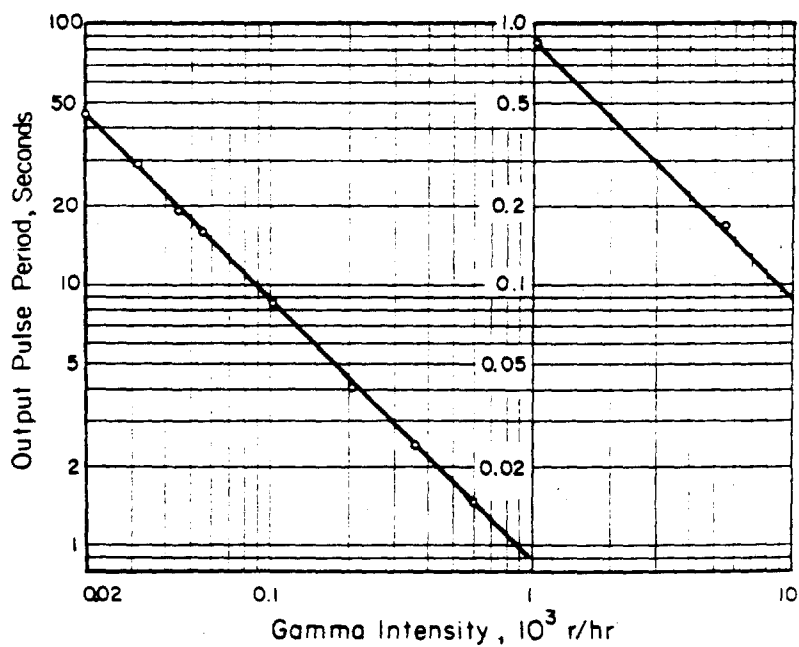

Figure B.2 GITR Model 103 high-range detector output pulse period as a function of gamma intensity for Co[60] and Cs[137]. The longitudinal axes of the detector and the beam were parallel, and the electronics housing was directed away from the source.

93

Figure B.4 Directional-response characteristics of the GITR Model 103 remote detector for parallel-beam radiation (Cs[137]). The detector was shielded by 0.13-inch of aluminum and rotated in the longitudinal plane.

* Response is normalized to 1.0 at 0 degree orientation. Response is symmetrical about the longitudinal axis of the detector for both the low and high ranges.
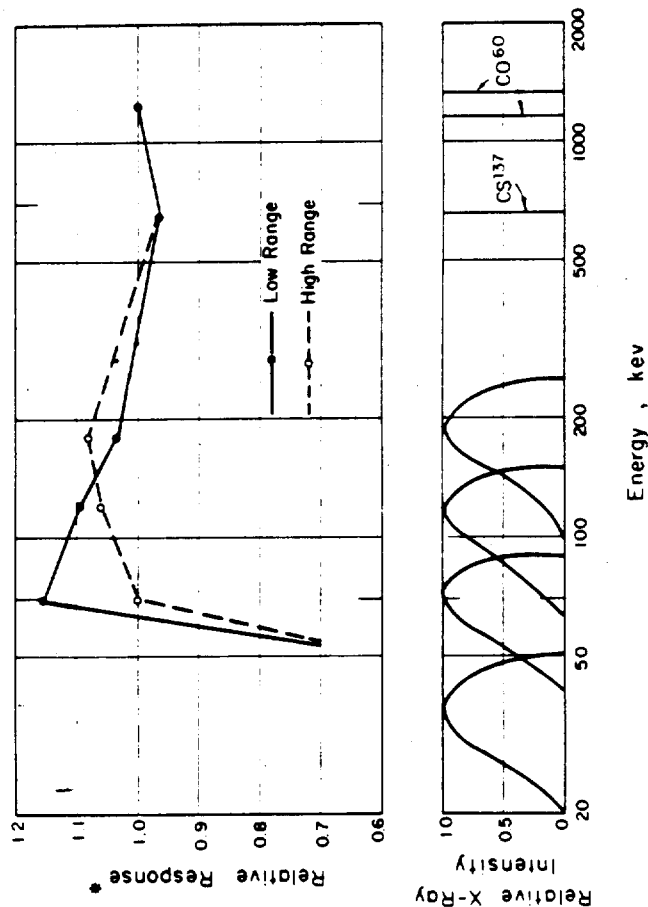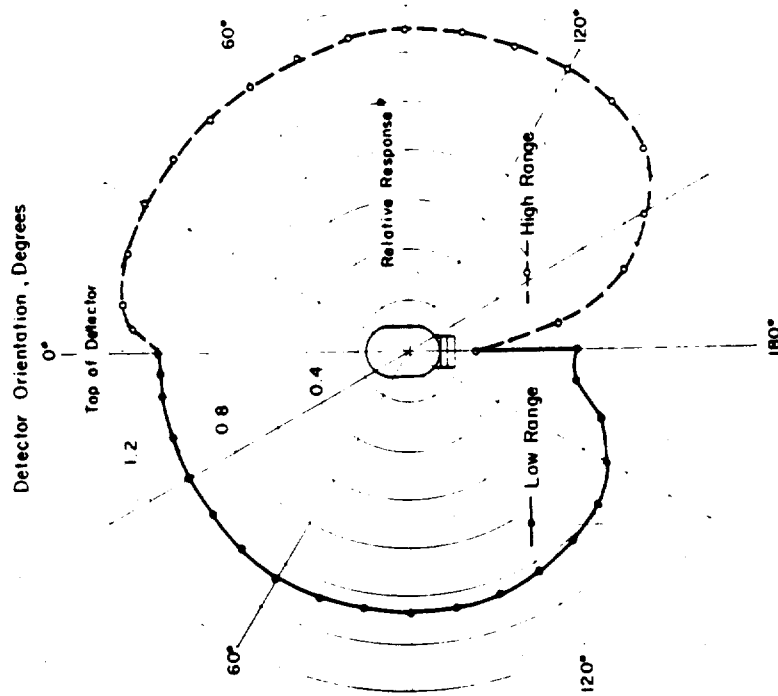

Figure B.3 Energy-response characteristics of the GITR Model 103 detector for parallel-beam radiations. The longitudinal axes of the detector and the beam were perpendicular. Values for 0.13-inch aluminum shield.

* Response is normalized to 1.0 for Co[60].

Figure B.6 GITR station response to monoenergetic radiation when radiation is horizontally incident compared with GITR response to Cs[137] radiation beam directed vertically at top of bare detector. Symbols: ⊙ standard interior station, ▲ standard exterior station, ▢ detector mounted inside GITR case.
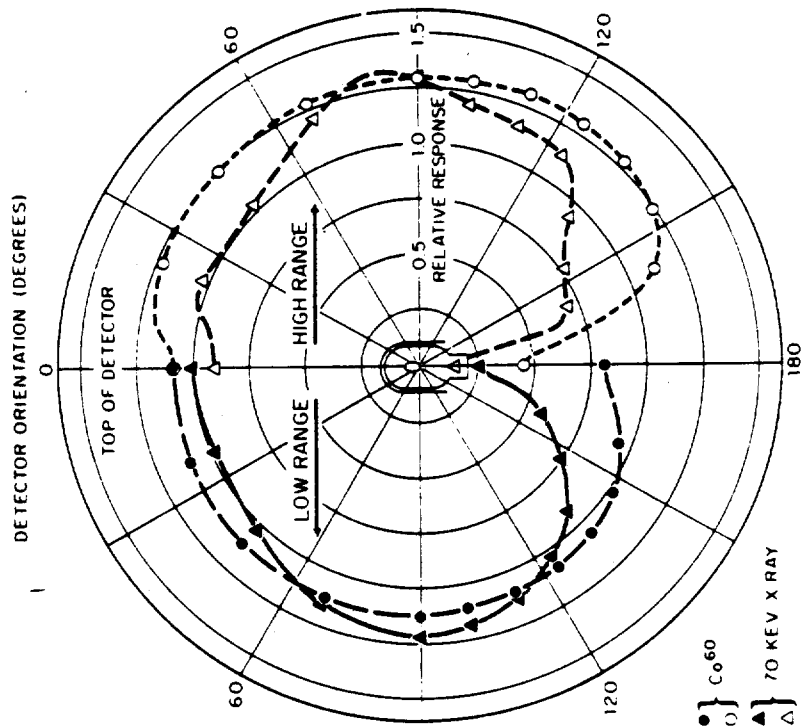

Figure B.5 Directional response of remote GITR detector (with 0.13 inch aluminum jacket) to 70-kev X-ray and Co[60] radiation beams. Values are comparisons to response of unshielded detector to Cs[137] radiation beam at 0 degree orientation. Detector was rotated in longitudinal plane. Response is symmetrical about longitudinal axis of detector.
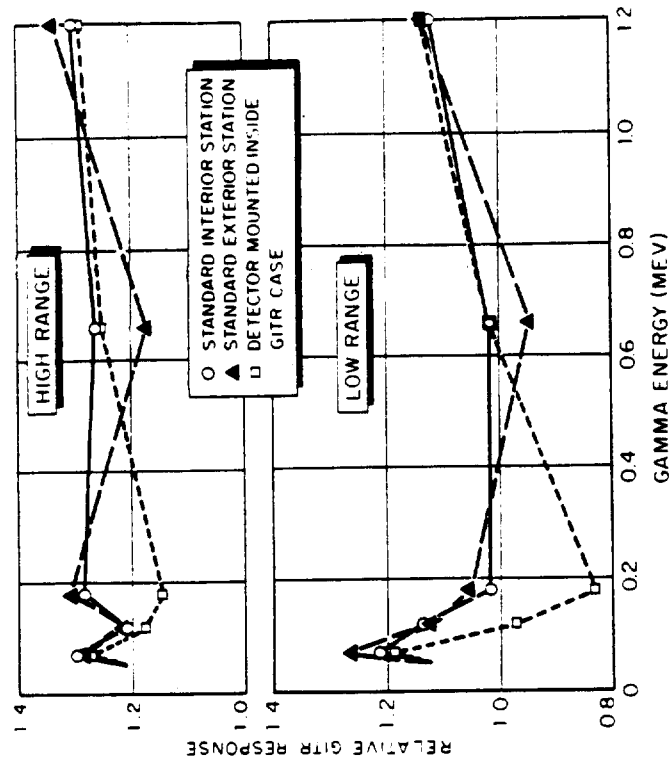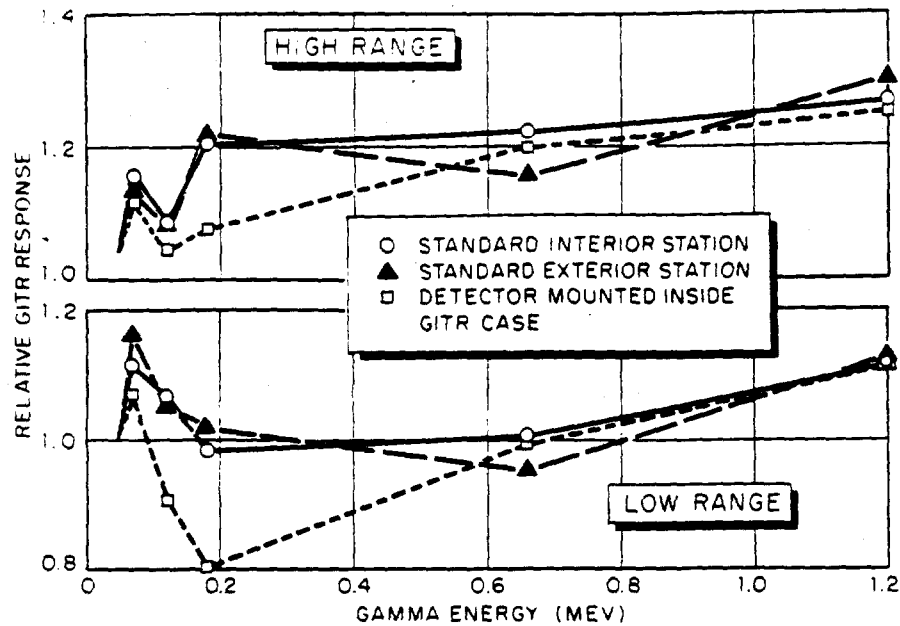
95

Figure B.7 GITR station response to monoenergetic radiation from hemispherical source above station compared with GITR response to Cs[137] radiation beam directed vertically at top of bare detector. Symbols: O standard interior station; △ standard exterior station; □ detector mounted inside GITR case.
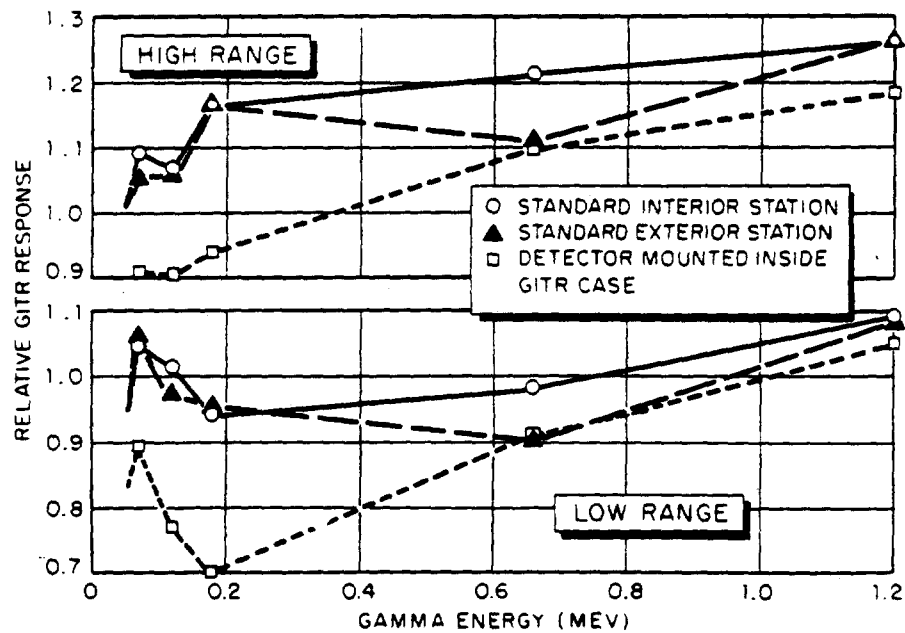

Figure B.8 GITR station response to monoenergetic radiation from spherical source around station compared with GITR response to Cs[137] radiation beam directed vertically at top of bare detector. Symbols: O standard interior station; △ standard exterior station; □ detector mounted inside GITR case.

Figure B.9 GITR station response to monoenergetic radiation from source presenting solid angle of 1.7-π steradians below station compared with GITR response to Cs^{137} radiation beam directed vertically at top of bare detector. Symbols: ○ standard interior station; △ standard exterior station, ▢ detector mounted inside GITR case.
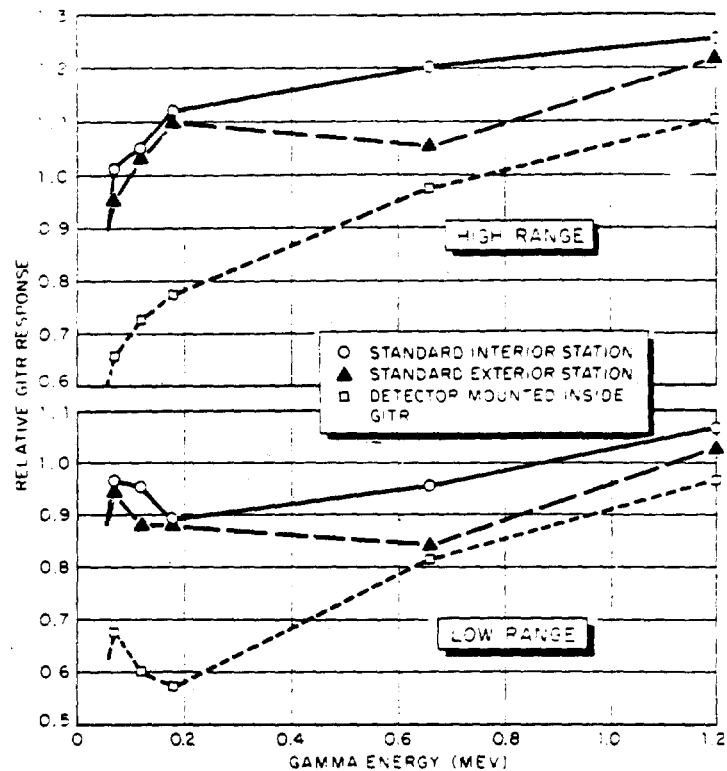

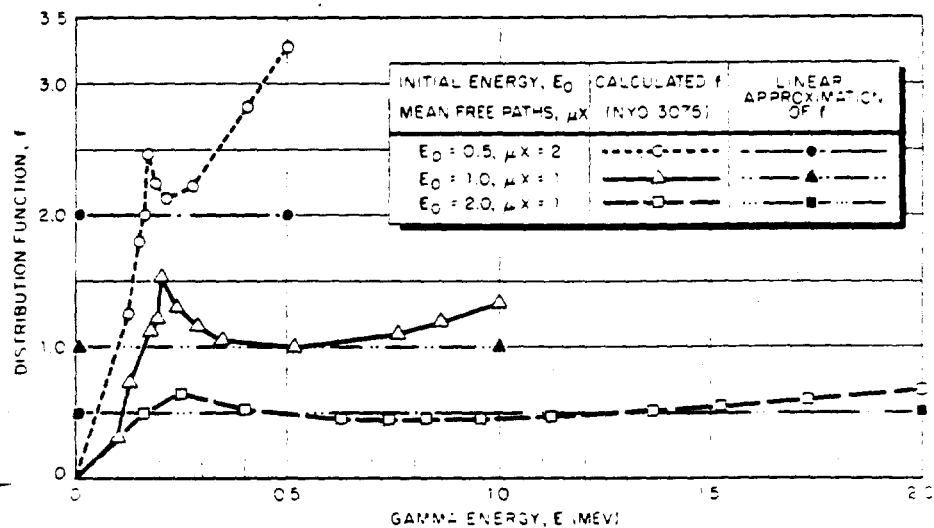Figure B.10 Degraded energy distributions of monoenergetic plane monodirectional gamma radiation after penetrating iron. Areas under curves equal 1 Mev of energy. f is defined by $\int_{0}^{E_0} f dE \equiv 1$ Mev.
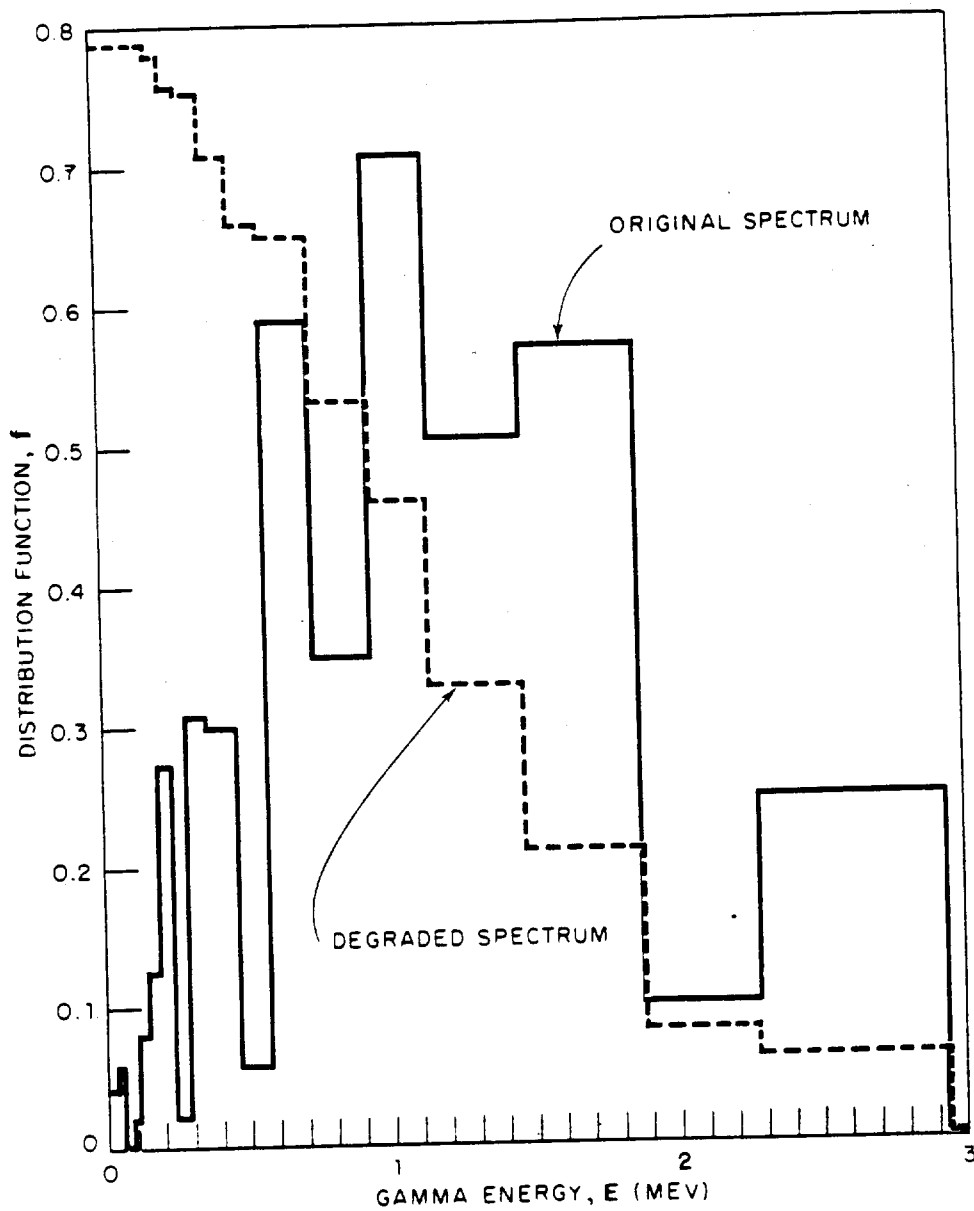
Figure B.11 Estimated degradation of gamma energy after penetrating 1 inch of steel. Original spectrum from Table 2, NBS 5853 (31 min, slow fission of U^{235}). f is defined by $\int f dE \equiv 1$ Mev.

FILM-BADGE DATA. CALIBRATION. AND ESTIMATES OF ERRORS

The nominally 24-hour gamma doses for the individual film badges aboard the three target ships for both shots are presented in Tables C.1 through C.19. The locations of the film-badge stations in the various compartments or areas are presented in Figures C.1 through C.19.

C.1 CALIBRATION

Calibration exposures of film badges were made by TU-6 on their calibration range at EPG, using Co^{60} sources of known strength at various distances and for various exposure times. Calculated doses were checked by means of a Victoreen r-meter. At EPG, the density of the developed film was read by means of an Eberline-Angus densitometer which gave digital average-density readings for a fixed $^5/_{16}$ by $^{11}/_{16}$ inch area of the film originally under the lead strip. A film-density-versus-dose plot, used for preliminary results. showed that there was considerable scatter in the data about the interim calibration curve.

Because damage to the film emulsion—such as pinholes. scratches. waterspots. and the like—would increase light transmission. all films were reread at NRDL, using a Macbeth-Ansco densitometer which permitted scanning $^1/_8$-inch-diameter areas. in order to find the maximum density of the film originally under the lead strip. Standard density wedges were used frequently to check the calibration of the densitometer.

According to Reference 16. characteristic curves of film density versus dose for gamma rays can be obtained with beta-ray plaques calibrated with film to indicate an equivalent gamma ray exposure. A group of sources with several levels of activity will allow a complete curve to be reproduced in a short period of time. The required activity is low and sources equivalent to many curies of gamma rays can be used directly in the laboratory without need for elaborate shielding. Sr^{90}-Y^{90} beta-ray sources were used to establish the shape of the characteristic curve for the film used by this project. The characteristic curve for Sr^{90}-Y^{90} sources was then normalized to give a good fit with various calibration points obtained by use of Co^{60} sources both at NRDL and EPG. This normalized characteristic curve was used as the final calibration curve from which the film-badge doses presented in this report were determined. Only the results from the high-range film (DuPont 834) are presented. because many inconsistencies were observed between the results from the low- and high-range films (in the same badge) that were supposedly exposed to identical doses.

C.2 ESTIMATES OF ERROR

Pairs of film badges were mounted at all stations. except that four badges were used at the GITR stations. In order to investigate random errors (not bias). the percentage difference in dose for each film-badge pair was calculated. For Shot Wahoo data. the average percent difference for 276 film-badge pairs was 7.7 ± 0.5 percent and the median value was 5.4 percent. For Shot Umbrella data. the average percent difference for 311 film-badge pairs was 2.3 ± 0.1 percent and the median value was 1.6 percent. The lower values for the Shot Umbrella data reflect improved handling and processing of the film badges.

The standard errors of the film-badge dose averages, expressed as percentages of the average dose in a compartment, are shown in Table C.20. These percentage standard errors were obtained from the expression: $100 \left[(\sum\limits_{i}^{n} x^2 - n\bar{x}^2)/n(n-1)\bar{x}^2 \right]^{1/2}$; where x is the individual film-badge dose, n is the number of film badges, and $\bar{x}$ is the average dose in the compartment.

All calibration films which had been exposed to known-strength Co^{60} sources (both at NRDL and EPG) were used to investigate the differences between the "actual" doses, i.e., calculated or measured on the calibration range, and the "assigned" doses (based upon use of film densities and the calibration curve discussed in Section C.1). The absolute magnitudes of the difference between the two doses varied from 0 to 32 percent of the assigned dose and had an average value of 7 percent in the 10-to-1,000-r dose range

(which is the recommended range for use of DuPont 534 film). For the 5-to-10-r dose range, the assigned doses averaged about 35 percent lower than the actual doses; and for the 1-to-5-r dose range, the assigned doses averaged about 67 percent lower than the actual doses.

Some of the film badges were in compartments that were both hot and humid for long periods of time. A cursory investigation of temperature and humidity effects on film-badge calibration was performed by exposing ten film badges to Co^{60} radiation and then immersing the badges for 24 hours in a water bath at 150 degrees F prior to film development. The films were developed from 3 to 14 days after exposure. Using the above-mentioned calibration curve resulted in assigned doses which averaged about 12 percent higher (and varied from 7 percent lower to 32 percent higher) than the actual doses. The conditions of this investigation are considered to have been more severe than the actual conditions encountered by the film badges aboard the test ships.

On the basis of the above discussion it would appear reasonable to say that film-badge dose averages are probably accurate to within 20 percent for the recommended dose range of 10 to 1,000 r. and are probably accurate to within a factor of two, i.e., the assigned doses are presumably too low, for doses lower than 10 r.

100

Pages 101 through 106
deleted.

TABLE C.20   STANDARD ERRORS OF FILM-BADGE DOSE AVERAGES

Values are expressed as percentages of the average dose in various compartments or areas.

Compartment or Area	Shot Wahoo			Shot Umbrella		
	DD 474	DD 592	DD 593	DD 474	DD 592	DD 593
Above waterline. 16 to 33 ft:						
Pilot house	—	5.2	14.3	2.9	2.5	2.4
Chart house	—	7.0	6.6	7.9	5.2	6.2
Main weather deck						
Midships	—	4.5	9.6	4.6	7.1	5.1
Fantail	—	—	13.0	—	4.2	0.6
Above waterline. 11 to 16 ft:						
Forward quarters	—	9.1	8.2	7.7	5.7	7.2
Radio central	—	17.5	5.2	8.1	12.6	8.5
Galley	—	5.2	4.5	4.2	3.5	2.4
Crew's washroom	—	7.1	8.0	4.2	2.0	3.9
Above waterline. 2 to 4 ft:						
Crew's mess	11.3	5.1	6.7	5.4	8.9	7.0
Forward fireroom	11.0	9.8	6.6	10.9	11.9	9.4
Forward engine room	12.2	5.9	6.6	7.2	9.0	6.5
Aft fireroom	—	7.6	—	—	11.1	—
Aft engine room	—	6.0	—	—	5.3	—
Aft quarters	—	12.8	5.7	3.1	5.2	3.3
Steering gear room	6.0	9.1	6.3	3.3	1.7	5.8
Below waterline, 3 to 6 ft:						
Magazine	6.8	4.8	4.0	8.4	3.0	6.2
Forward fireroom	8.4	7.2	11.0	5.9	10.0	10.4
Forward engine room	8.9	6.7	9.6	8.5	6.8	—
Aft fireroom	—	7.0	—	—	8.2	—
Aft engine room	—	8.7	—	—	8.5	—

107

MESS ROOM

CPO

3 Berths

CPO QUARTERS

3 Berths

154 ●

152

150 ●

5" AMMUNITION
HANDLING ROOM
AND PASSAGE

151 ●

153 ●

CPO QUARTERS

3 Berths

155 ●

4 Berths

Lkr

Lkr

Lkr

Lkr

Lkr

Lkr

Lkr

Lkr

Lkr

Lkr

Lkr

Lkr

Lkr
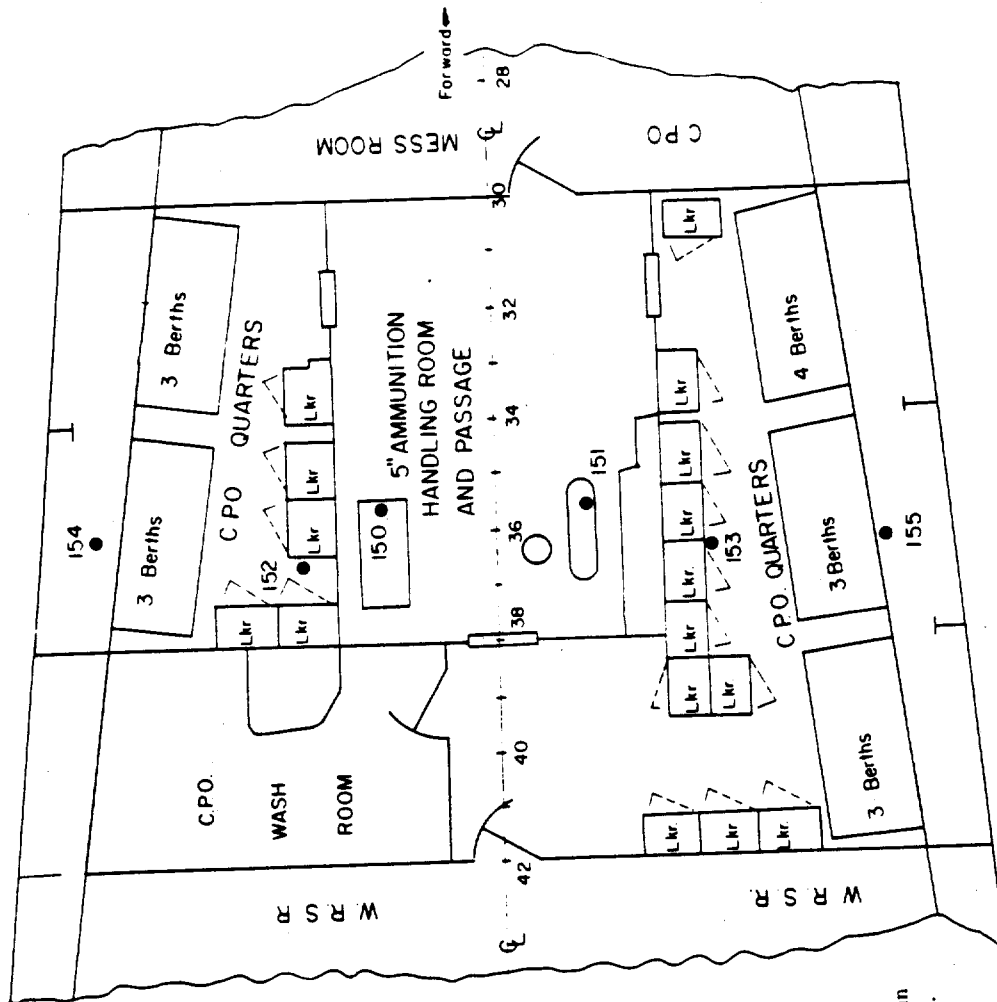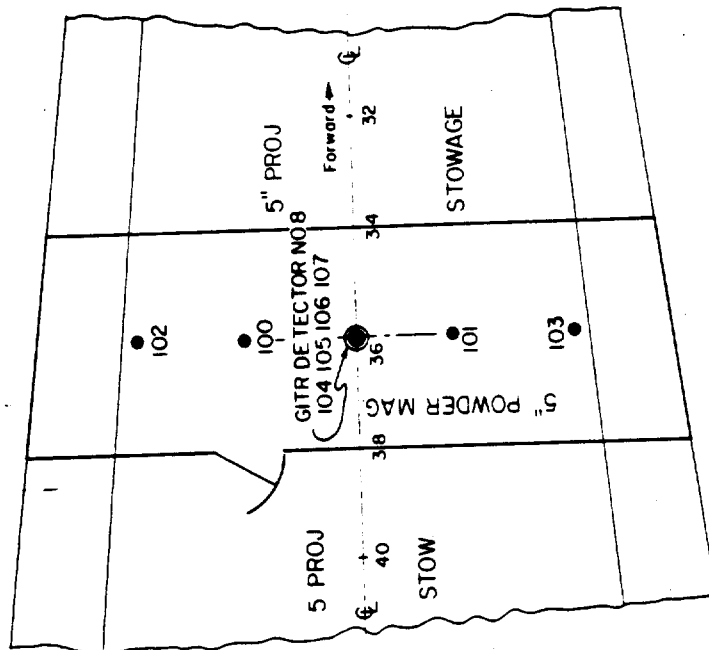
Lkr

CPO.

WASH

ROOM

WRSR

WRSR

Forward

28

30

32

34

36

38

40

42

Figure C.2 Location and designation of film-badge stations
in forward quarters (first platform) aboard target ships.

5" PROJ

STOWAGE

102 ●

100 ●

GTR DETECTOR NO8
104 105 106 107

36 ●

101 ●

103 ●

5" POWDER MAG

5 PROJ
STOW

Forward

32

34

36

38

40

Figure C.1 Location and designation of film-badge stations in
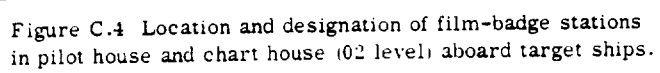5-inch powder magazine (third platform) aboard target ships.

108
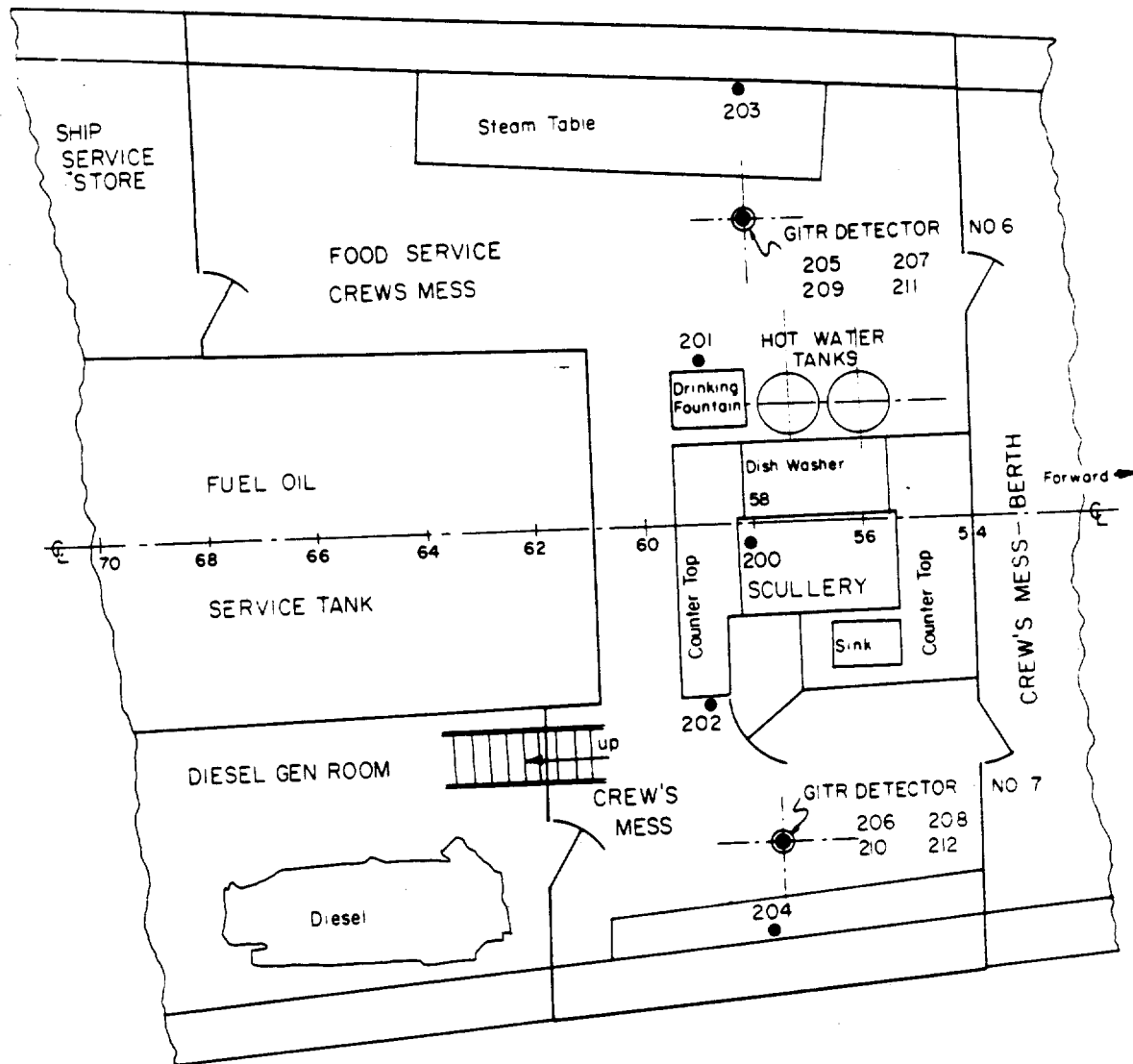
Figure C.3 Location and designation of film-badge stations in crew's mess (second platform) aboard target ships.

Figure C.4 Location and designation of film-badge stations
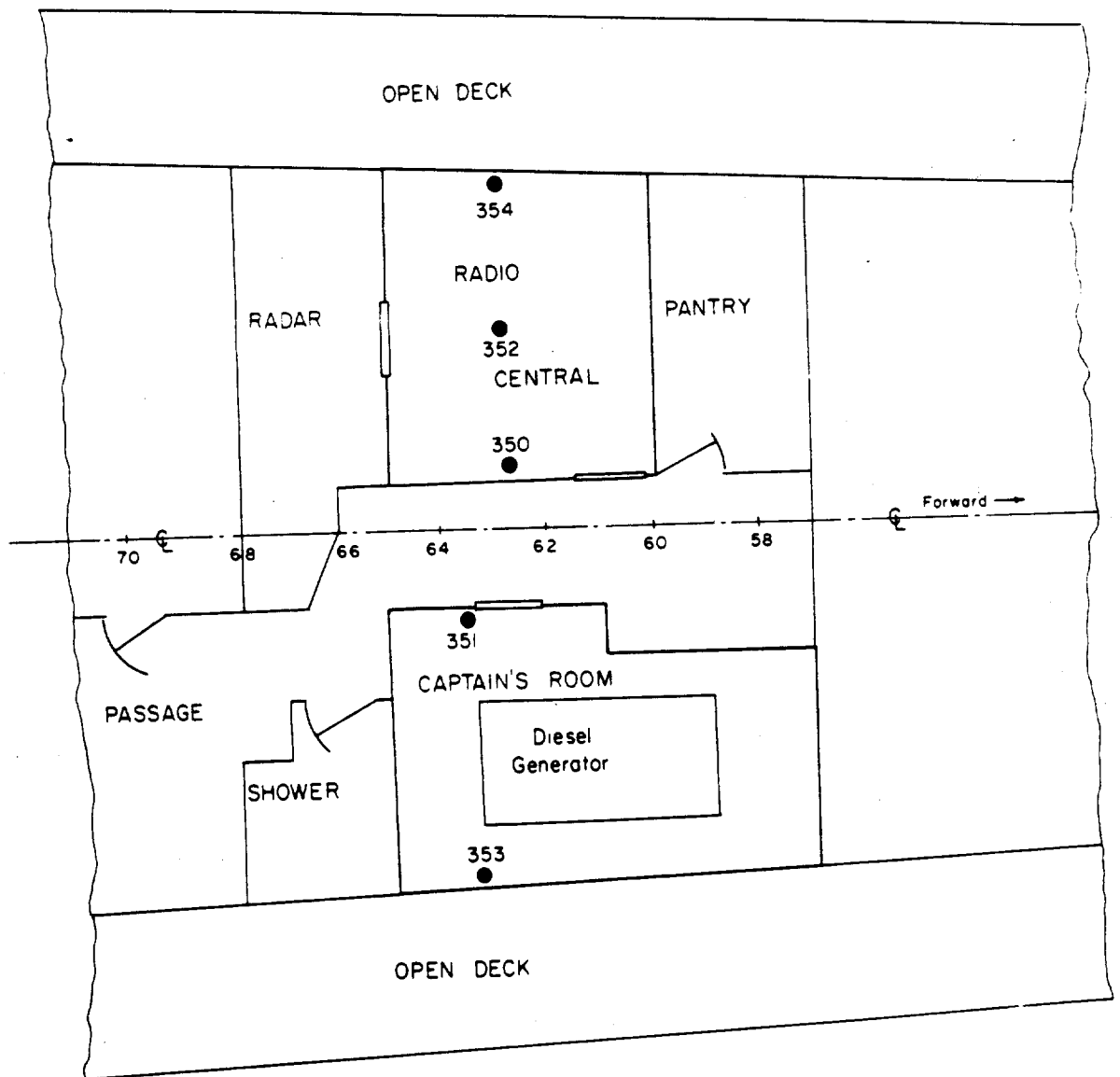in pilot house and chart house (02 level) aboard target ships.

Figure C.5 Location and designation of film-badge stations
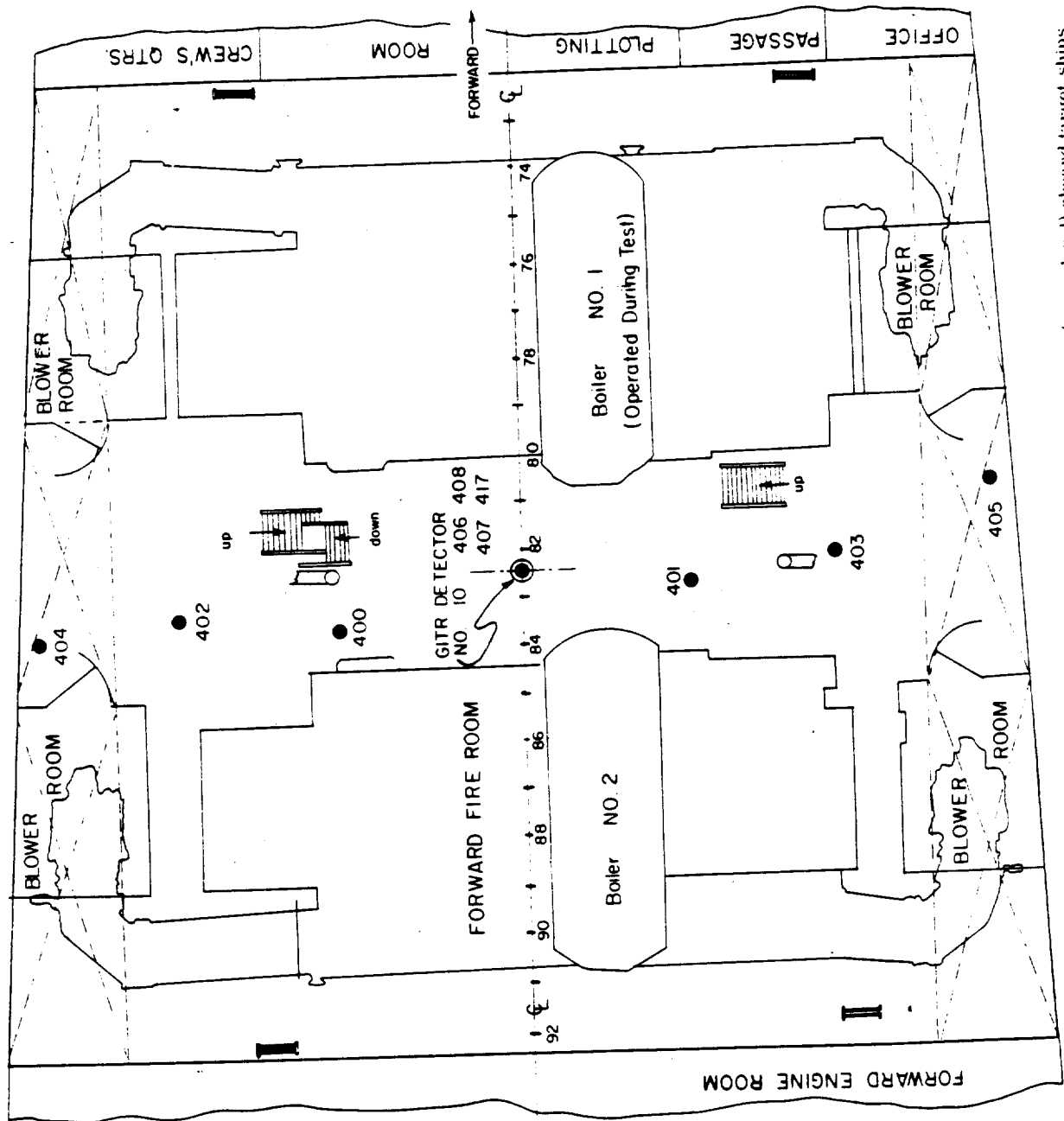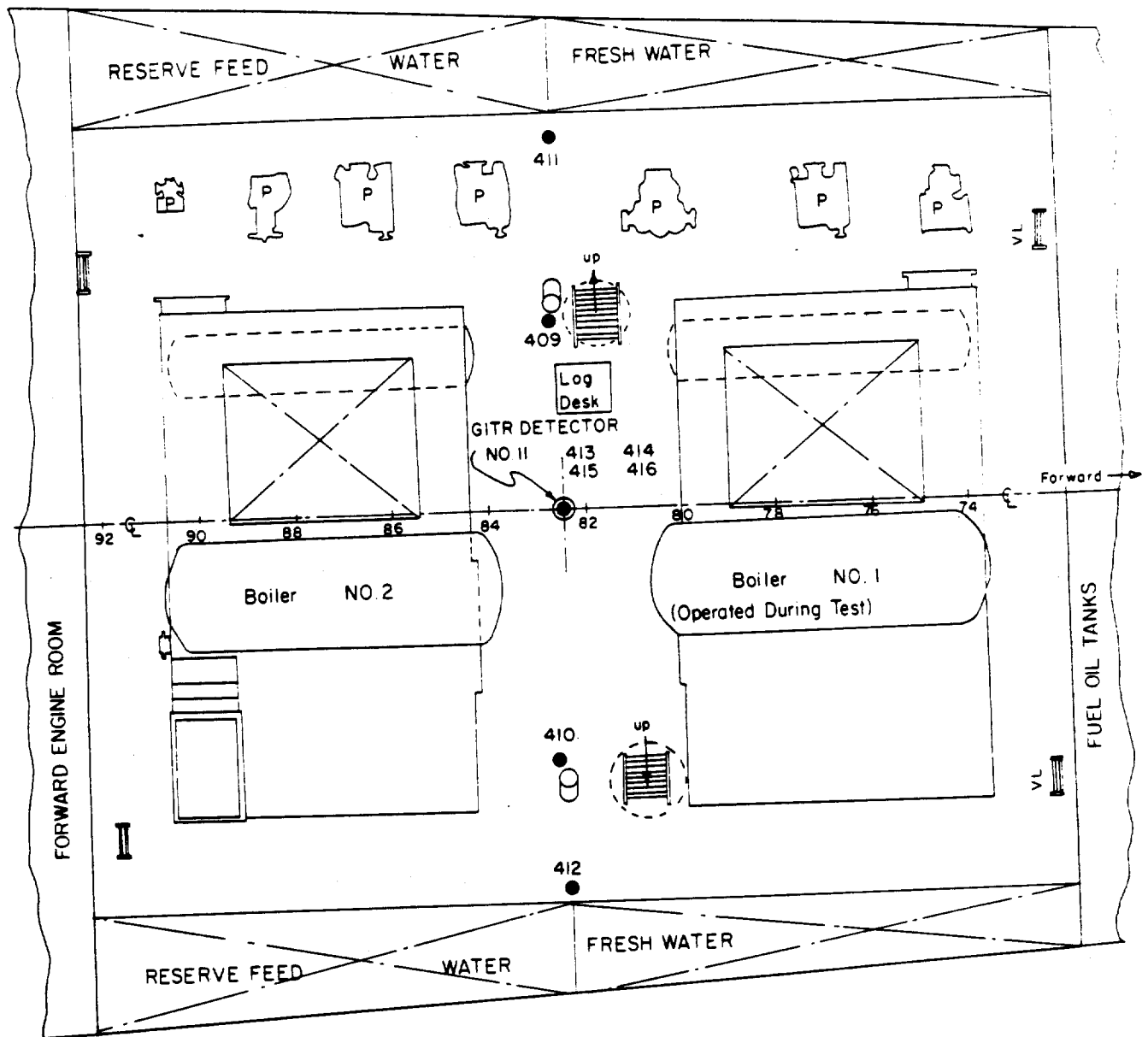in radio central (main deck) aboard target ships.

Figure C.6 Location and designation of film-badge stations in forward fireroom (upper level) aboard target ships.

112

RESERVE FEED   WATER   FRESH WATER

411

409

Log
Desk

GITR DETECTOR
NO. 11   413   414
          415   416

Forward

92   90   88   86   84   82   80   78   76   74

Boiler   NO. 2

Boiler   NO. 1
(Operated During Test)

FORWARD ENGINE ROOM

FUEL OIL TANKS

VL

410.

up

412

FRESH WATER

RESERVE FEED   WATER

Note. Items Marked "P" are Pumps

Figure C.7 Location and designation of film-badge stations
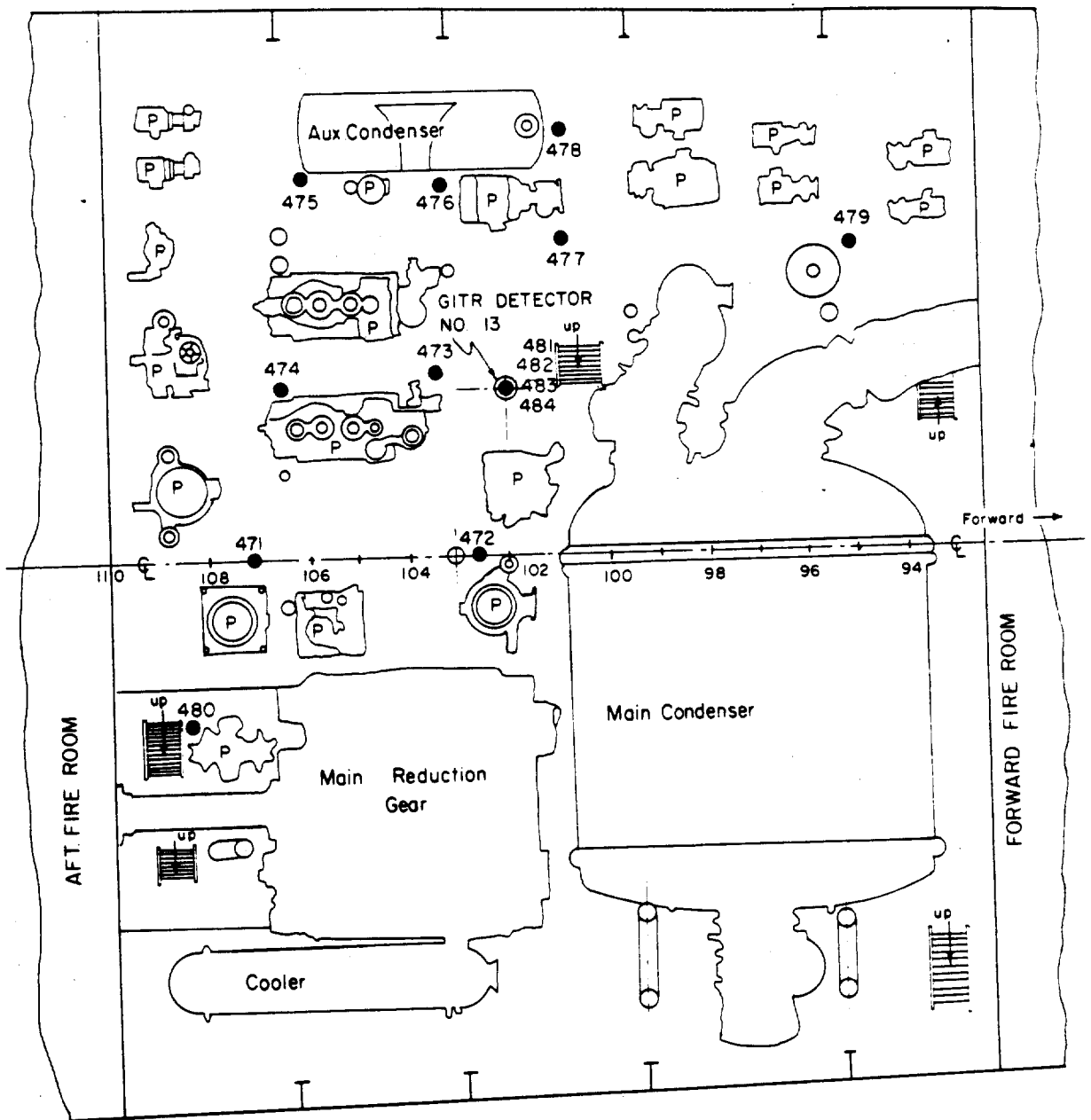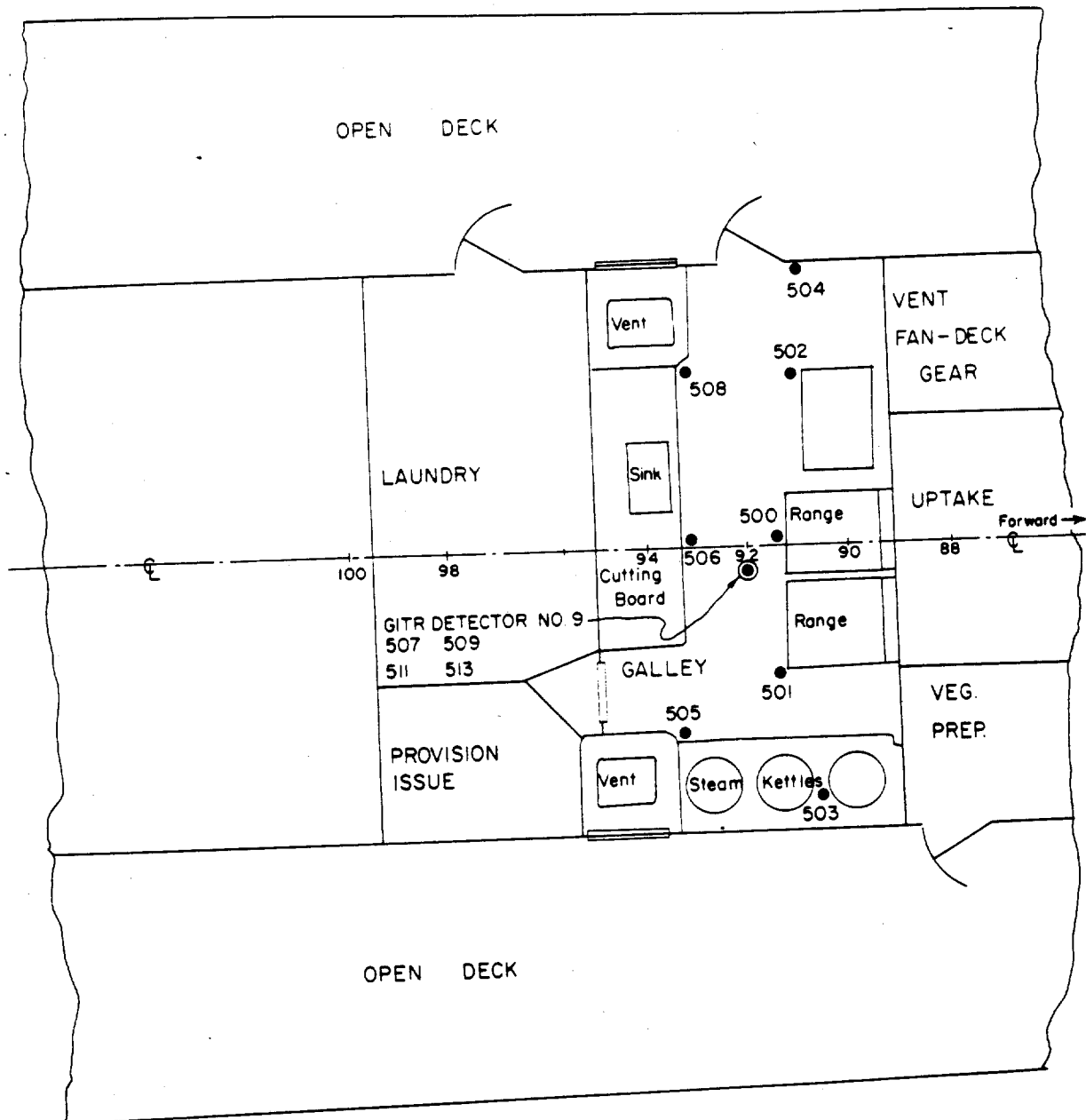in forward fireroom (lower level) aboard target ships.

113
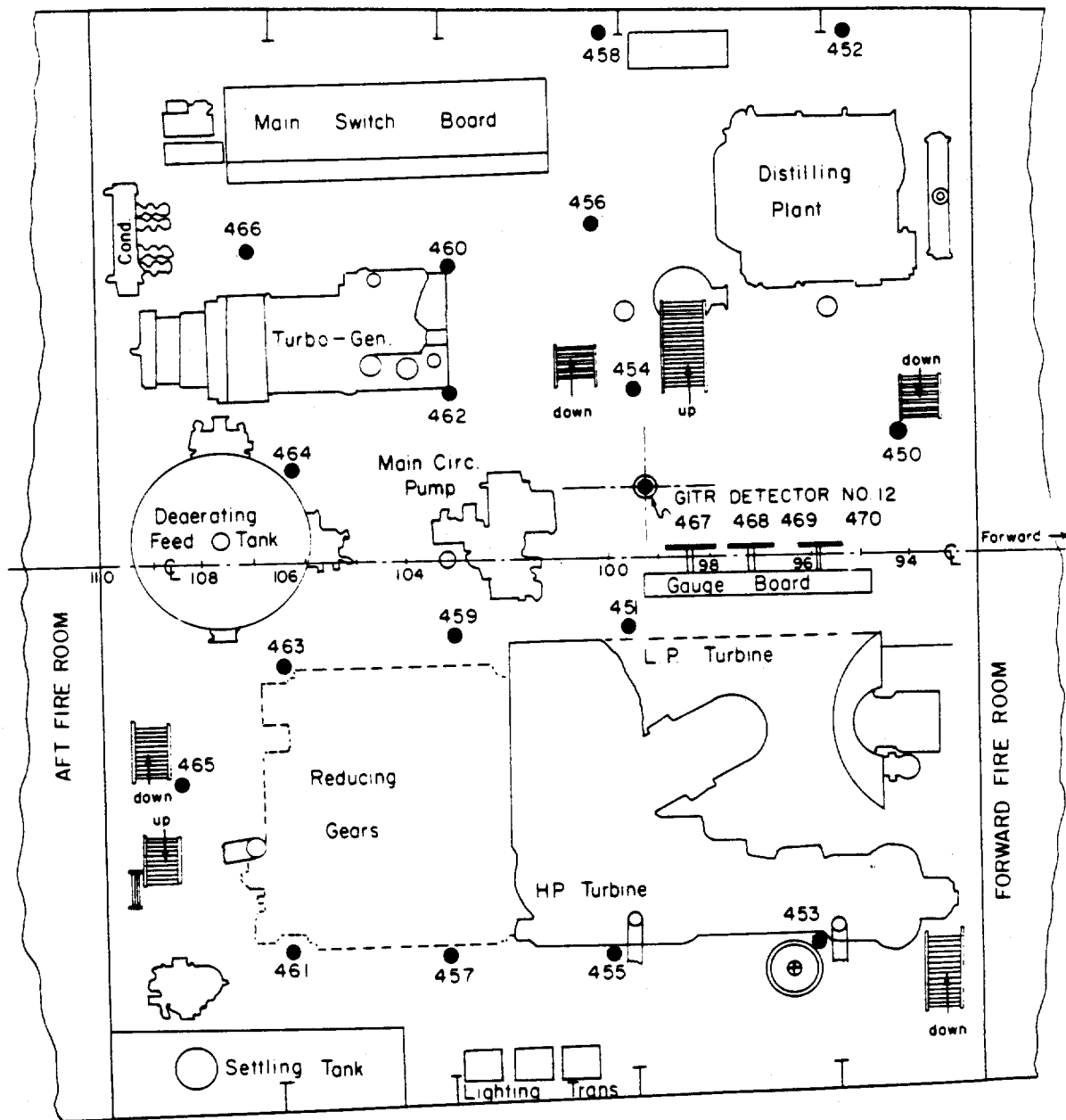
Figure C.8 Location and designation of film-badge stations
in forward engine room (upper level) aboard target ships.

Note: Items Marked "P" are Pumps

Figure C.9 Location and designation of film-badge stations
in forward engine room (lower level) aboard target ships.

OPEN DECK

VENT FAN-DECK GEAR

LAUNDRY

UPTAKE

Forward →

PROVISION ISSUE

VEG. PREP.

GALLEY

OPEN DECK

Note. DD 592 Galley Eqipment Removed Prior to Tests

Figure C.10 Location and designation of film-badge stations in galley (main deck) aboard target ships.
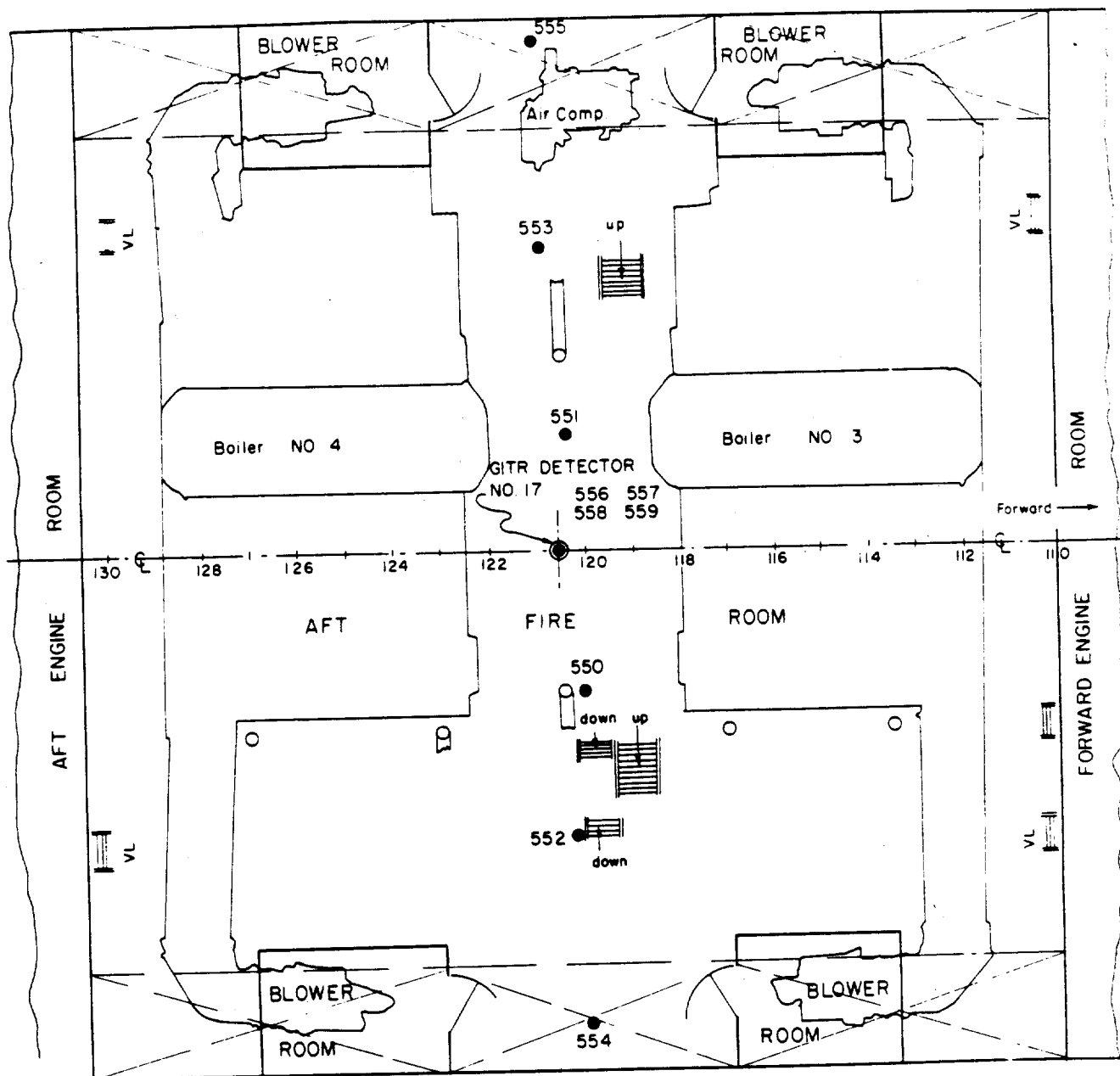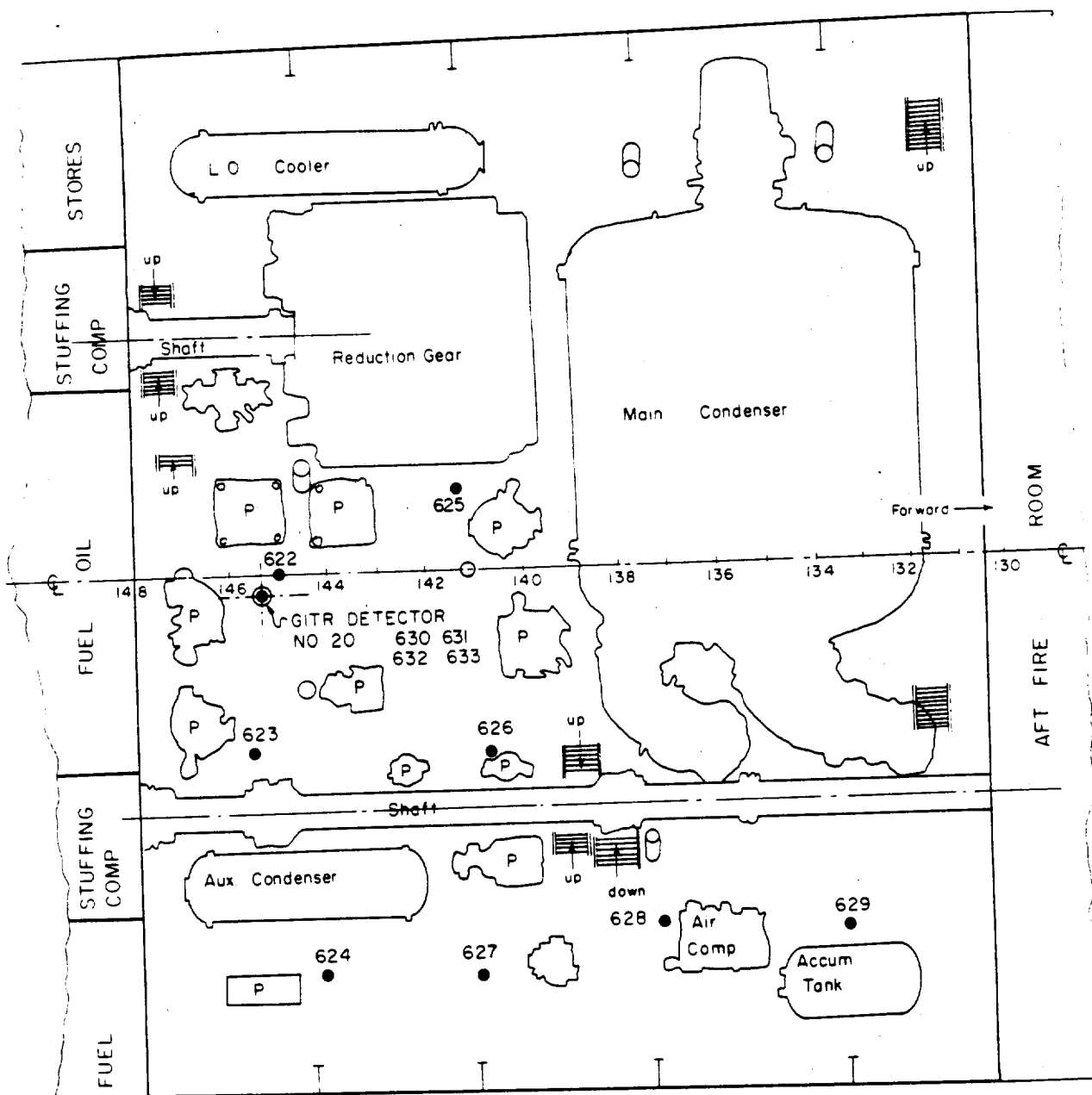
116

Figure C.11 Location and designation of film-badge stations in aft fireroom (upper level) aboard DD 592.

117

Figure C.12 Location and designation of film-badge
stations in aft fireroom (lower level) aboard DD 592.

118

Note: Items Marked "P" are Pumps

Figure C.13 Location and designation of film-badge
stations in aft engine room (upper level) aboard DD 592.

Note. Items Marked "P" are Pumps

Figure C.14 Location and designation of film-badge
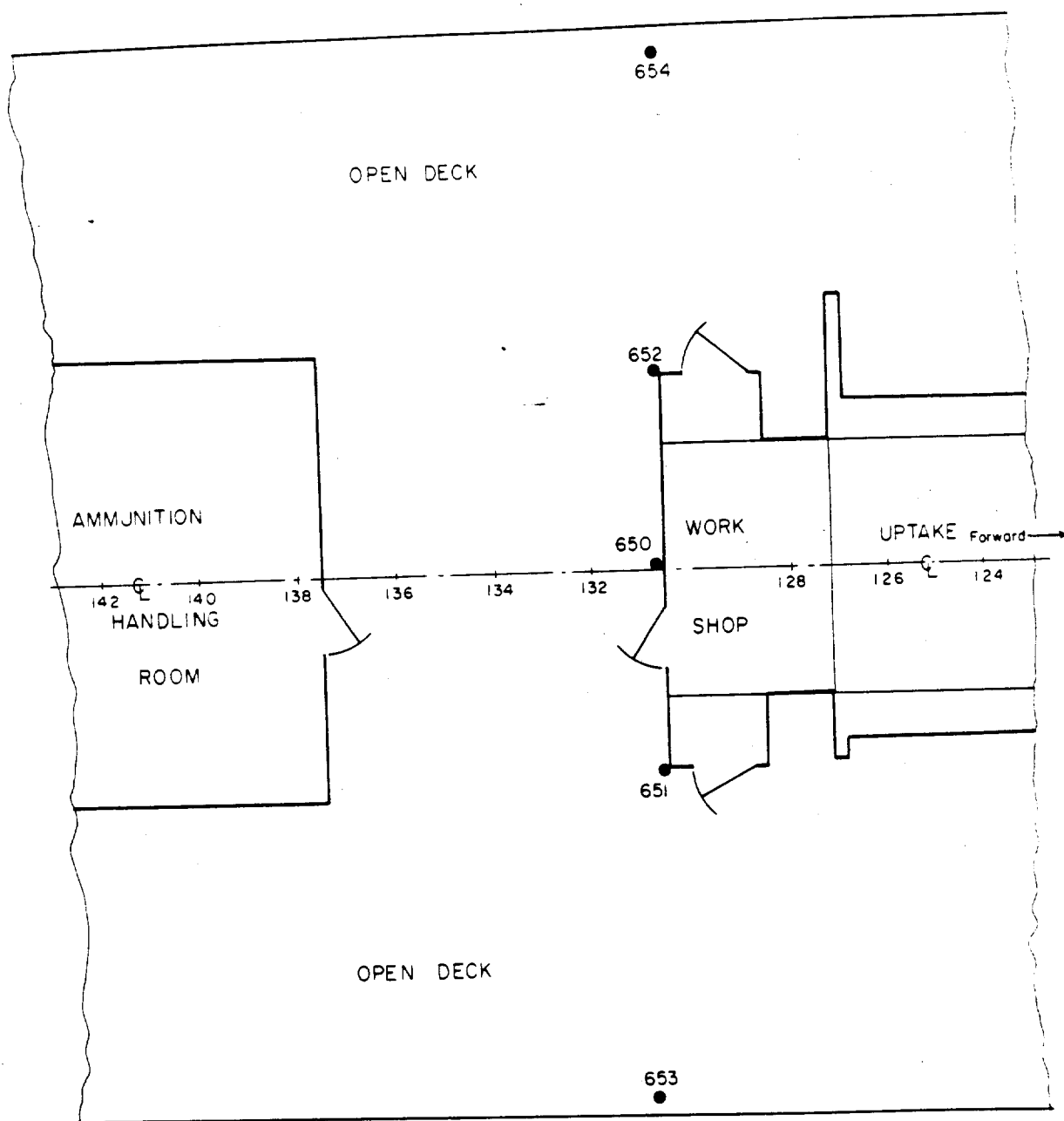stations in aft engine room (lower level) aboard DD 592.

Figure C.15 Location and designation of film-badge
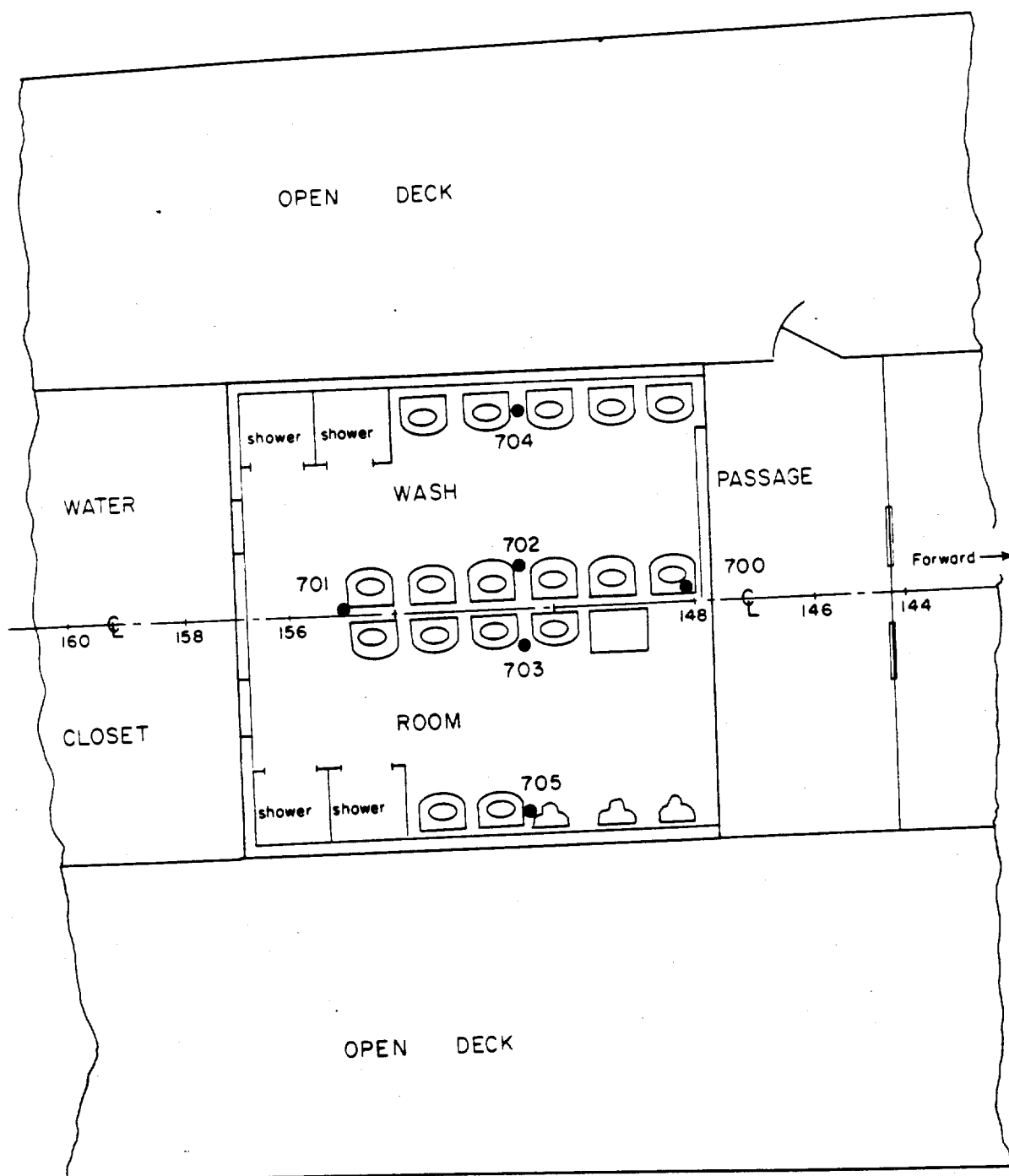stations on main deck (midship) aboard target ships.

121

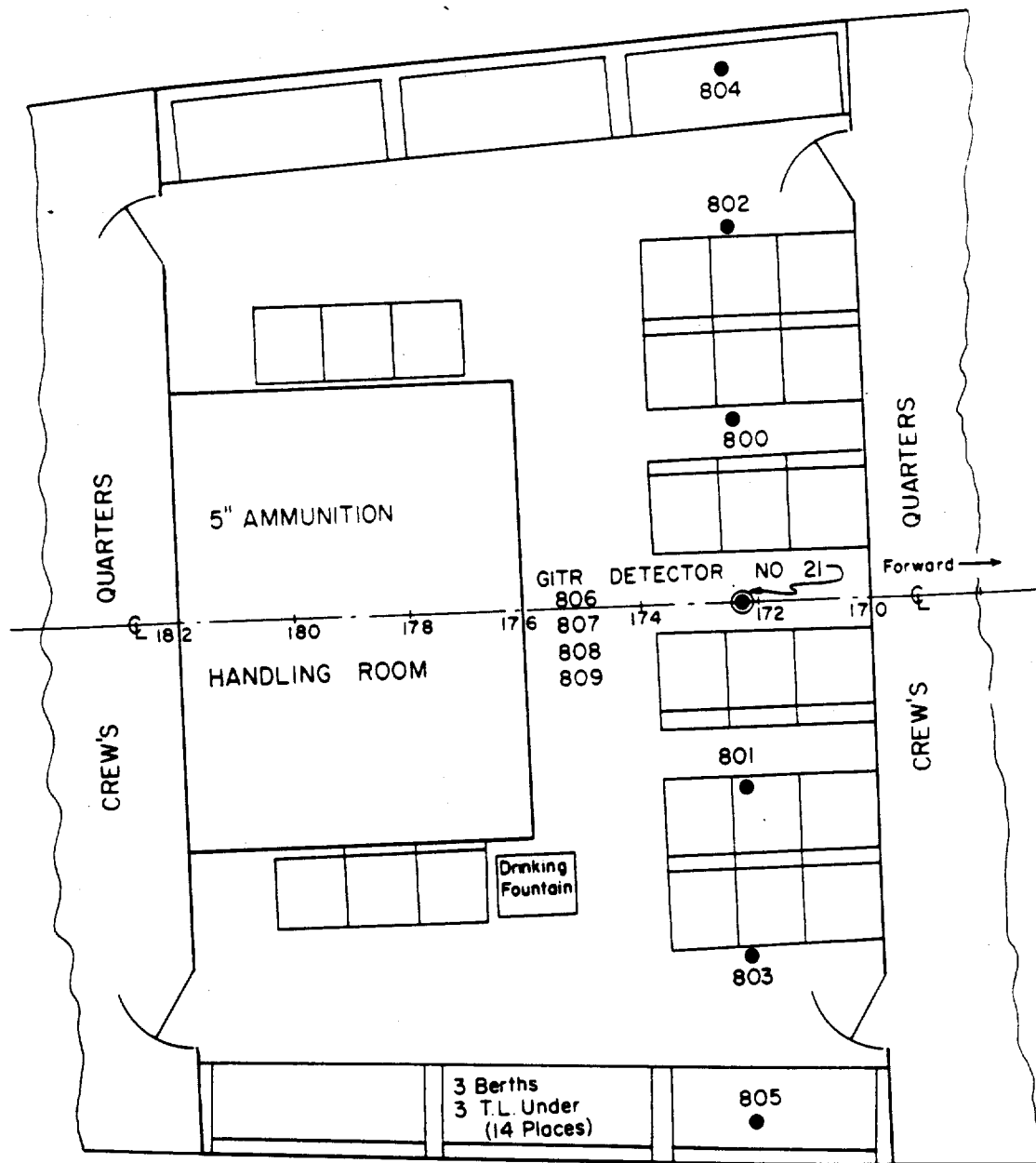Figure C.16 Location and designation of film-badge stations in crew's washroom (main deck) aboard target ships.

122

Figure C.17 Location and designation of film-badge stations in aft quarters (first platform) aboard target ships.

OPEN DECK

854

OPEN DECK

852

5" GUN

Forward →

850

210   208   206   186   184   182   180   178

MOUNT

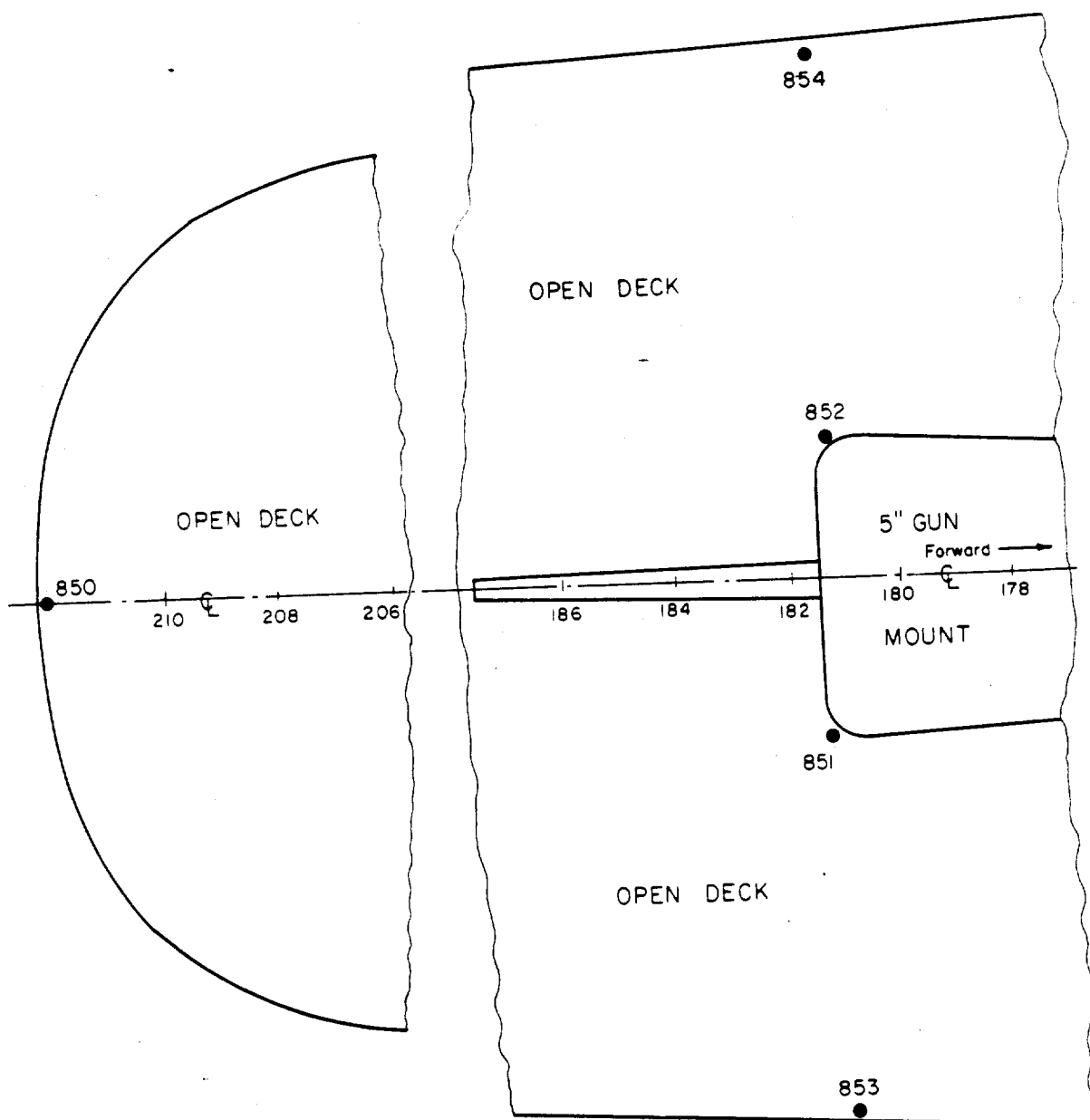OPEN DECK

851

OPEN DECK

853

Figure C.18 Location and designation of film-badge
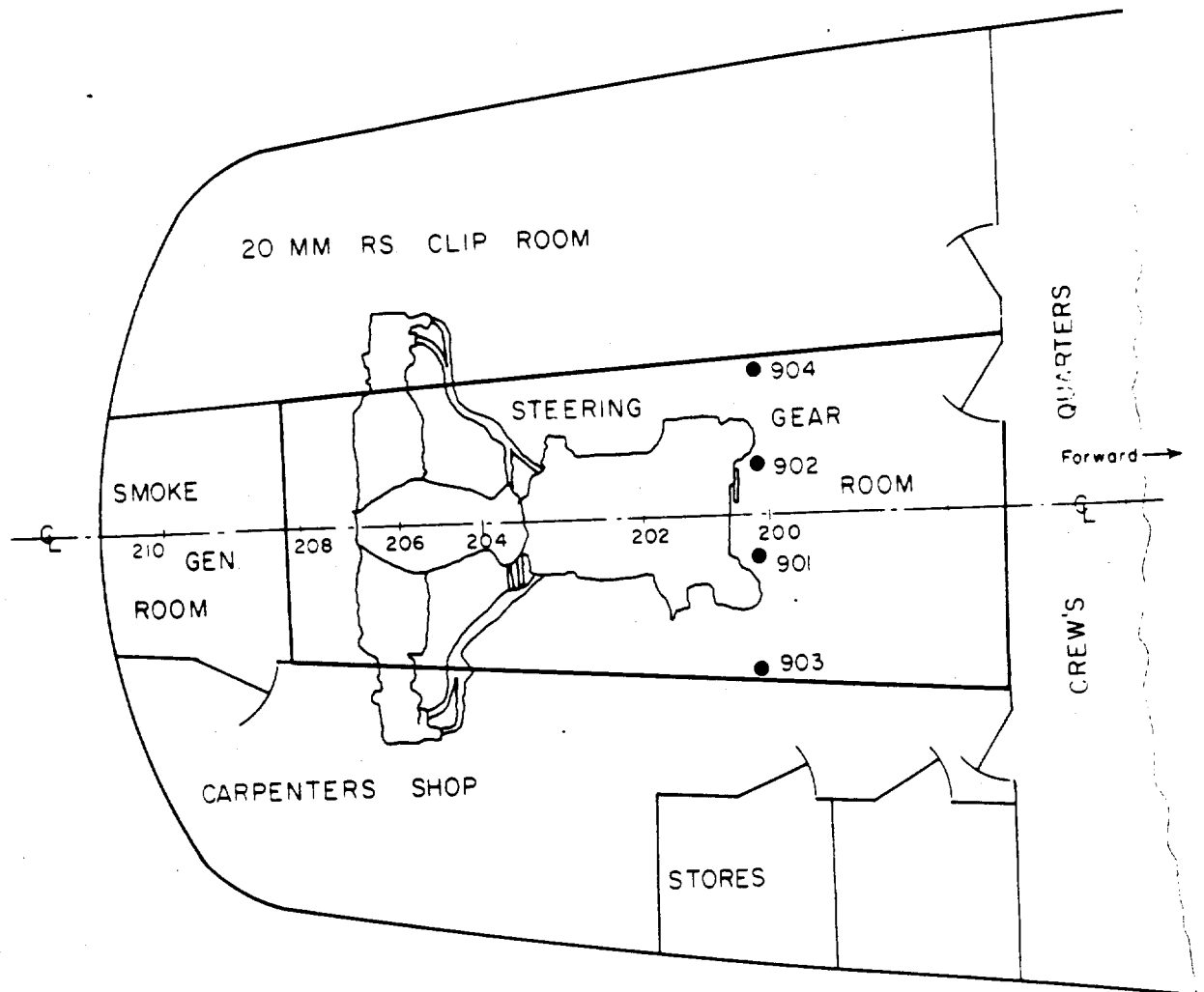stations on main deck (fantail) aboard target ships.

124

Figure C.19 Location and designation of film-badge stations in steering gear room (first platform) aboard target ships.

125

Appendix D

TABULATIONS OF GAMMA-RADIATION HISTORIES

Appendix D is not being published.

The appendix consists of 2 pages of text. 366 pages of numerical data tables (dose rates and doses versus time and location, and the like). and 3 figures that depict the estimated probable errors in average gamma dose rates and doses (versus time) on the weather decks of the target ships.

Pages 127 and 128 deleted.